

**A STUDY OF ALUMINUM-GERMANIUM-NICKEL OHMIC CONTACT  
METALLURGICAL EFFECTS AT THE GALLIUM ARSENIDE INTERFACE**

By

**WILLIAM V. LAMPERT**

**A DISSERTATION PRESENTED TO THE GRADUATE SCHOOL OF THE  
UNIVERSITY OF FLORIDA IN PARTIAL FULFILLMENT OF THE  
REQUIREMENTS FOR THE DEGREE OF DOCTOR OF PHILOSOPHY**

**UNIVERSITY OF FLORIDA**

**1992**

## ACKNOWLEDGMENTS

The author would like to thank all of the members of his supervisory committee for both their patience and assistance throughout his research. In particular, he appreciates the guidance and constant encouragement of his committee chairman and advisor, Dr. P. H. Holloway, and also that of his committee member and group leader at the Wright Laboratory Materials Directorate, Dr. T W. Haas. He would also like to thank Eric Lambers for the assistance with the Auger Electron Spectroscopy, Dr. Baoqi Li for assistance with the room temperature I-V measurements, Chris Roubelet for the assistance with the real time heat treatment and I-V measurements, co-workers Dr. Scott Walck and Dave Tomich for their help with data translation for the computer, and his other co-workers at the Materials Directorate for their help and agitation to finish.

The author would most like to express his gratitude to his sons, Curt, Thomas, and Doug and especially to his wife, Nancy for the constant love, support, and sacrifice they gave without question over the many long years he pursued his education. Special thanks also go to his parents, Thomas and Edna for their support and instilling in him the belief that anything was achievable given enough effort.

Acknowledgment is also due the United States Air Force for their Long-Term Training Program which made it possible for the author to pursue this work.

## TABLE OF CONTENTS

ACKNOWLEDGMENTS .....	ii
ABSTRACT .....	v
CHAPTERS	
1 INTRODUCTION .....	1
2 REVIEW OF LITERATURE .....	6
Au/Ge/Ni Ohmic Contacts to GaAs .....	6
Other Metals and GaAs .....	15
Background for Aluminum Based Ohmic Contacts to GaAs .....	19
3 EXPERIMENTAL PROCEDURE .....	30
Sample Preparation .....	30
Metal Deposition .....	32
Electrical Measurement .....	37
Heat Treatment .....	39
Real Time I-V Measurement and Heat Treatment .....	40
Auger Electron Spectroscopy .....	41
Thin Film X-ray Diffraction .....	42
4 RESULTS .....	44
Sample Preparation .....	44
Sample Deposition .....	45
Heat Treatment .....	47
Electrical Measurement .....	48
Real Time I-V Measurement and Heat Treatment .....	56
Summary of Current-Voltage Data .....	59
Elemental Depth Profiles .....	62
Three Element Contacts .....	62
Two Element Metallizations .....	69
Summary of Elemental Depth Profiles .....	71
Diffraction Analysis of Phase Formation in Al-Ge-Ni Thin Films .....	73
Three Element Metallizations on GaAs .....	73
Three Element Metallizations on Sapphire .....	80
Two Element Metallization .....	80
Summary of Phase Formation in Al-Ge-Ni Thin Films .....	82

5 DISCUSSION .....	86
Reaction Path Analysis .....	87
Mechanism of Doping .....	90
General Model of Ohmic Contact Formation .....	90
6 CONCLUSIONS .....	94

## APPENDICES

A GaAs SUBSTRATE AND SAMPLE CLEANING .....	97
B METALLIZATION SEQUENCE, HEAT TREATMENT, AND ELECTRICAL CHARACTERIZATION .....	103
REFERENCES .....	109
BIOGRAPHICAL SKETCH .....	116

Abstract of Dissertation Presented to the Graduate School of the University of Florida  
in Partial Fulfillment of the Requirements for the Degree of Doctor of Philosophy

**A STUDY OF ALUMINUM-GERMANIUM-NICKEL OHMIC CONTACT  
METALLURGICAL EFFECTS AT THE GALLIUM ARSENIDE INTERFACE**

By

William V. Lampert

August 1992

Chairman: Paul H. Holloway

Major Department: Materials Science and Engineering

Electrical and metallurgical properties of layered thin film Al-Ge-Ni ohmic contacts to GaAs have been studied with current-voltage (I-V) measurements, Auger electron spectroscopy, and X-ray diffraction. The objective of this study was to identify the interfacial reactions which took place upon heating. These data were correlated with elemental profiles and alloy formation to rationalize models of formation of ohmic contacts.

I-V data collected by a transmission line method demonstrate dramatic differences existed in the time and temperature required to convert Al-Ge-Ni on GaAs to ohmic behavior. For samples with Ge adjacent to heavily doped GaAs (Si,  $\sim 1 \times 10^{18} \text{ cm}^{-3}$ ), heat treatments of 500° C and 425° C required times up to 9 and 20 minutes, respectively, for conversion to ohmic behavior. Similarly, for low doped substrates (Si,  $\sim 5 \times 10^{16} \text{ cm}^{-3}$ ) heat treatment at 500° C required 42 minutes, while for heat treatment at 425° C the conversion was not complete after 100 minutes. These data show the time required to convert to ohmic behavior varied inversely with doping concentration and directly with temperature. For samples with the Ni layer at the

interface of both heavily and low doped GaAs, the time required to convert was 2 to 3 minutes for either 500° C or 425° C. Thus, conversion to ohmic behavior was much less dependent on doping concentration or temperature with Ni adjacent to GaAs.

Simultaneous with the transition to ohmic behavior, Auger electron spectroscopy and X-ray diffraction show that interdiffusion took place across the metal-semiconductor interface and between metal layers. Neither Ga nor As were found in the Al overlayer, while Ni diffused into the Al and Ge layers and formed both solid solutions and intermetallic phases (e.g. Al<sub>3</sub>Ni, GeNi, and Ge<sub>3</sub>Ni<sub>5</sub>). However, Ga and As did alloy with Ni to form phases such as Ni<sub>4</sub>GaGe<sub>2</sub>, NiAs, Ni<sub>5</sub>As<sub>2</sub>, NiAs(Ge), and Ni<sub>2</sub>Ga<sub>3</sub>. Only limited phase formation was found between Ge and Al. As a result, the Ni-Ge, Ni-GaAs and Ge-GaAs reactions control the ohmic contact formation. Formation of Ni-GaAs compounds followed by degenerative doping of the substrate by Ge best explain the change from rectifying to ohmic contacts.

## CHAPTER 1 INTRODUCTION

The desire to have faster electronic components that were capable of operating at higher temperatures precipitated this study of Al-based ohmic contacts for the III-V semiconductor GaAs. Zuleeg et al.<sup>1,2</sup> originally proposed the use of the Al-Ge-Ni ohmic contact system for n-type GaAs because of its potential to operate at higher temperature and be more radiation hard as compared to the more commonly used Au-Ge-Ni ohmic contact system. GaAs was of interest because, in comparison with Si, it has higher electron mobility, greater radiation hardness, can operate at higher temperature, uses less power, absorbs sunlight more efficiently and can alloy with additional elements to form materials with continuously variable properties. Possibly most important, GaAs is a direct bandgap semiconductor and therefore efficiently converts electrical power to light. Thus the opportunity for integration of opto-electronic devices with electrical integrated circuits exists for GaAs.

All semiconductor devices require contacts to communicate with the outside world. Metal/semiconductor contact literature dates back to at least 1874, when Braun<sup>3</sup> published a paper on the asymmetric relationship of electrical conduction between metals and semiconductors. In 1938 Schottky<sup>4</sup> and Mott<sup>5</sup> independently published the first acceptable model of metal-semiconductor contacts, explaining the mechanism of barrier formation based on the barrier height which depended on both the work function of the metal and the electron affinity of the semiconductor. According to their model, a contact metal whose work function is less than the electron affinity of the n-type semiconductor should exhibit ohmic properties. The model works reasonably well for semiconductors such as Si; however, experimental evidence shows this is not the case for most

circumstances with a low work function metal on n-type GaAs. A model, proposed by Bardeen<sup>6</sup> in 1947, attributes deviations from the model of Schottky and Mott to a large density of surface states. These states are distributed in the forbidden energy gap between the conduction band and the valance band energy levels, and can trap both electrons and holes near the surface. For an n-type crystal these states will trap electrons, producing a negative charge on the surface that shifts the valence and conduction band edges up in energy relative to the bulk semiconductor. To maintain electronic charge balance these electronic defects near the surface of GaAs pin the Fermi level over a rather narrow energy range at the middle of the bandgap, which renders the Schottky relationship invalid. According to Bardeen's model, this problem will develop when the population of surface states is large ( $>10^{13} \text{ cm}^{-2}$ ). A number of explanations advanced more recently have described the origin of the surface states and resultant Fermi level pinning.<sup>7-10</sup> These models were based on either atomic rearrangements near the metal-semiconductor interface, or on redistribution of valence electron charge density at this interface. The unified defect model,<sup>7</sup> chemical reactivity model,<sup>8</sup> and effective work function model<sup>9</sup> are examples of explanations for the Fermi level pinning. Derivations of these models were based on data from metals deposited on vacuum cleaved (110) GaAs and air exposed (100) GaAs. The existence of the Fermi level pinning was important for this study; however, the exact cause of its formation was not critical to the formation of ohmic contacts.

Under ideal circumstances, the current carrying capacity of an ohmic contact obeys Ohm's Law; that is, the current flow between the metal and the semiconductor is linearly proportional to the voltage under both positive and negative biases. Practically, an ohmic contact is defined as a metal-semiconductor contact that has a negligible contact resistance relative to the bulk or spreading resistance of the semiconductor. An ohmic contact will supply the current with a sufficiently small voltage drop such that the device will perform properly.<sup>11</sup> Various metals and metal alloy systems were used as ohmic

contacts to GaAs over the years. Alloyed contacts generally form a phase which melts at low temperature and a dopant for the type of GaAs of interest (n or p type). For a typical process the metals were deposited onto the GaAs substrate and heated above a eutectic temperature. A portion of the GaAs dissociates and mixes with the alloy, resulting in a degenerative doped layer of GaAs beneath the contact because of dopant incorporation during GaAs regrowth. Charge is transported across the interface by a combined thermionic and field emission conducting mechanism.<sup>11</sup>

There is an incredibly large body of literature discussing the many aspects of ohmic contacts to GaAs. There have also been many different types of ohmic contact metallizations developed for GaAs. For a comprehensive review of this literature before 1984 see the articles of Rideout<sup>12</sup> and Piotrowska et al.<sup>13</sup> For more recent reviews see the articles of Sands,<sup>14</sup> Murakami,<sup>15</sup> and Piotrowska and Kaminska<sup>16</sup> as well as the reference books and book chapters of Williams,<sup>17</sup> Sharma,<sup>18</sup> and Robinson.<sup>19</sup> In this dissertation, the literature on Au-Ge-Ni and Al-Ge-Ni ohmic contacts will be reviewed in detail. The rest of the ohmic contact systems will be referenced only as they specifically apply to the present study.

As stated earlier, Zuleeg et al.<sup>1,2</sup> originally proposed the use of an Al-Ge-Ni contact system as a substitute for the Au/Ge/Ni contact system, predicting that the Al-based metallization would provide higher radiation tolerance and improved thermal stability for higher temperature applications. This contact system has been investigated much less than the Au-Ge-Ni contact system.<sup>20-23</sup> However, the initial ohmic contact properties were promising both due to the potential for higher temperature applications and to the uniformity of the metal-semiconductor interface. The existing literature suggests that the metallurgy of Al-Ge-Ni ohmic contacts differs from Au-Ge-Ni ohmic contacts. However, the relationship between ohmic behavior and microstructure of the Al/Ge/Ni/GaAs ohmic contact as a function of thermal processing is unknown. The

objective of this dissertation was to study the interfacial reactions between the Al-Ge-Ni metallization and the surface of clean GaAs, then to correlate this information with phase diagram data to rationalize alloy formation and elemental profiles. These data were then used to study any correlation between phase formation and ohmic behavior. A model to explain these observations based upon a decomposition and regrowth mechanism will then be postulated. The variables studied were the component sequencing, layer thickness and thermal processing of the Al, Ge, and Ni thin films to determine their effects on elemental distributions and phase formations after the conversion from Schottky to ohmic behavior. The data show that the layer sequence of Ni versus Ge adjacent to GaAs dramatically affects the kinetics of the reactions between the metals and semiconductor. While the sequence of metals has been shown to affect the quality of ohmic contacts in some other systems, it has not previously been reported to affect the reaction rates which control the conversion from Schottky to ohmic behavior. Electrical measurements will be presented which show the dramatic effect upon kinetics of first depositing Ni at the metal/semiconductor interface.

In Chapter 2, Review of the Literature, the general ohmic contact literature and the Au-Ge-Ni contact system are reviewed first. Also included is a detailed review of the Al-Ge-Ni contact system, literature which describes ohmic contact formation by a decomposition and regrowth mechanism, and phase diagram literature related to ohmic contacts. In Chapter 3, Experimental Procedures, sample preparation, sample deposition, and thermal processing methodology are described. Details of the analytical procedures are also included in this chapter. In Chapter 4, Experimental Results, changes in electrical properties are reported in the first section. Interdiffusion of Al, Ge, Ni, and the GaAs substrate was studied by Auger electron spectroscopy as reported in the section entitled Elemental Depth Profiles. The effects of interdiffusion on formation of both solid solutions and intermetallic phases are reported in the third section, Phase Formation in Al-Ge-Ni Thin Films. These results are then discussed in Chapter 5,

Discussion, and a model to explain the observations is postulated. Finally, conclusions regarding the effects of metal layer sequence, temperature, time and dopant level upon formation of ohmic contacts between Al-Ge-Ni and GaAs are summarized in Chapter 6.

## CHAPTER 2 REVIEW OF LITERATURE

Various metals and metal alloy systems have been used as ohmic contacts to GaAs over the years. An alloyed contact generally contained a low melting phase and a dopant for the GaAs. The alloy was deposited onto the GaAs substrate and then heated until a portion of the GaAs dissociated and mixed with the alloy resulting in a degenerative doped layer of GaAs beneath the metal contact. Charge is transported between the metal and semiconductor by a combined thermionic and field emission conducting mechanism. While the exact mechanism responsible for the degenerative doped surface layer is still controversial, there is no doubt that the contact resistance can be made low enough ( $\sim 10^{-7} \Omega\text{-cm}^2$ ) to be functional in nearly all applications.

### Au/Ge/Ni Ohmic Contacts to GaAs

The most commonly used metal alloy system for ohmic contacts to n-type GaAs is the Au-Ge-Ni metallization introduced by Braslau et al.<sup>24</sup> They were in search of contacts which would provide low linear series resistance, were noninjecting in the presence of high applied fields, could be manufactured and processed in a uniform and reproducible manner, could form patterns of controllable size and shape, and would be adaptable to batch fabrication. These contacts were intended for use instead of the common contacts of the day: Sn, In, Au, Ag, as well as alloys of Sn-Ni, Ni-In, and Au-In. Tin had been widely used as an alloyed contact for GaAs, but the large contact angle of liquid Sn on GaAs causes it to form into islands on the GaAs surface which, unless

constrained, causes nonuniform morphology. Sn also has a tendency to form conducting channels in the semiconductor when subjected to high electrical fields, and the electrical properties depend rather critically on the alloying temperature.<sup>25</sup> This led Braslau et al.<sup>24</sup> to search for a system not involving Sn. They found that Au and Ge, evaporated from a eutectic composition, could form ohmic contacts to n-type GaAs. However, like Sn, the deposition from the Au-Ge eutectic also formed minute droplets on the GaAs surface. Even though good wetting was attained at the higher temperature at which alloying took place, the resulting film had an island structure similar to Sn. Braslau et al.<sup>24</sup> resolved this problem by adding a small amount of Ni (2-11 % by weight) to their eutectic Au-Ge evaporant. Though these films were evaporated from a single mixture, they did not evaporate congruently, which resulted in a layered structure. During heat treatment above the eutectic temperature the Au and Ge recombined, while the Ni layer remained intact owing to its low solubility in Au-Ge at this temperature. Braslau et al.<sup>24</sup> speculated that the presence of the solid Ni overlayer held the Au-Ge melt in intimate contact with the substrate at the alloying temperature, resulting in the contact being uniform over the surface of the semiconductor after solidification.

To be useful a metallization must form an ohmic contact over a broad range of doping concentrations in the contact layer of the GaAs. The Au-Ge-Ni contact system has worked over a wide range of doping concentrations from lightly doped Gunn oscillators to degenerative doped injection lasers.<sup>26</sup> Owing to its practical importance, a substantial body of literature exists concerning formation and characterization of the Au-Ge-Ni contact system by various processing and analysis techniques. As stated earlier, there are a number of review papers as well as the reference books and book chapters describing ohmic contacts to GaAs.<sup>12-19</sup> The Au-Ge-Ni contact system is thought to behave according to the general model for an ohmic contact to GaAs as described above. Au-Ge forms a low melting eutectic and Ge is a dopant for the GaAs. The effects of Ni are still controversial. Ni causes a portion of the GaAs to dissociate with in-diffusion of

the Ge resulting in a degeneratively doped layer of GaAs beneath the metal contact according to one model.<sup>27, 28</sup> An alternative model suggests a regrowth mechanism of the highly doped layer during cool down or heat treatment rather than the diffusion mechanism.<sup>29-35</sup> The regrowth mechanism will be discussed later in more detail.

To develop a better understanding of the Al-Ge-Ni contact system, an understanding of the materials and processing of the Au-Ge-Ni contact system is useful. Therefore, a more detailed description of the effect of each of the components and their interrelationships on the complete metal and semiconductor contact system follows. The well-known high concentration of surface states, present under ordinary processing of GaAs, pins the Fermi level near midgap. Deposition of most metals onto a cleaned n-type GaAs surface results in a Schottky contact with a barrier height of ~0.8 eV. To lower the contact resistance, it is necessary either to reduce the barrier height to allow greater electron transport by thermionic emission or to increase the doping concentration so that the electron transport by thermionic emission is enhanced by field emission (tunneling). As stated earlier, Ge is believed to degenerative dope the GaAs so that the contact conducts through the combination thermal activation assisted tunneling mechanism. However, Ge is amphoteric in GaAs. Andrews and Holonyak<sup>36</sup> reported that bulk Ge-doped GaAs grown from a Ga rich solution is p-type, while bulk Ge-doped GaAs grown under conditions of exact stoichiometry or excess As is n-type. Evidence that Ge formed a degenerative doped n<sup>+</sup> layer was provided by Anderson et al.<sup>27</sup> and later confirmed by Heiblum et al.<sup>37</sup> Anderson et al. deposited the Ge and Ni onto a p-type Zn doped GaAs substrate and produced a pn junction with Ni and Ni-Ge contacts. The pn junction indicated that Ge in-diffused to compensate the p-type substrate.

There are several opinions as to whether Ge could diffuse into GaAs to accomplish this fact. According to Aina et al.<sup>38, 39</sup> Ge is a substitutional diffuser with diffusion properties similar to other substitutional diffusers such as Te, S, and Sn. Auger depth profiles were used to show the Ge diffused from the metallization toward the

metal-semiconductor interface.<sup>40</sup> Ge penetrates the GaAs by way of a Ga vacancy dependent diffusion model according to Gupta and Khokle.<sup>41</sup> Dell et al.<sup>42</sup> showed that a critical amount of Ge was required for the Au-Ge-Ni metallization to convert to ohmic behavior by varying the total amount of each of the metals deposited while maintaining the overall ratio. The resistance increased dramatically when the total amount of metal was less than 600Å. They used a single source of Au-Ge eutectic with ~5 % Ni. They concluded a sufficient amount of Ge was needed to produce the tunneling. Robinson suggested the formation of an n<sup>+</sup> layer resulted from Ge penetration of the dissociating GaAs.<sup>40</sup> He further concluded that Ge replaced the Ga to dope the GaAs. The role of Ge was reported to be involved in the dissociation of GaAs as well as serving as the n<sup>+</sup> dopant to GaAs by Iliadis and Singer.<sup>43</sup> However, Anderson et al.<sup>27</sup> found that even Ge layers grown by liquid phase epitaxy did not significantly penetrate the GaAs without the presence of a Ni overlayer. Ge combined with the Ni as long as the amount of Ni was sufficient to consume the Ge. If so, the contact remained uniform; however, if the ratio of Ge was greater than Ni, the contact layer became laterally nonuniform.<sup>44</sup> Thus the ratio of Ge to the other materials was important. Excess Ge caused out diffusion and precipitation on the surface during heat treatment.<sup>28, 44-46</sup> Crouch et al. reported a dendritic growth of 1 to 1 Ge to Au precipitated on the surface of Au-Ge contacts heat treated by rapid thermal annealing (RTA).<sup>45</sup>

As stated earlier, Braslau et al. originally concluded the Ni only served to cap the eutectic Au-Ge melt and to hold the Au-Ge in place during solidification and prevent it from balling up due to surface energy.<sup>24</sup> It was later reported that Ni aided the wetting rather than serving as a cap to hold the Au-Ge in place.<sup>40, 47</sup> The Auger depth profiles of Robinson indicated that Ni also diffused to the metal-semiconductor interface during heat treatment. For samples heat treated below the eutectic temperature of the Au-Ge, Ni was also found to diffuse rapidly through the separated Au and Ge layers to the GaAs interface.<sup>40</sup> His results demonstrated GaAs decomposition and interdiffusion of Ni, Au,

and Ge during alloying. Ogawa found Ni to be a very fast diffuser in both the contacts and in GaAs.<sup>28, 48</sup> He further suggested that Ni also served to catalyze the reaction between Au and the GaAs. Auger depth profiles were used to show out-diffusion of the Ga and As. Ni and As Auger depth profile peak overlap was used to infer formation of a NiAs phase or at least the formation of Ni and As grains.<sup>28, 40, 49</sup> They suggested that the Ni increased the solubility of GaAs and enhanced the in-diffusion of Ge so that Ge sat on substitutional Ga sites and created the n<sup>+</sup> layer. Ogawa<sup>28</sup> also reported X-ray diffraction results which indicated that the NiAs was textured during the early stages of heat treatment and that it incorporated Ge during the high temperature stage of the heat treatment. He made a case for shorter heat treatment times at higher temperatures (e. g. 500° C), to avoid the deeper penetration of the contact metals such as Ni into the GaAs substrate. Later Ogawa studied only the Ni-GaAs reaction and identified the ternary Ni<sub>2</sub>GaAs.<sup>48</sup> The Ni<sub>2</sub>GaAs formed at ~200° C, but decomposed to NiGa and NiAs above 400°C. Similar observations of a ternary phase decomposition for the Ni-GaAs system were made by others.<sup>50-53</sup> The depth of penetration by the various Au-Ge-Ni components has been reported to be from 1000Å to 3000Å using analytical techniques such as Rutherford Backscattering, RBS, SIMS, backside SIMS, and transmission electron microscopy (TEM).<sup>50, 51, 54-55</sup> The ratio of Ni to the other materials was also reported to be important. For example, Patrick et al.<sup>56</sup> found that the heat treating temperature required for forming low resistance contacts was lower when the ratio of 5% Ni to Au-Ge was maintained. As stated above, excess Ni has led to excessive out-diffusion of Ga, leaving excess Ga vacancies and too little Ge to fill these donor sites.

The noble metal gold was the part of the metallization to which the outside connections were made. The eutectic of Au and Ge provided a lower melting alloy for lower temperature heat treatment of the ohmic contact metallization. The Au-Ge eutectic composition evaporates upon deposition into the two terminal phases. The Auger depth profiles indicated a separate though overlapping layered structure in the as-deposited

contacts.<sup>28, 40, 45, 49</sup> Au was found to diffuse to the metal-semiconductor interface and react with the GaAs during heat treatment. Au is a fast interstitial diffuser ( $D_0=10^{-3}$  cm<sup>2</sup>/sec,  $E_a=1.2\text{eV}$ ) in GaAs.<sup>39</sup> Liliental et al. showed Au rich protrusions into the GaAs.<sup>57</sup> At a temperature of 300° C, Au began to react with the GaAs.<sup>28</sup> Whether the heat treatment was above or below the eutectic temperature, GaAs dissociated until one component reached its saturation limit in the metal layer.<sup>26</sup> Dissociation and out-diffusion of Ga and As had been observed for Au-Ge contacts.<sup>43, 58</sup> Similar results were reported for the Au-Ge-Ni contacts.<sup>26, 28, 40, 49, 58</sup> The Ga out-diffusion was by way of grain boundary diffusion according to Gupta and Khokle.<sup>41</sup> The studies of Kulkarni and Lai<sup>59</sup> also supported a grain boundary diffusion mechanism. A significant dissociation of the GaAs at the interface and Ga out-diffusion allowed Ga accumulation at the surface. Robinson characterized the Ga out-diffusion as having a low activation energy.<sup>40</sup> As in the case of excess Ni, excess Au also led to more out-diffusion of Ga which caused greater decomposition of the interface; if too little Ge was present, the Au or Ni might compensate as p-type dopants.<sup>26, 58</sup> Auger studies showed in-diffusion of Au and Ni and out-diffusion of Ga, which was correlated with a decrease in resistivity during aging.<sup>58</sup> Auger studies also showed that the solid phase reactions were not complete at the lower temperatures and continued with time and electrical stress, leading to long-term degradation to the contact resistance.<sup>60</sup> Braslau<sup>60</sup> also stated that the 500° C thermal cycle with short alloying times at temperature led to better aging results. That is, contacts reached their lowest contact resistance for high temperature heat treatment, especially for short times.<sup>26, 45</sup> Robinson suggested this was due to Ge penetration of the dissociating GaAs when the Au-Ge melted and led to an n<sup>+</sup> layer and ohmic behavior.<sup>40</sup> He further stated that this was made possible by the out diffusion of the Ga allowing the formation of Ge doped, As rich GaAs at the interface. The out-diffusing Ga and in-diffusing Au formed a Ga-Au layer at the surface. The Au and Ga formed a  $\beta$ -AuGa phase at heat treatment temperatures below approximately 550° C and an  $\alpha$ -AuGa

phase at heat treatment temperatures above approximately 600° C.<sup>61, 62</sup> The  $\beta$ -AuGa phase, with a hexagonal crystal structure, was stable above 275° C and ranged in composition between about 26.5 and 29.2 at.% Ga.<sup>63</sup> The  $\alpha$ -AuGa phase was an Au-rich boundary solid solution with Au composition up to 12.5 at. % at 455° C.<sup>59</sup> The spatial distributions of these constituents of the contact were related to the electrical properties. Ni and As rich grains at the metal-semiconductor interface have been correlated with lower resistivity, while resistance degradation was correlated with  $\beta$ -AuGa and/or  $\alpha$ -AuGa phases at the metal-semiconductor interface.<sup>49, 61, 62</sup>

Since the Au-Ge eutectic source materials did not deposit congruently, there were studies using separate evaporation of the components as well as studies varying the deposition sequence and both of which showed that these variations had little or no effect on the resistivity of the ohmic contacts.<sup>28, 40, 45, 49, 64</sup> For example, Robinson grew contacts with Ni at the metal-semiconductor interface.<sup>40</sup> He suggested that the order of deposition and whether the Au and Ge were evaporated separately, co-evaporated, or evaporated from a eutectic did not affect the ohmic contact. Thus it was suggested that the sequence of deposition had little effect on the contact. The sequence of evaporation did not seem to matter to the final arrangement of constituents after heat treatment.<sup>38, 37, 40, 45, 47, 49, 64</sup> The elemental Auger depth profile distributions at the metal-semiconductor interface were very similar after the metallization becomes ohmic and similar Ni-Ge-As phases were present as determined by X-ray diffraction, XRD.<sup>28</sup> Likewise, Kuan<sup>65</sup> used TEM and EDS to show that the as-deposited samples were not completely intermixed, but that a portion of the Ge separated from the Au even when the metals were co-evaporated. The lowest resistivity was achieved for a heat treatment of 410° C for 115 sec and he correlated the phase formation of Ni<sub>2</sub>GeAs with lower resistance. Initially NiAs and NiGe formed, and the Ni<sub>2</sub>GeAs was said to have formed from these two phases. This phase was also identified by Lahav and Eizenberg<sup>50, 51</sup> using Auger and XRD, and by Chen et al.<sup>53</sup> using TEM to study lateral diffusion

samples. It should be pointed out that selected area diffraction, SAD, patterns are very similar for Ni<sub>2</sub>GeAs and NiAs. Prolonged heat treatment caused a decrease in the amount of Ni<sub>2</sub>GeAs and an increase of both the resistivity and the amount of Au at the GaAs interface.

Contrary to the above conclusion about layer sequence, several authors have reported the sequencing arrangement of the components did affect the resistivity of the contacts.<sup>37, 47, 61, 62</sup> Heiblum et al. deposited 50 Å of Ni first and found a correlation with lower resistance and smaller, dense clusters of NiGe.<sup>37</sup> They proposed a high resistance layer formed under the metal transmission line measurement (TLM), lines. The sequencing also was found to affect the amount of the Ni<sub>2</sub>AsGe formed.<sup>66</sup> Ni at the metal-semiconductor interface was also credited with initially acting as a sink for Ge. Then during heat treatment, NiGe was a source of Ge and a diffusion barrier against too great of out-diffusion of Ga and As.<sup>66, 67</sup> Both Murakami et al. and Shih et al. have reported that the sequencing of the materials does affect the contact resistance.<sup>61, 62</sup> They varied the sequence of the metallization and the amount of Ni at the metal-semiconductor interface and found that 50 Å of Ni at the interface caused the onset of ohmic behavior at lower temperature and that the spread in the measured resistance versus temperature was also reduced. This behavior was correlated with the formation of a NiAs(Ge) phase similar to that identified by Kuan et al.<sup>64</sup> However, based on Auger depth profiles, Murakami et al. suggested that the phase was not Ni<sub>2</sub>GeAs but rather was a NiAs phase with a small amount of Ge.<sup>61</sup> The diffraction patterns for these two phases are similar. Liliental et al.<sup>57</sup> found a Ni-Ge-As phase but the convergent beam electron diffraction pattern, CBED, was not that of Ni<sub>2</sub>AsGe. This was in disagreement with the results of Kuan et al.<sup>64</sup>

In summary, it is generally accepted that Ge dopes the GaAs when aided by the presence of Ni in the Au-Ge-Ni metallization. Ni wets the substrate surface to prevent the irregular contact surface morphology due to Au-Ge balling up. Au provides the

material to which the outside leads are attached and forms Au-Ga phases. The contact interface morphology is very rough, with deep penetration of Au and Ni. Ni and Ge diffuse to the metal-semiconductor interface and combine with As to form compounds which appear to be necessary to produce a low resistivity ohmic contacts. Important compounds have been identified as either  $\text{Ni}_2\text{AsGe}$  or  $\text{NiAs}$  with some Ge ( $\text{NiAs}(\text{Ge})$ ). Au and Ga formed compounds, such as  $\beta$ -AuGa and/or  $\alpha$ -AuGa which were postulated to create the vacancies necessary to allow doping by Ge. The compounds also contributed to the degradation of the ohmic contact when they diffused to the metal-semiconductor interface. The recommended heat treatment process was for temperatures near 500° C and for short periods of time. Contrary to earlier literature, the more recent literature indicates that the sequence of the materials does influence both the final resistivity and the scatter in the resistivity data. There is disagreement over the mechanism by which the heavily doped layer of  $\text{GaAs}(\text{Ge})$  is formed. However, the disagreement is best illustrated by data from other ohmic contact metallization systems, as will be discussed in the next section.

As stated earlier, the Au-Ge-Ni ohmic contact literature is not without disagreements and controversy. Some of this is probably due to the dependence of the quality of contacts on metal and semiconductor starting materials, and on processing procedures for substrate preparation, metal deposition, and sample heat treatment. In many of the papers the substrate cleaning procedures and the contact doping concentration levels or type were not reported. The absence of this information frequently makes comparisons difficult. The same concerns exist when comparing the Au-Ge-Ni ohmic contact literature with the Al-Ge-Ni ohmic contact literature. However, the vast amount of work on the Au-Ge-Ni ohmic contact system provides a great background for the subject of this study, the Al-Ge-Ni contact system, when care is taken and an effort is made to understand the inherent differences.

Other Metals and GaAs

The Au-Ge-Ni literature can be used to explain many of the results observed in this study. However, there were a number of observations made in other metal systems which more adequately describe the mechanism believed to cause the conversion to ohmic behavior in this study. Several of these other metal ohmic contact systems and theoretical and experimental studies of single metal-GaAs or ternary systems are discussed below. A number of papers have suggested an alternative mechanism to Ge diffusion to explain the formation of ohmic contacts. For example, a series of papers on Pd containing contacts have reported evidence of Pd<sub>4</sub>GaAs ternary formation at low temperatures that resulted in regrowth of a heavily doped GaAs layer after higher temperature heat treatment.<sup>31-34</sup> It was proposed that if a thin, highly doped GaAs layer was formed during ohmic contact formation, it could have resulted either from diffusion of a dopant into the GaAs or from solid phase regrowth of GaAs incorporating the dopant.<sup>34</sup> A regrowth mechanism has been used to explain the behavior of Pd-Ge and Pd-Si metallizations deposited onto GaAs. Both contact metallizations have shown conversion to ohmic contacts began with a limited low temperature (~100° C) reaction to form and decompose the ternary Pd<sub>4</sub>GaAs at the metal/GaAs interface. The thickness of the GaAs reacting with the Pd was uniform and estimated to be 60-150Å.<sup>31</sup> Ge/Pd/GaAs contacts have been shown to be rectifying at this stage, 100-225° C, and a correlation between the onset of ohmic behavior and heat treatment between 225 and 250° C has been reported.<sup>33</sup> However, RBS spectra before and after the onset of ohmic behavior were nearly identical.<sup>33</sup> Subsequent reaction at higher temperatures (~325° C) between the Ge overlayer and the intermediate Pd<sub>4</sub>GaAs phase resulted in formation of PdGe phases and decomposition of the Pd<sub>4</sub>GaAs phase and the epitaxial regrowth of a Ge doped n<sup>+</sup>-GaAs surface layer, GaAs(Ge).<sup>34</sup> It was suggested that any excess Ge (beyond PdGe) migrated across the PdGe layer and was regrown epitaxially on the GaAs substrate.<sup>33</sup>

The Si-Pd system behaved in an analogous manner, but without a Si epi-layer at the metal/semiconductor interface.<sup>31, 32</sup> Enhanced probability of electron tunneling through the n<sup>+</sup> regrown GaAs layer was proposed as the primary reason for ohmic behavior.<sup>31-34</sup> A secondary reason suggested for the Ge-Pd system was the small conduction band discontinuity between the epitaxial Ge layer and the GaAs substrate.<sup>31, 32</sup>

Holloway et al.<sup>29</sup> demonstrated that pure Au contacts on GaAs converted to ohmic behavior as the result of segregation of Si dopant in areas where GaAs had decomposed by reacting with the Au overlayer. SIMS data were used to show segregation of Si from the metal solid solution to the GaAs surface. Ohmic behavior of Au-Ge-Ni contacts can also be induced by regrowth of GaAs and dopant incorporation as shown by Li et al.<sup>68</sup>

The Ni-GaAs system has also been experimentally treated by several authors. Using TEM, electron diffraction, EDS, and RBS, Sands et al.<sup>52</sup> identified the first phase formed during heat treatment to 480°C to be Ni<sub>x</sub>GaAs, where x is ~3. They reported Ni reacts with GaAs during deposition or during TEM sample prep to form a thin layer of Ni<sub>x</sub>GaAs under the native oxide. Equally important, Sands et al.<sup>52</sup> noted the ability of Ni to penetrate thin native oxides to react with the GaAs in this study. The Ni<sub>x</sub>GaAs was formed during their 220° C heat treatment and decomposed about 400° C to NiGa and NiAs. Sand et al. also demonstrated that regrowth of GaAs occurred when the Ni<sub>x</sub>GaAs phase decomposed.<sup>35</sup>

Recently several authors have attempted to use multidimensional phase diagrams to better understand existing ohmic contact literature and to use the basic thermodynamic principles to explain metallization processing problems. For example, Tsai and Williams<sup>69</sup> concluded that Au and GaAs will not react unless gas phase As species were allowed to form. In an open system, if As sublimes or crystallizes, pseudobinary phases between several intermetallic Au-Ga phases can form from reactions between Au and GaAs. Because the solubility of Ga in Au decreases to near zero at room temperature

GaAs should regrow in all instances during cool down. Instead Au-Ga phases are observed because the As vapor was not given enough time to diffuse back into the solid during cool down.<sup>69</sup> However, utilizing phase diagrams rather than trial and error experimental methods to determine phases formed may be more useful for ternary systems than for the larger multicomponent systems. The number of possible reactions and the number of stable or metastable phases are large in the ternary systems, but much larger in the multicomponent systems of most ohmic contact systems. Therefore, predictions quickly become much more difficult without understanding of the thermodynamics and phase relations.

Beyers et al.<sup>70</sup> and Schmid-Fetzer<sup>71</sup> have calculated ternary phase diagrams for a number of metal-semiconductor systems. Beyers et al.<sup>70</sup> proposed a classification scheme for phase equilibria in seven generic elemental metal-GaAs systems. Their purpose was to describe how phase diagrams can provide a framework for interpreting previous results and for identifying suitable materials for stable contacts. They compared one of their generic ternary phase diagrams to that of Ni and the ternary Ni-Ga-As phases identified by Ogawa,<sup>28</sup> Sands et al.,<sup>35, 52</sup> and Lahav and Eizenberg.<sup>50, 51</sup> Because of uncertainty between bulk versus thin film results, they indicate that either the ternary Ni<sub>2</sub>GaAs is a metastable intermediate phase or a low temperature phase with tie lines to GaAs. Later Schmid-Fetzer<sup>71</sup> calculated the ternary phase diagrams for 19 different metal-GaAs systems using bulk thermodynamic data and an approximation suggested by a personal communication with Y.A. Chang. Schmid-Fetzer also pointed out the difficulties arising from inferring phase diagrams from thin film experiments. For metal-GaAs, the identification of phases in thin films is more ambiguous due to As loss during vacuum processing. More seriously, the limited amount of metal may exclude the occurrence of certain phases, thus turning the film thickness into another degree of freedom.

Guivarc'h et al. studied the solid portion of the bulk Ni-Ga-As ternary phase diagram.<sup>72</sup> Their samples were prepared in closed, small volume containers to prevent formation of gas phase products. They used XRD of powders and single crystals to determine that neither Ni nor any of 4 possible ternary phases were in thermodynamic equilibrium with GaAs below ~800° C. They showed instead binaries of NiGa, Ni<sub>2</sub>Ga<sub>3</sub>, and NiAs were in thermodynamic equilibrium at lower temperatures. However, cooling from above 800° C, several Ni rich phases, including ternary phase compositions in regions of 3 or 2 phase equilibria, likely preceded the formation of the final equilibrium products. Based on their results NiGa and NiAs phases would be expected, as seen by others, after 400° to 500° C heat treatment for sufficiently long times.<sup>28, 35, 50-52</sup> In a second paper Guivarc'h and Guerin conducted a similar study on molecular beam epitaxy (MBE) grown Ni thin films on (100) and (111) GaAs.<sup>73</sup> These films were grown simultaneously in the MBE system by indium bonding different substrates to a Mo sample holder. After heat treating the samples for 1 hour at temperatures from 200° C to 600° C, a series of ternary phases was formed. However, at the 600° C heat treatment, the binary phases of NiGa and NiAs again formed along with a ternary of Ni<sub>3</sub>Ga<sub>1.5</sub>As<sub>0.5</sub>.

Care must be taken when referring to the above calculated phase diagrams. Some of the conclusions were inferred from chemical ratios rather than from diffraction experiments. Most of the phases identified by Guivarc'h and Guerin<sup>72, 73</sup> were based on a single 001 X-ray diffraction line due to the epitaxial nature of their MBE films. As they pointed out, there were inherent differences in studies of bulk materials grown in a closed environment and thin film studies carried out in a vacuum or another open system. It must also be remembered that interdiffusion can and will take place without formation of new phases. In addition, phase formation in thin films is often determined by kinetics rather than thermodynamics. Nucleation and growth, diffusion, and short circuit diffusion paths through intervening layers are just a few of the likely examples of

important kinetic effects. In spite of these cautions, the phase diagrams can be used as guides to determine likely paths for a reaction to proceed. At the very least, thermodynamics will determine the reaction direction and the final equilibrium position of the phases, given enough time at temperature.

The previous sections on Au-Ge-Ni and other metals reviewed the general literature required to better understand the Al-Ge-Ni literature and the observations reported in this study. The final section of the Review of Literature will give an in-depth description of the Al-Ge-Ni ohmic contact system.

#### Background for Aluminum Based Ohmic Contacts to GaAs

As stated earlier, Zuleeg et al. originally proposed the use of an A-/Ge-Ni metallization system as an ohmic contact for n-type GaAs.<sup>1,2</sup> Zuleeg et al. predicted the Al based metallization would provide a number of benefits, as follows. It would have improved thermal stability and therefore reliability, especially in higher temperature applications since the eutectic temperature of Al-Ge (424°C) is higher than that of Au-Ge (356°C). Since Al has a lower atomic number than Au, it should have higher radiation tolerance. It could have lower interconnect resistance because evaporated Al has a lower interconnect resistance than sputtered Au. Better definition of fine patterns would be possible by dry etching as used for Al metallization on Si Very Large Scale Integrated, VLSI, circuitry. According to R. Zuleeg, the metallization should be ohmic for both n- and p-type GaAs. And finally, Al would be less expensive than Au.

The Al-Ge-Ni ohmic contacts studied by Zuleeg et al.<sup>1,2</sup> were prepared by separate evaporation in sequence of 400Å of Ge, 300Å of Ni, and 2000Å of Al onto Liquid Encapsulated Czochralski, LEC, semi-insulating GaAs substrates which were ion implanted with Si. The Si content was in the range of  $10^{17}$  to  $10^{18}$  cm<sup>-3</sup>. The ion implanted substrates were activated by RTA at 825°C prior to metallization. Samples

prepared with a TLM test structure were heat treated in a reducing atmosphere of hydrogen using a graphite strip heater at 500° C for 1 to 30 minutes. Contact resistance as low as  $1.4 \times 10^{-6} \Omega \cdot \text{cm}^2$  were observed. Zuleeg et al. also reported the successful fabrication of a set of 50 JFET (junction field-effect transistor) devices with this metallization as the first-level interconnect. They proposed the mechanism causing the metallization to become ohmic was similar to that commonly attributed to the Au-Ge system, i.e., heat treating above the eutectic temperature caused the Al-Ge to melt and the liquid state enhanced Ge diffusion into the GaAs. After solidification, this resulted in a metal alloy n<sup>+</sup> semiconductor contact. The Ni was added to prevent balling up of the Al-Ge similar the Au-Ge based contacts.<sup>24, 40</sup> The presence of Ni afforded good wetting properties of the molten Al-Ge and led to smooth surface texture and contact uniformity. Zuleeg et al. later reported that their specific contact resistance measurement versus doping concentration correlated with the theory for the field emission (tunneling) conduction mode ( $R_C \propto (N_D)^{-1/2}$ ), rather than the mixed mode conduction model ( $R_C \propto 1/N_D$ ) which fits the behavior of the Au based contacts.<sup>2</sup> They also reported less resistance degradation during thermal aging at 250° and 300° C for their Al-Ge-Ni versus Au-Ge-Ni ohmic contacts.

Liliental-Weber et al.<sup>20</sup> reported an investigation of the structure and composition of Al/Ge/Ni ohmic contacts by TEM, SIMS, and depth profiling with Auger electron spectroscopy. Two types of contacts (A and B) were examined in this study. Type A contacts, fabricated by Zuleeg, were similar to those mentioned above except the layer thickness of Ge and Ni was 300 Å each. The type A contacts were on ion implanted substrates. Liliental-Weber et al.<sup>20</sup> reported that Zuleeg had not previously been able to fabricate Al-Ge-Ni ohmic contacts on LEC substrates that were not ion implanted. These contacts were heat treated in a reducing atmosphere of hydrogen on a graphite strip heater at 500° C for 1 minute. The type B contacts were evaporated from Knudsen cells with Al<sub>2</sub>O<sub>3</sub> crucibles, using a different layering sequence, onto semi-insulating LEC GaAs

without an n-type contact layer. The type B LEC substrates received no chemical etching or cleaning prior to the deposition of the contact metallization. The metallization layering was 50Å of Ni on 1000Å of Al-30.3 at. % Ge, coevaporated at the eutectic ratio, followed by 300Å of Ni, and finally 500Å of Al. The type B contacts were heat treated at 500° C in forming gas for 3.5 minutes. These contacts were not characterized electrically since they were deposited on undoped GaAs. Both types of samples were prepared as TEM cross-section samples by gluing two pieces, with thin metal layers adjacent, using silver epoxy (the epoxy was cured by heating at 90° C for 30 minutes to allow hardening). Mechanical polishing was used to thin to ~50 µm, and then Ar<sup>+</sup> ion milling with a low energy ion gun and cold stage was used to make electron transparent samples.

After heat treating the A-type contacts at 500° C for ~ 1min the contact resistance was 1.4 X 10<sup>-6</sup> Ω·cm<sup>2</sup>. TEM analysis of the A-type metal layers, after heat treatment, showed an increase in thickness and their interface was more uniform than the as-deposited samples. Primarily Ni<sub>5</sub>Ge<sub>3</sub> and Al<sub>3</sub>Ni phases were found in contact with the GaAs. This indicated that the Ni and Ge layers were being dispersed during the heat treatment and that Al was diffusing toward the GaAs. A hexagonal ternary Al-Ni-Ge phase was identified as the top layer and the composition was tentatively determined to be Al<sub>3</sub>NiGe<sub>4</sub> based on elemental ratios from energy dispersive spectroscopy, EDS, of fluorescent X-rays. EDS also indicated that Ga and As diffused out into the contact, with ~15% more Ga than As. The Ga and As were believed to be in solid solution since no phases containing Ga or As were found in the TEM investigation, unless new ternary or quaternary phases containing Ga or As had formed with lattice structures and parameters close to that of Ni<sub>5</sub>Ge<sub>3</sub> or Al<sub>3</sub>Ni. SIMS data showed that the Ge penetrated the substrate. By comparison with EDS data, it was suggested that the Ge concentration was less than 1%, the detection limit for EDS. For type B samples after heat treatment, there was not an increase in metal layer thickness, but an amorphous metal/GaAs interfacial oxide layer

remained intact. The interface of these samples was very flat. A thin layer of Ge, 70Å-150Å thick, was just above the amorphous layer, and the next layer consisted of mostly Al with embedded Ni<sub>5</sub>Ge<sub>3</sub> and Al<sub>3</sub>Ni grains. Again, Ga and As were found to have diffused into the metal by both EDS and Auger depth profiling. In this case the Ga to As ratio was that of the bulk as determined by EDS. It was noted again that the oxide served as a reaction barrier for GaAs in the type B sample, and this was suggested to be due to the Ni layer at the interface. It was also suggested that the oxide may also prevent Ge diffusion into the GaAs. It was suggested that the type A contacts became ohmic due to the diffusion of Ge into the substrate and substitution on the Ga sites forming an n<sup>+</sup> layering in the GaAs. It was further suggested that lack of phase formation between Al and Ga or As was responsible for extra flat interfaces found in the Al/Ge/Ni ohmic contact metallization system.

Since the original efforts of Zuleeg and his various co-authors, only one other group has studied the Al/Ge/Ni ohmic contact system.<sup>21-23</sup> This group has written a series of papers detailing work with the deposition of Al/Ge/Ni contacts onto both n-type and p-type GaAs with objectives of understanding the contact system and optimizing its performance.<sup>21, 22</sup> Research was conducted to correlate the contact microstructure with electrical performance. Initially Al/Ge/Ni contacts were deposited onto bulk doped GaAs that were polished, degreased, and chemically etched prior to deposition of the layering sequence of Zuleeg et al.,<sup>1,2</sup> which was 400Å of Ge deposited first, followed by 300Å of Ni and then 2000Å of Al. The metals were deposited by electron beam evaporation through a shadow mask onto n-type (Si @ N<sub>D</sub>=10<sup>18</sup> cm<sup>-3</sup>) and p-type (Zn @ N<sub>A</sub>=10<sup>19</sup> cm<sup>-3</sup>) GaAs, then heat treated at 425°C in forming gas for 1 to 4 minutes. The mask arrangement allowed only qualitative determination of contact ohmicity. Later, in an attempt to study factors governing ohmic contact formation and to measure specific contact resistance as a function of contact layer deposition, additional samples were prepared using less heavily doped n-type GaAs substrates.<sup>23</sup>

In the as-deposited samples, although evaporated separately, the Ni and Ge layers were found by CBED and EDS to have alloyed to produce a layer (~600Å thick) consisting of a hexagonal Ni<sub>1.7</sub>Ge (Ni<sub>5</sub>Ge<sub>3</sub>) phase, unreacted Ge, and possibly other Ni-Ge phases as well. It should be pointed out that during sample preparation for TEM cross-sectioning, the temperature may increase to at least 100° C during the epoxy cure which could contribute to the diffusion of the as-deposited samples. The authors state that a temperature of 100° C was also expected due to the heat of condensation during metal deposition. Parallel electron energy loss spectroscopy (PEELS) showed that a thin (10Å-50Å) layer between the GaAs substrate and the Ni-Ge layer contained oxygen, presumably the native oxide on the GaAs surface which was not removed during surface preparation. Columnar Al grains were observed between the Ni-Ge layer and the ambient interface.

In the first paper, all the contacts were described as lustrous and uniform prior to heat treatment, but the contacts on p-type GaAs became matte in appearance while the contacts to n-type material remained largely lustrous after the 425° C heat treatment. All contacts deposited onto the heavily doped p-type GaAs became ohmic; however, on the heavily n-type GaAs contacts heat treated for 1-2 minutes remained rectifying while those heat treated for 3 and 4 minutes were ohmic as determined by the qualitative current-voltage (I-V) measurements. Following electrical characterization, planar and cross-sectional samples were prepared for TEM examination. Large microstructural differences between p-type and n-type samples were reported in the first paper. A thick amorphous layer with a web-like structure consisting of Al and Ni was found in the p-type ohmic contacts. EDS of this layer indicated a ratio of 6:1 for Al:Ni. Contrary to these results, in the second paper the microstructures were reported to be independent of the type of doping. For all samples, the contact/semiconductor interface was reported to be extremely flat at the atomic level, while the metal/ambient interfaces were nonuniform. Graham et al.<sup>21-23</sup> cautioned that the TEM results on the surface were thought to be

affected by the etching procedure used to remove the GaAs from the back of the contact and possibly could account for the discrepancy between the first and second reports. Using TEM and EDS, no Ge was found in the metal-semiconductor interface region of the heat treated specimens after they became ohmic. Instead the surface became decorated by a Ge rich growth. EDS identified this floret-like surface precipitate to be primarily Ge interspersed on a background of Al and Ni. Below this floret precipitant they found a nearly uniform continuous layer adjacent to the GaAs. The continuous layer at the interface was identified as mainly an orthorhombic  $\text{Al}_3\text{Ni}$  with excess unreacted Ni. The interface was observed to be extremely flat and uniform without penetration into the GaAs but with a thin native oxide layer between the metal and semiconductor, similar to those observed by Liliental-Weber et al.<sup>20</sup> Some As and slightly more Ga were found in the metal after heat treatment.

In order to analyze selected contacts with SIMS since the surfaces were non-uniform due to the florets, the metallization was removed by a chemical etch to improve depth resolution. A secondary electron microscope (SEM) examination of adjacent etched and unetched regions of contact viewed edge-on indicated that their procedure did not remove any underlying GaAs. It was possible for them to successfully etch away the metallization only from contacts heat treated for the longest times, a fact ascribed to the complete formation of the  $\text{Al}_3\text{Ni}$  phase. Al, Ni, and Ge all were found to have diffused into the substrate up to several hundred Angstroms, while Ga and As profiles remained essentially flat. Ni diffused about the same distance in both n and p substrates, while the Al profile fell off much more abruptly in p-type material. Similarly, Ge penetrated much further ( $500^\circ \text{ C}$ ) in n-type material, with the diffusion depth being similar to that reported previously by Liliental-Weber et al.<sup>20</sup> An interfacial accumulation of Zn dopant in the p-type GaAs was also found. They stressed that they did not believe this to be an artifact of the SIMS measurement. They also believed the Al penetration to

be real, although they were unable to quantify the depth since calibration standards were unavailable.

Quantitative I-V measurements of less heavily doped contacts were reported in a third paper.<sup>23</sup> Contacts were deposited onto semi-insulating GaAs substrates with an n-type layer ( $\text{Si} @ N_D = 6-10 \times 10^{17} \text{ cm}^{-3}$ ) grown by MOCVD (metal-organic chemical vapor deposition). Utilizing photolithography, mesas of conducting material were etched in epitaxial films, the metallization deposited, and the TLM pattern was produced by a lift-off process. These samples were made to quantitatively evaluate specific contact resistance. However, samples with the same intended metallization ratio as previously reported were incorrectly made without Ge. For n-type contacts, only the sample with a 200Å Ge layer was actually made and measured. For  $N_D @ 10^{17}-10^{18} \text{ cm}^{-3}$  the specific contact resistance was found to vary from  $1.8 \times 10^{-3}$  to  $3.6 \times 10^{-5} \Omega \cdot \text{cm}^2$ . A correlation was reported between electrical data and structural properties of the n-type contact. For shorter than 3-minute heat treatment times, the contacts were rectifying and the layer closest to the GaAs was a NiGe phase. Contacts heat treated for longer than 3 minutes were found to be ohmic and the NiGe phases had disappeared while an Al<sub>3</sub>Ni phase was adjacent to the GaAs. They therefore attributed the formation of n-type ohmic contacts to the formation of this Al<sub>3</sub>Ni phase at the GaAs interface and speculate that in-diffusion of the contact components, particularly Ge, contribute to ohmic formation.

For the p-type GaAs with  $N_A @ 3.5 \times 10^{18}$  to  $1.4 \times 10^{19} \text{ cm}^{-3}$ , all contacts were ohmic as-deposited, the specific contact resistance did not change appreciably with alloying, the contact resistance decreased with increasing doping but increased with increasing Ge layer thickness and with increased heat treatment time. The specific contact resistance varied from  $4.0 \times 10^{-4}$  to  $3.6 \times 10^{-5} \Omega \cdot \text{cm}^2$ . Graham et al. suggested that for the p-type contact, almost any metallic system would provide a suitable contact to such a heavily doped material, but also pointed out that the dopant levels studied were about those used in common p-type devices. Graham et al.<sup>22, 23</sup> were unable to explain why

the metallization functioned as an ohmic contact. However, they did point out a number of unresolved dilemmas. For n-type systems it is generally said that Ge diffuses into GaAs to heavily dope the semiconductor to allow charge transport and ohmic behavior by a tunneling mechanism resulting from band bending. Band bending obviously would be counter-productive for p-type systems since the bands would be bent in the wrong direction, making the contact less ohmic. They propose Al diffusion onto vacant Ga sites, thus forcing the amphoteric Ge to locate on As sites. In this way, the Ge atoms were either adding themselves to the existing acceptor population or were introducing themselves in donor-acceptor pairs that do not alter the original band bending at the surface. Graham et al. further speculate that the smooth morphology of the interface probably leads to quite a different transport mechanism than that of the Au-Ge-Ni/GaAs system whose interface is usually characterized by irregular morphologies and concomitant high-field regions. They state that the Al/Ge/Ni contact system was originally intended for use on n-type materials, and that on p-type materials the decrease in specific contact resistance may be due to the amphoteric nature of Ge. Ge may prefer the Ga site at the low temperature of heat treatment and thus actually compensate the Zn.<sup>43</sup> They attribute negligible electrical effects to the Ni.

To explain their observations Graham et al. made sometimes contradictory arguments. They initially proposed that Al diffused into the Ni-Ge layer via grain boundaries and formed an Al-Ge eutectic during the heat treatment. Recall that in as-deposited contacts, the Ge and Ni layers were said to combine to form a single reacted layer during the deposition. The eutectic would then melt and in this molten state the Ge could more easily penetrate the substrate to allow Ge doping. In this way, the GaAs was doped heavily enough that the Al-Ge-Ni contact can work in the same manner as the Au-Ge-Ni contacts. Graham et al. attributed the floret structure on the surface to liquid Al-Ge eutectic formation during heat treatment. Thus, during heat treatment Al diffused into and reacted with the Ni-Ge layer to form the thin polycrystalline layer of  $\text{Al}_3\text{Ni}$  and larger

single crystals of the same phase. The Ge released was more than sufficient to form a eutectic liquid with the remaining Al which "balls up" on the contact surface to produce the observed "floret" structures. In the absence of asperities on the contact surface in the form of the  $\text{Al}_3\text{Ni}$  single crystals, Graham et al. believe the balling up would probably be more severe and result in a less uniform contact surface. They express surprise at the abrupt, flat, uniform, intact interface at the metal-native oxide-semiconductor interface considering the slight excess Ga observed in the metal. They further suggested that uniformity of the continuous layer of the  $\text{Al}_3\text{Ni}$  at the interface meant that the liquid Al-Ge eutectic never came in direct contact with the GaAs. They pointed out that one might expect to observe contact metal-arsenide phases or a poor lattice image due to disorder immediately under the native oxide, but that neither of these were seen. They offer as a possible explanation for this that Al diffused into the GaAs during heat treatment and occupied the Ga vacancies to create a graded layer of AlGaAs at the interface. The layer would be very thin, perhaps  $100\text{\AA}$  thick, with a low Al content lattice matched to the underlying GaAs. They further suggested that Al in-diffusion was made possible by the dissociation of the GaAs in the presence of the Ni at the GaAs surface as reported by Ogawa.<sup>28</sup> However, they were unable to verify this suggestion and their SIMS data suggested that such an AlGaAs layer did not exist. They then suggested that an alternative possibility for the very flat interfacial morphology was the apparently strong tendency for Al and Ni to react and form a single phase alloy rather than Ni causing GaAs to dissociate, as happens in Au based contact system. In the third paper Graham et al. pointed out that the earlier explanation in which the eutectic composition became liquid and led to ohmic contact formation did not appear to be appropriate since the only evidence of liquid formation was the dendritic decoration at the surface. Furthermore, EDS data indicated that the surface precipitates were too Ge rich to be entirely the result of the eutectic solidification.

In summary, both Zuleeg et al.<sup>1,2</sup> and Graham et al.<sup>21, 22</sup> have been able to produce ohmic contacts on heavily doped n-type GaAs. Both Liliental-Weber et al.<sup>20</sup> and Graham et al.<sup>21, 22</sup> found the contacts to be very uniform and flat at the semiconductor-metal interface. The electrical data of Zuleeg et al.<sup>2</sup> suggested that field emission is the conduction mechanism and that Al-Ge-Ni contacts were stable at elevated temperatures. Liliental-Weber et al.<sup>20</sup> and Graham et al.<sup>21, 22</sup> observed Ge-Ni and Al-Ni compounds at the semiconductor interface utilizing EDS and TEM. These were identified as Ni<sub>5</sub>Ge<sub>3</sub> and Al<sub>3</sub>Ni. Both groups determined that a small amount of Ge penetrated the GaAs substrates, but did not find any compounds containing both metals and semiconductor components.

Thus the Al-Ge-Ni ohmic contact literature is also subject to disagreements and controversy. Some of this may be due to the dependence of the contact quality on the starting materials, both metals and semiconductor, and the processing procedures for sample preparation, contact deposition, and sample heat treatment. Similar to the Au-Ge-Ni contacts, the reactions occurring during the deposition and heat treatment of the Al-Ge-Ni contacts are apparently quite complex.

On the basis of the Al-Ge-Ni literature, the present study should expect to find Al<sub>3</sub>Ni and Ni<sub>5</sub>As<sub>3</sub> as the primary phases formed upon heat treatment of the ohmic contact metallizations. Since the heat treatments of the contacts in this study were at 425° or 500° C, the ternary phases of Ni-Ga-As described in the phase diagram literature (Ni<sub>x</sub>GaAs) would not be expected. However, NiGa, Ni<sub>2</sub>Ga<sub>3</sub> and NiAs phases were said to be equilibrium phases after heat treatment of 400-500° C and therefore should form, although formation of these phases has not been previously reported in the Al-Ge-Ni contact literature. The Au-Ge-Ni contact literature has identified the key phases of Ni<sub>x</sub>As(Ge) (e. g. Ni<sub>2</sub>AsGe or NiAs with some Ge in solid solution), β-AuGa and/or α-AuGa, which were postulated to create the vacancies necessary to allow doping by Ge. Based on the work of Sands et al.<sup>35</sup> a Ni<sub>x</sub>GaAs phase might also form for Ni adjacent to

GaAs, a condition used as part of one of the layering sequence in this study. An analogous  $Ni_xAs(Ge)$  phase for the Al-Ge-Ni system would seem possible, but based on previous works, an Al-Ga phase seems unlikely. Therefore, if the Al-Ge-Ni contact system is to achieve ohmic behavior by degenerative doping of GaAs, the reactions taking place during heat treatment must allow Ge incorporation on Ga sites and in addition to the  $Al_3Ni$  and  $Ni_5As_3$  phases previously identified,  $Ni_xAs$  and  $Ni_xGa$  phases should be found. In fact, the regrowth mechanism which has been used to explain the formation of ohmic contacts for several other metallization systems will be used in this dissertation to explain a dramatic effect in the conversion to ohmic behavior which results when Ni is deposited onto the GaAs first. The effects of layering sequence upon the kinetics of ohmic formation have not been previously reported. Further the equilibrium phases predicted from the phase diagram literature will be correlated with X-ray diffraction analysis.

## CHAPTER 3 EXPERIMENTAL PROCEDURE

The experimental work for this dissertation was carried out at both the Materials Directorate of Wright Laboratory, Wright-Patterson Air Force Base, Ohio, and at the Department of Materials Science and Engineering at the University of Florida, Gainesville, Florida. The samples were grown and the X-ray diffraction was accomplished at the Materials Directorate, while the heat treatment, electrical characterization, and the Auger depth profiling were conducted at the University of Florida.

### Sample Preparation

A number of different types of GaAs substrates were selected for this study to test the effects of bulk doping versus ion implantation over a range of doping levels, and the influence of the various growth techniques to produce epitaxial doped layers. Specifically, contacts were deposited on 1) semi-insulating LEC GaAs substrates with silicon ion implanted active and contact layers, 2) semi-insulating LEC GaAs substrates with Si doped active and contact layers grown by vapor phase epitaxy, 3) semi-insulating LEC GaAs substrates with a Si doped contact layer and an arsenic passivation cap grown by MBE, 4) conductive horizontal Bridgeman (HB) GaAs substrates bulk doped with Si, and 5) single crystal sapphire substrates. Substrates were implanted with  $2.9 \times 10^{17} \text{ cm}^{-3}$  Si to a depth of  $0.34 \mu\text{m}$  as an active layer and a higher doping density of  $1.0 \times 10^{18} \text{ cm}^{-3}$  Si to a depth of  $0.16 \mu\text{m}$  as a contact layer in undoped semi-insulating

substrates with a resistivity of  $> 10^7 \Omega\text{-cm}$ . The vapor phase epi-substrates were doped at  $2.7 \times 10^{17} \text{ cm}^{-3}$  Si to a depth of  $0.63 \mu\text{m}$  as an active layer and at  $1.6 \times 10^{18} \text{ cm}^{-3}$  Si to a depth of  $0.25 \mu\text{m}$  as a contact layer, also on undoped semi-insulating LEC GaAs substrates with a resistivity of  $> 10^7 \Omega\text{-cm}$ . Both of these substrates were cut with an orientation of  $2^\circ$  off  $\{100\}$  toward  $\{110\}$  and polished on both sides. The ion implanted and vapor phase epi substrates were used both as-received and with a mild etch of 1:1:4 -  $\text{NH}_4\text{OH}: \text{H}_2\text{O}_2:\text{H}_2\text{O}$  for 20 seconds followed by a rinse with  $17 \text{ M}\Omega$  water and blown dry with filtered dry nitrogen. The horizontal Bridgeman grown GaAs substrates were bulk doped with  $2.6\text{--}3.5 \times 10^{16} \text{ cm}^{-3}$  Si and were cut on axis and polished on both sides. These substrates were subjected to the same sample cleaning procedures.

The quality of devices grown on GaAs substrates can be dramatically influenced by the effect of substrate processing, packaging, and preparation. Historically a great deal of effort has gone into the determination of proper sample preparation and packaging prior to device fabrication. In order to avoid the complications presented by surface preparations, some of the substrates used in this study had contact layers grown by MBE with an As overlayer to protect the surface. The As overlayer oxidizes upon exposure to air, but it passivates the GaAs surface by preventing it from forming a native oxide. While the actual removal of the As cap layer took place in the metal deposition chamber, it was a form of in-situ vacuum sample preparation. Thus, the GaAs substrate surface was not exposed to the atmosphere prior to the metal deposition.

The MBE substrates used in this study were LEC semi-insulating with a resistivity of  $>10^7 \Omega\text{-cm}$ , were cut on axis  $\{100\} \pm 0.5^\circ$ , whole wafer etched, and polished on the top side only. Prior to MBE growth, these wafers were chemically cleaned with a 6 minute 1:1:5  $\text{NH}_4\text{OH}:\text{H}_2\text{O}_2:\text{H}_2\text{O}$  etch, followed by a rinse with  $17 \text{ M}\Omega$  water and blown dry with filtered nitrogen. The substrate was then mechanically mounted, rather than using the typical indium mounting, and loaded into the MBE system. After the native oxide was thermally desorbed, a  $2.0 \mu\text{m}$  layer of Si doped

n-GaAs was grown. This surface was then As capped by cooling the wafer to room temperature in an overpressure of As. Wafers were grown with Si doping levels at the mid  $10^{18} \text{ cm}^{-3}$  range and also with the Si doping levels in the low  $10^{16} \text{ cm}^{-3}$  range.

In addition to the various types of GaAs substrates, sapphire was also used as an inert substrate for the metal depositions. The sapphire substrates were used as-received and chemically cleaned in the same manner as the GaAs wafers. Since the metals, the semiconductor, and the interface contamination make this a many component system, the use of sapphire substrates allowed for potentially simpler determination of phase formation between the Al, Ge, Ni, Ga, and As components. The inert sapphire substrate will not react with the contact metals making it easier to determine the phases formed when all the materials were present.

### Metal Deposition

All of the metal depositions were carried out in an all metal-sealed stainless steel ultrahigh vacuum chamber, which was configured to include a Perkin Elmer model TBNX 3, 300 liter/sec vac-ion pump with a titanium sublimation pump, a Spectramass Selectorrr Residual Gas Analyzer, an Inficon Leybold Heraeus model 751-001-G1 quartz crystal oscillator, a Thermionics sample manipulator with a home-made sample heater and dc power supply, and a Thermionics three position electron beam evaporator, model 010-0030, with both beam steering and rastering options.

Chemically etched samples were loaded into the deposition chamber immediately after they were dried with nitrogen. The GaAs substrates were loaded into the heater portion of the sample manipulator while the sapphire was loaded into a position on the sample manipulator which was not heated. The sample manipulator, with the samples, was then loaded into the vacuum chamber. The sample manipulator was positioned with the substrates facing up and away from the electron beam evaporator. The vacuum

chamber was pumped down using sorption pumps, and the bake-out was begun at this time using the sorption pumps. After the pressure reached the mid  $10^{-5}$  Torr range, the system was switched to the vac-ion pump and baked at approximately 125° C for 18 to 60 hours (overnight to over-the-weekend). Typical background pressure after the bake and at least an overnight cool down was 2 to  $4 \times 10^{-10}$  Torr. The titanium sublimation pump was sublimed several times before the metal deposition was begun to provide additional pumping capacity.

The As capped MBE grown samples were heated as quickly as possible to approximately 600° C by turning the dc power supply to full power. When the sample reached 600° C the power supply was turned off, allowing the sample to cool. Due to the mass of the sample heater and poor thermal contact, it required 6 to 8 minutes for the sample to reach 600° C and 30 to 40 minutes to return to room temperature. The sample temperature was monitored by both an IR pyrometer and a platinel thermocouple attached to the sample holder. The As capped samples had a matte finish as-deposited, but after desorption at 600° C the sample had a mirror-like appearance. The reflectivity change was also used as an indicator of desorption. Only the MBE grown, As capped substrates received the thermal 600° C treatment.

Electron beam evaporation, in principle, is a simple, efficient method of deposition of uniform pure thin contact layers onto GaAs and sapphire substrates. The source material was placed in a crucible liner made of graphite to avoid contamination from both the evaporator hearth and any previously evaporated materials. Then a beam of electrons was directed onto the source material. In larger production systems, the material is generally only melted at the point of impingement of the electron beam and evaporated from a relatively small melted pool at this position. The rest of the material is heated only through conduction and cooled at the crucible by cooling water circulating through the evaporator hearth. Therefore the source material acts as its own container. In the small system used in this project, the entire source load melted. Prior to proper

outgassing, the source materials tended to spit if heated too quickly. If the sample was too close to the evaporator, small balls of the source material deposited onto the substrate. Thus it was important to slowly heat and outgas each source prior to deposition. For the Ge and Ni sources this did not pose a problem after the materials were sufficiently outgassed. However, for the evaporation of Al it did cause major problems. In addition to its tendency to spit, the Al also broke its crucible during cool down and solidification. When the Al was evaporated, it melted and wetted the surface of the crucible walls. The Al would adhere to the walls of the crucible so well during cool down that it would pull the walls of the crucible in and break them during the solidification process. Slower heating and cooling, especially through the melting point of Al, was used in an attempt to keep the crucible from breaking. This slower cool down procedure is a common practice used in MBE systems to prevent crucible breakage. This approach proved fruitless in the electron beam evaporator. Eventually it was determined that simply adding more and more Al to the broken crucible, until it overflowed both the broken crucible and the hearth, allowed the remaining Al to act as its own crucible. The Al overflowed its crucible, made contact with the cold hearth of the evaporator and solidified. This overflow formed into a bowl-like configuration somewhat like the top of a volcano and behaved much like a larger crucible allowing evaporation of the Al in a more controlled manner (Figure 1). Another important key in allowing this procedure to work, was the addition of the beam steering apparatus to the electron beam evaporator. This allowed the electron beam to be very accurately placed in the center of the Al source.

Prior to deposition of each metal layer, each source was thoroughly outgassed and a small amount of material,  $\sim 100\text{\AA}$ , was evaporated to clean up the source surface. During outgassing, the sample was left face up in the deposition chamber to prevent any undesired deposition. Initially the outgassing of the sources was monitored with the Residual Gas Analyzer, (RGA). The gases were found to be primarily hydrogen, with lesser amounts of water, carbon monoxide and carbon dioxide. During the outgassing



Figure 1. The Al source and crucible after many depositions.

the base pressure usually rose for only a brief period (10-15 sec) into the  $10^{-7}$  Torr range then quickly fell to the mid  $10^{-8}$  to the mid  $10^{-9}$  Torr range during the actual metal deposition. Following the outgassing of all three sources, the layering was done sequentially from a three source electron beam evaporator. Thus only single component layers of Al, Ge, and Ni in various ratios were possible from the pure source materials. Typical evaporation rates were approximately 0.5-1.5 Å/sec for Ge and Ni and approximately 1.0-5.0 Å/sec for Al. The actual deposition of each layer of metal was monitored using the quartz crystal oscillator placed symmetrically with the sample above the evaporator. Each of the source materials in their graphite crucibles were moved into position under the immobile electron gun and evaporated onto the substrates in the

desired amount and sequence. On several occasions the evaporation of Al would climb as high as 10-20 Å/sec for brief periods (typically only a few seconds) due to the difficulties of electron beam evaporation of Al as mentioned earlier. The choice of the slower deposition rates was the result of trying to keep the evaporation of Al under control, and also to keep the deposition chamber background pressure as low as possible.

Just prior to the deposition, a movable Ta mask was positioned over the substrate. The mask was not in intimate contact with the sample in the up position, since the sliding may have caused scratching and or contamination of the substrate. However, when the substrate was turned face down for deposition the substrate laid on the mask. The mask was used to define the three thin lines on one quarter of the sample, see Figure 2. The electrical lines, ~0.5 mm X ~4 mm with spacings of ~875 µm and ~2150 µm, were later used to electrically characterize the contact via the TLM test structure.

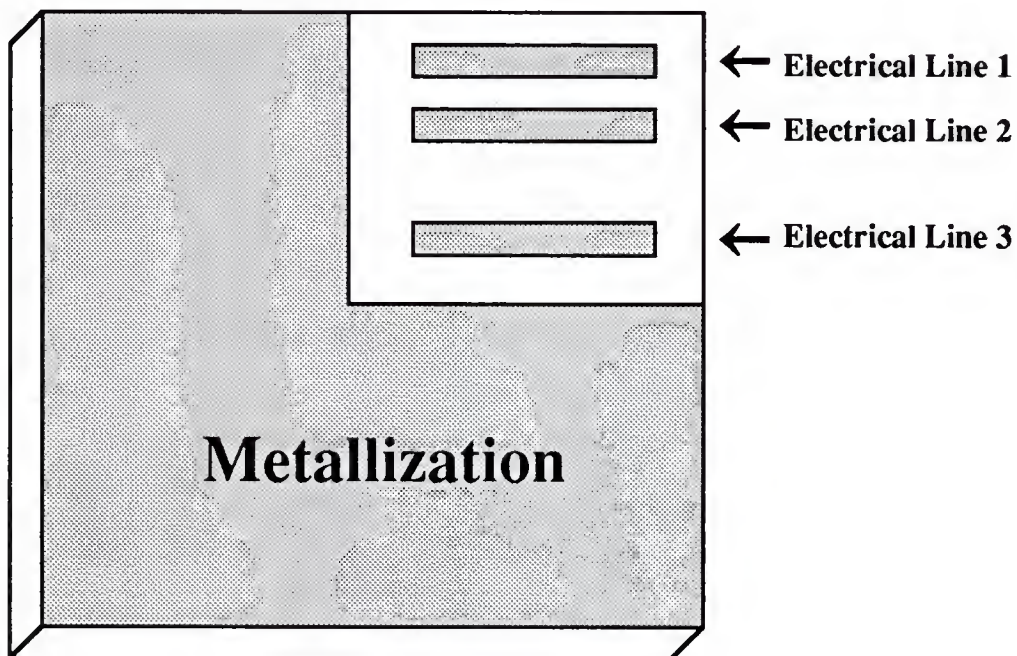


Figure 2. Sample metallization configuration.

Once the difficulties of deposition were overcome, the samples were then able to be made routinely. The deposition sequence of elements and the ratio of elements were chosen as variables. These were simultaneously deposited on both GaAs and sapphire substrates. For each different ratio of materials at least four samples were made, two for each heat treatment temperature. Samples were made for two different purposes. First, sets of samples were made which were intended to become ohmic contacts. Second, sets of samples were made to help delineate which materials reacted and which phases formed. There were two types of samples in the first group, one with Ni as the initial layer on the substrate, and one with Ge as the initial layer on the substrate. Examples of these types of samples were deposited onto all of the different types of GaAs substrates and also onto sapphire substrates. The second group of samples were made of combinations of only two of the Al-Ge-Ni components grown on both GaAs and sapphire substrates. These were made in ratios of materials similar to those of the ohmic contacts and also in equal parts of the two components. A list of the samples, their description, and electrical results can be found in the Appendices A and B.

### Electrical Measurements

Electrical characterization was required to determine if the Al/Ge/Ni metallization deposited upon GaAs had become ohmic. Transmission line measurement (TLM) current versus voltage (I-V) measurements<sup>74</sup> were chosen to provide this determination because the complete contact system can be deposited onto one side of the substrate. With the one sided contacts, the deposition process was accomplished without having to break vacuum and expose the sample surfaces to atmosphere. The metals were deposited, as stated earlier, through a Ta shadow mask. Therefore, the choice of the TLM method was also an indirect means to avoid additional contamination of the semiconductor surface. As indicated in Figure 3, the I-V measurement was made three times on each sample,

measuring between electrical lines 1 and 2, 2 and 3, and 1 and 3. I-V measurements were made on nearly all of the metallization samples.

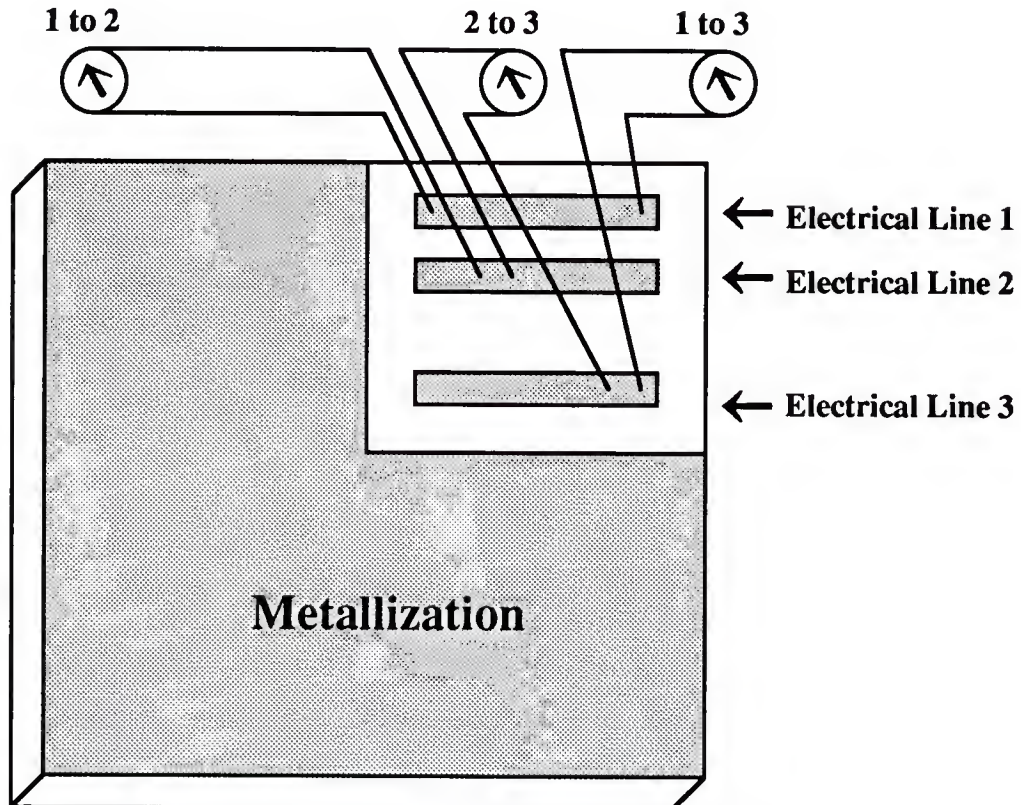


Figure 3. I-V probe contact to sample electrical lines.

Most of the I-V measurements were made using a system that consisted of a Hewlett Packard model 3478A multimeter, a Hewlett Packard model 6112A DC power supply, and a Hewlett Packard 59501B power supply programmer. It was automated and controlled through an IBM PC with an IEEE-488 computer interface. This was a table top system with the measurements made in atmosphere at room temperature. Some of the measurements made on the as-deposited samples were made on a Tektronics curve tracer oscilloscope with Polaroid photos taken of the curves. Contact to the metallization was made using tungsten tipped probes. The I-V measurements were made on the as-deposited samples first, then the samples were heat treated generally in 2 or 3 minute

increments, and the heat treatment was followed by another I-V measurement. This process was repeated until the contact became ohmic or no further change was observed in the plots of the I-V measurements. Each I-V measurement consisted of three actual measurements made across electrical lines 1 to 2, 2 to 3, and 1 to 3.

### Heat Treatment

The choice of heat treatment temperatures was influenced by the references of Zuleeg et al.<sup>1</sup> and Graham et al.<sup>21-23</sup> Zuleeg et al. heat treated their samples at 500° C and Graham et al. heat treated their samples at 425° C. The 500° C heat treatment temperature is also a common temperature recommended for heat treating Au-Ge-Ni ohmic contacts on GaAs for short periods of time.<sup>28, 60</sup> It is high enough to allow interdiffusion of the metal alloyed contacts but low enough to avoid too great a decomposition of the GaAs. Thus it was thought that if the metallizations on low doped GaAs were to become ohmic, the 500° C heat treatment temperature was a likely choice. Graham et al. did not explain their choice of the 425° C heat treatment temperature. It was chosen for this effort because it was approximately the eutectic temperature of Al-Ge and should slow any diffusion or intermixing of the metals by more than a factor of two, according to the rule of thumb, which states that the diffusion distances are usually a factor of two smaller for each 50° C decrease in temperature. Also, by using both temperatures the parameters of both of the other groups could be duplicated, and used to gain some insight into the existing literature.

Prior to heat treatment, the GaAs and the sapphire samples were each split into two pieces. After the initial I-V measurement, the part of the GaAs with the electrical measurement lines and a piece of the sapphire were then heat treated. Both samples were heat treated in a 3-zone furnace with a 10 cm flat zone with a flowing forming gas atmosphere, 10 % H<sub>2</sub> and 90 % N<sub>2</sub>. One set of samples was heat treated at 425 ° C and

a second set of samples was heat treated at 500° C. In both cases the heat treatments were carried out in a similar manner. Several samples were loaded into a quartz boat and slowly inserted into the center of the 3-zone furnace, the elapsed time for insertion was about 20 to 30 seconds. The samples were then held at the center for a short time, generally 2 or 3 minutes. The listed heat treatment times were the elapsed time the sample was held at the center hot zone of the furnace. No correction was made for either heat up or cool down time. The samples were then slowly removed from the center of the furnace, the elapsed time for removal was about 30 to 45 seconds. The samples were removed from the quartz boat and the next I-V measurement was made immediately. The quartz boat was stored at the end of the furnace between heat treatments. This process was repeated until the contact became ohmic or no further change was observed in the plots of the I-V measurements.

#### Real Time I-V Measurement and Heat Treatment

Because the two heat treatment temperatures apparently affect the contacts differently it was decided to use a real time heat treatment and I-V measurement to investigate the time effects. Two different types of the samples were measured in this second system, which consisted of a Hewlett Packard curve tracer oscilloscope, a tube furnace, a combination quartz holder and insertion rod equipped with thermocouple and electrical leads. Both type of leads were spring loaded to make contact with the TLM pads 1 and 3 on the sample. The output of the I-V and temperature measurements were sent to the curve tracer and a digital thermocouple meter. Polaroid photos were used to record the output of the curve tracer. Two samples were taken from the same 3 inch GaAs. The initial I-V curve of the as-deposited metallization of both samples was that of a Schottky barrier. This measurement was made on the same non real time system at room temperature as the other samples. The sample was then mounted in the real-time

system, and the initial I-V measurement was also initially rectifying. The temperature at the center of the furnace was set at 425° C, but 74° C at the end of the furnace. The sample was left at the end of the furnace approximately 1 minute, then slowly inserted to the center of the furnace. The changes were so rapid that there was not enough time to photograph the curves on the oscilloscope. After the sample was observed to exhibit ohmic behavior, it was slowly removed from the furnace. After removal from the furnace, an I-V of the sample was again taken on the non-real time system at room temperature.

#### Auger Electron Spectroscopy

Auger depth profiling was the technique chosen to investigate the interdiffusion of the metals and semiconductor both as-deposited and after the sample had become ohmic. In addition, Auger survey scans were used to characterize the contamination. The sensitivity of AES is in the range of 0.1 to 1 atomic percent, therefore the technique is capable of monitoring the alloy interdiffusion and the penetration of the alloy into the semiconductor. But, AES is not capable of monitoring the degenerative doping of the semiconductor by the metal alloy. The goal of the surface analysis was to use the Auger techniques to characterize the movement of these materials in the samples to complement the XRD measurements, and to correlate these changes with the electrical properties.

Auger electron spectroscopy was performed in a Perkin-Elmer Physical Electronics Model 660 Scanning Auger Microscope (SAM). Typical electron beam parameters were a 5 keV primary electron beam energy with a 30 nA beam current. The data were collected in the N(E) mode with repetitive scans to increase the signal to noise ratio, summing 20 scans in an elapsed time of approximately 17 minutes. The electron beam was rastered during data collection to reduce the possibility of beam-induced changes in the surface such as contamination by electron beam cracking of the residual

gases in the vacuum. The electron spectrometer was a cylindrical mirror analyzer. The system base pressure was typically in the low  $10^{-10}$  Torr range. For Auger depth profiling a 3 keV Ar ion gun with a rastered current density of 25 mA was used for sputtering. The raster size was varied from 2 mm x 2 mm to 5 mm x 5 mm to control the sputter rate. The differentially pumped ion gun was operated with an Ar pressure of 15 mPa inside the gun. The pressure during sputtering was in the mid to the high  $10^{-8}$  Torr in the analyzing chamber. The electron beam was positioned near the center of the sputtered crater and rastered over a sufficiently small area to avoid crater edge effects. The system was also configured with a secondary electron detector so that it would function as a secondary electron microscope (SEM).

#### Thin Film X-ray Diffraction

X-ray diffraction was chosen to identify the phase formation resulting from the interdiffusion of the ohmic contact metals and semiconductor. Glancing angle X-ray diffraction was performed in a computer controlled Rigaku X-ray diffractometer using a thin film attachment and Cu K $\alpha$  radiation from a tube operated at 40 kV and 30 mA. The X-ray source has a line focus, with divergence of the incident X-rays in the vertical direction limited by the vertical divergence Soller slit, and narrowed by a 0.6° incident slit combined with a 5 mm incident height limiting slit. The diffracted X-rays from the thin film sample pass through the receiving Soller slit with a 1° width limiting receiving slit and without a scatter slit, are again diffracted by a single crystal graphite monochromator, and are counted by a scintillation counter. Because the thin films yield low intensities, the data was collected for very long times, up to nearly 3 full days in many cases. The metal films of Ni and Ge were relatively thin, 500 Å and 250 Å respectively, with an overlayer of Al of 2000 Å for most of the ohmic contact samples. Glancing angle or thin film X-ray diffraction was used for the measurement of thin films.

It is generally difficult to obtain a distinct diffraction pattern from thin film samples using conventional X-ray diffraction techniques because the diffracted intensity of X-rays are very weak and on relatively high backgrounds. The conventional diffractometer utilizes  $\Theta - 2\Theta$  scans where the movement of both sample and detector allows the X-ray incidence angle to be equal to the take-off angle. The angular resolution and the diffracted intensity are both a function of the take-off angle. The constant take off angle maintains constant angular resolution and intensity. In the case of thin film X-ray diffractometer the incident angle,  $\Theta$ , is held constant to maximize the intensity through maximizing the interaction volume between the incident X-rays and the diffracting material over the entire  $2\Theta$  scan. The smaller the incidence angle, the greater the interaction volume and thus the intensity is relatively greater.

Phase identification was accomplished by comparing standard peak position and intensities from International Centre for Diffraction Data (ICDD) cards<sup>75</sup> with the XRD data collected from the deposited samples. Peak position was the primary source of identification, but peak intensity was also used for verification where possible. There are a number of reasons for the measured intensities to vary from those reported on ICDD cards. For example, a sample with preferred orientation within a metal layer results in intensity changes and alters the measured intensity values relative to the values given on the ICDD cards. Poor crystallinity caused by defect structures, small size, or stress will also alter the measured peak intensity. Most importantly, for this study, overlapping of peaks from one or more phases will cause large errors. A number of the identified phases have peaks which overlap, which is common in systems with a large number of components. Because of the likely occurrence of several of these sources of error as well as the single crystal nature of the GaAs and sapphire substrates and the possibility of epitaxy, the samples were run at two different glancing angles to increase the chance of detection from oriented thin films and substrates.

## CHAPTER 4 RESULTS

### Sample Preparation

As stated in Chapter 3, the quality of devices grown on GaAs substrates can be dramatically influenced by the effects of substrate processing. None of the more exotic methods, such as ozone treatment, and low energy ion sputtering at elevated temperatures have been used in this study to clean the substrate prior to deposition. Substrates with ion implanted active and contact layers, substrates with vapor phase epitaxy doped active and contact layers, HB grown, bulk-doped substrates, and sapphire substrates were used as-deposited or cleaned with a mild etch. Though sample prep has evolved in an attempt to reduce the general contamination levels, even today there is disagreement over which processes are necessary and whether or not the surface states which result from the contamination can be removed, reduced, or at least passivated. Therefore, because of concern over potential complications presented by surface preparations, some of the substrates used in this study had contact layers grown by MBE with an As overlayer to protect the surface. As described earlier, the thermal desorption of the As cap proved to occur quite easily. The sample was simply heated until the surface became mirror like.

In one instance two pieces of the same substrate were mounted in the sample heater to desorb the As cap for later use in a Hall Measurement to check doping concentration. When the As cap began to desorb, as indicated by a pressure increase in the deposition chamber, the As cap of only one of the pieces appeared to coalesce then disappear from the surface completely. When the surface of this piece appeared

mirror-like, the heater was turned off. The second of the two pieces apparently was not making as good as thermal contact with the sample holder as the first piece. At the time the sample heater was turned off, the second piece of GaAs was still covered with As as indicated by a matte surface. Its covering of As also desorbed during the cool down and its surface became highly reflective. The removal of As from the second piece of GaAs gave confidence that the desorption process was somewhat forgiving and that the surface reflectivity could generally be taken as an indicator of its removal.

In addition to reducing the potential effects of surface contamination, the MBE grown samples also allowed a selection of substrates with various doping concentration levels for the contact layer. To date the Al-Ge-Ni ohmic contact literature only contains reports for doping concentration levels in the high- $10^{17}$  cm<sup>-3</sup> range and above. To prove that the Al-Ge-Ni metallization was a viable candidate to become a generally accepted ohmic contact material for GaAs, the metallization must convert to ohmic when deposited on the full range of doping concentration levels, from lightly doped ( $10^{16}$  cm<sup>-3</sup>) to heavily doped ( $10^{18}$  cm<sup>-3</sup> and above). The MBE grown substrates doped with Si in the  $10^{16}$  cm<sup>-3</sup> range were important samples to prove that the Al/Ge/Ni ohmic contact system will work at low concentrations.

### Sample Deposition

Once the rate of heating of the source materials was under control, the Al source material was used as its own crucible, and the electron beam steering apparatus was added to the deposition system, sample deposition was accomplished routinely in ultrahigh vacuum. Over 75 samples were deposited, but the first 30 were quite variable while learning how to control the system, to test the various deposition parameters, and to determine proper analysis parameters. Approximately 45 samples were made after the deposition system was under control. Samples were made for two different purposes.

Samples made in set I were intended to become ohmic contacts. Samples made in set II were intended to help delineate which materials reacted and which phases formed. There were two types of samples in set I. The first, sample set Ia had Ni deposited first on the GaAs and sapphire substrates with a layering sequence of ambient/Al/Ni/Ge/Ni on GaAs or sapphire. The second, sample set Ib had Ge deposited first on the GaAs and sapphire substrates with a layering sequence of ambient/Al/Ni/Ge on GaAs or sapphire. The metallizations were therefore a series of diffusion couples. Different phases should form depending on which components were next to one another in the contact layers, how much of the component was present, and at which temperature they were heat treated. The starting sequence of the deposited materials were representative of the starting positions in a multidimensional phase diagram. These sets of samples were therefore meant to test the hypothesis that the sequence in which the metals were deposited would influence the resulting phase formation. While other recipes were also used, most of these samples were made using a total ratio of material of 2000Å of Al, 500Å of Ni, and 250Å of Ge. The total amount of material was held constant for samples in sets Ia and Ib, in this way the reactions if driven far enough would proceed to the same end point, only their pathways would be different. Thus, samples in set Ia were deposited in the sequence of Al (2000Å)/Ni (450Å)/Ge (250Å)/Ni (50Å) and samples in set Ib were deposited in the sequence of Al (2000Å)/Ni (500Å)/Ge (250Å) on GaAs and sapphire. This layer identification scheme will be used throughout the dissertation, i.e. the first metal layer contacts the environment and the last metal layer contacts the substrate. The substrate was GaAs unless specified as sapphire. This ratio of materials was a slight variation of the ratio of materials used in the previous Al/Ge/Ni ohmic contact literature.<sup>1, 2, 20-23</sup> It was selected over the other ratios used due Ge out-diffusion, which will be described later. These types of metallization schemes were deposited onto all of the different types of GaAs substrates and also onto sapphire substrates. Set I consists of approximately 20 of the samples. A complete list of the last 45 samples, their

description, heat treatment processing, and electrical characterization can be found in the Appendices A and B.

Samples in set II consisted of combinations of only two of the three metal Al/Ge/Ni components grown on GaAs and sapphire. These two element layers were made in ratios of materials similar to those of the ohmic contacts, i.e. Ni (450Å)/Ge (250Å)/Ni (50Å), as well as samples with layers of equal thicknesses, i. e. Ni (250Å)/Ge (250Å)/Ni (250Å)/Ge (250Å). Since the metals, the semiconductor, and the interface contamination make this a many component system, the use of two rather than three component layers on GaAs or sapphire substrates allowed for potentially simpler determination of the interdiffusion and phase formation. There were approximately 20 samples made for set II. Again, the complete list and description of these samples is in the Appendices A and B. Further effects of sample deposition will be discussed in the following characterization subsections.

### Heat Treatment

As stated in the Chapter 3, the choice of heat treatment temperatures was influenced by the references of Zuleeg et al.<sup>1</sup> and Graham et al.<sup>21-23</sup> Zuleeg et al. heat treated their samples at 500° C and Graham et al. heat treated their samples at 425° C. The 500° C heat treatment temperature is also a common temperature recommended for heat treating Au/Ge/Ni ohmic contacts on GaAs for short periods of time.<sup>28, 60</sup> The heat treatment was accomplished routinely. A complete list of heat treatment times is in Appendix B. Further effects of heat treatment will be more thoroughly discussed in the following characterization subsections.

### Electrical Measurement

As stated in chapter 3, electrical characterization was required to determine if the Al/Ge/Ni metallization deposited upon GaAs had become ohmic and the TLM type I-V contacts were deposited onto one side of the substrate without breaking vacuum.

Figure 4 is an example of an I-V curve of the three TLM measurements made on the as-deposited sample 47. The contact layer for sample 47 ( $\text{Si} @ 5.0 \times 10^{16} \text{ cm}^{-3}$ ) was grown in the MBE system, As capped, and the As cap was desorbed in the vacuum chamber immediately before deposition of the metal layers with a sequence of Al/Ni/Ge/GaAs. The three curves in Figure 4 correspond to the three I-V measurements made on the TLM electrical lines of the sample.

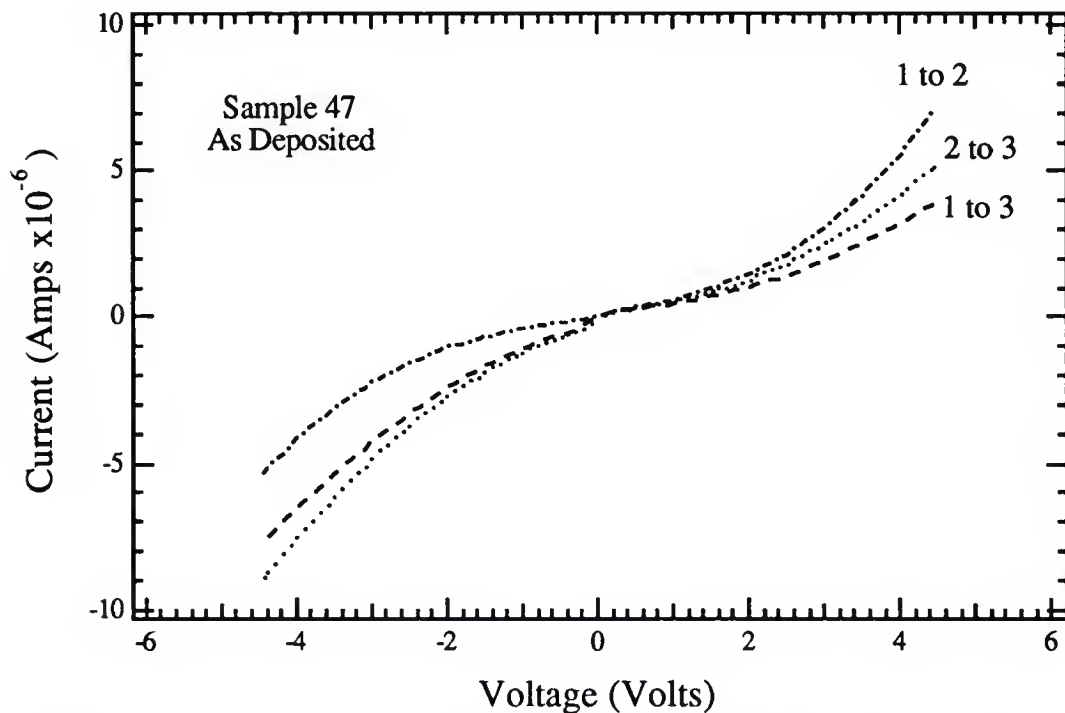


Figure 4. I-V curves of as-deposited metallization Al/Ni/Ge/GaAs, sample 47.

Although the I-V measurements indicated some of the metallizations deposited onto heavily doped substrates were ohmic as-deposited, all of the as-deposited contacts on lightly-doped substrates exhibited Schottky behavior. The I-V curves of the contacts indicate back-to-back Schottky barriers which result from the TLM type of measurement on two front surface contacts, both of which were rectifying. Thus, one metal contact was a diode under forward bias while the second metal contact was under reverse bias. The resulting I-V curve indicates rectification under both voltage biases. After the contact converts from Schottky to ohmic behavior the contact resistance will be independent of the bias voltage direction, (Fig. 5). The three separate measurements differ in the length of the current path through the substrate, and this resistance increases with the spacing between the metal contact pads.

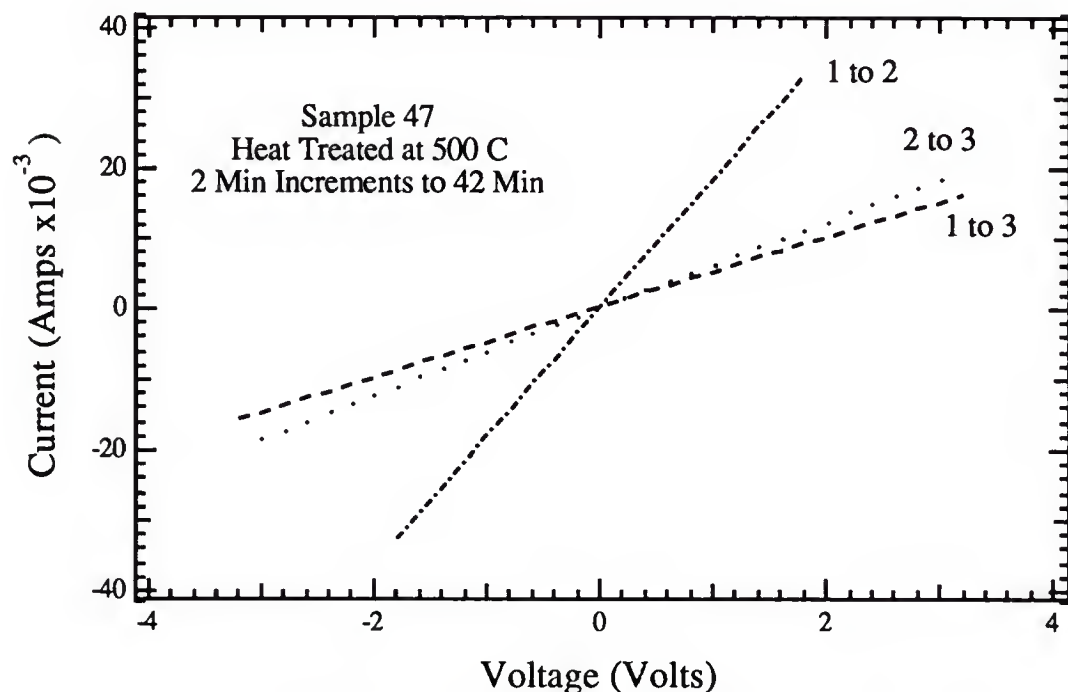


Figure 5. I-V curves after heat treatment of 42 minutes to become ohmic of metallization Al/Ni/Ge/GaAs for sample 47 .

After the initial I-V measurement the samples were heat treated in 2 or 3 minute increments. Sample 47 was heat treated in 2 minute increments at 500° C. After each 2 minute heat treatment another set of I-V data were collected. The sample underwent 21 of these iterations before it became ohmic (total time of 42 minutes). Figure 5 shows the I-V data from sample 47 after it became ohmic, as demonstrated by the straight lines. As in the as-deposited sample, the three separate curves indicate the three separate measurements made between line 1,2, and 3 on sample 47.

The iterative heat treatment and measurement process was originally chosen because the time required for the contact to become ohmic was unknown. A series of the I-V curves versus time can be plotted, as shown in Figure 6 for sample 47. To simplify the graph, only the data between lines 1 and 2 were plotted from each set of I-V measurements. Data from the other sets of lines would have produced a similar plot. Note that the current scale has changed for the as-deposited I-V curve from Figure 4 to Figure 6, because this sample was highly resistive as-deposited but very conductive after it became ohmic. Thus, the as-deposited contacts appear to be carrying nearly zero current. The changes taking place in the I-V measurement of this sample, which result from the increased heat treatment time, were initially very gradual. Little, if any, change was observed in the I-V curve in approximately the first 15 minutes of I-V measurement and heat treatment. In the next 15 minutes of heat treatment the I-V curve did begin to change gradually and over the last 12 minutes of heat treatment the rate of change in the I-V measurement increased. As shall be demonstrated, the changes in the series of I-V curves reflect metallurgical changes taking place in the contact metal layers and at the metal-semiconductor interface.

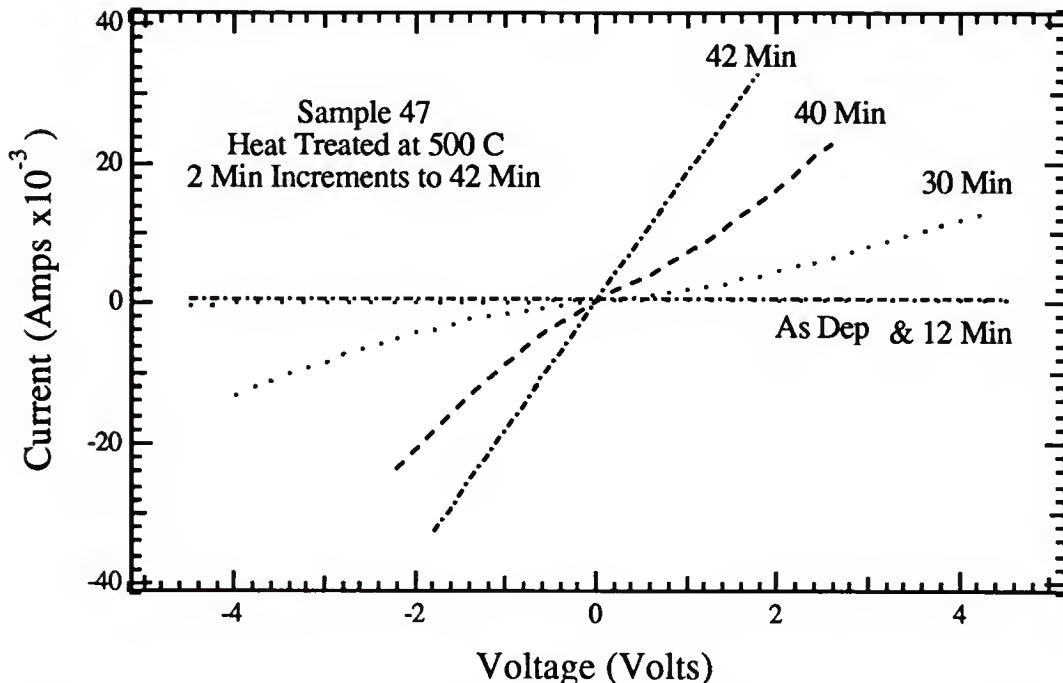


Figure 6. Series of I-V curves for sample 47, selected electrical measurements between lines 1 and 2 with increasing heat treatment time.

The time required for the metallization to become ohmic was found to be dependent on the deposition sequence, particularly whether Ni or Ge was immediately adjacent to the metal-semiconductor interface. Sample 43 was taken from the same wafer and MBE growth as sample 47, which was a 3 inch semi-insulating GaAs wafer. However, the metallization sequence for sample 43 was Al/Ni/Ge/Ni/GaAs rather than Al/Ni/Ge/GaAs as for sample 47. The metals were deposited as 50Å of Ni, 250Å of Ge, 450Å of Ni, and 2000Å of Al. Therefore sample 43 was identical in all aspects to 47 except 50Å of Ni was moved to the first layer of metal on the GaAs, rather than the 250Å of Ge on sample 47. The total amount of Ni in sample 43 remains the same as sample 47, a total thickness of about 500Å. For all of the samples discussed in this section (unless otherwise noted) the same ratio of 250Å of Ge, 500Å of Ni, and 2000Å of Al was maintained.

Sample 43, like sample 47, was heat treated in 2 minute increments at 500° C, but it became ohmic after just one 2 minute heat treatment cycle, rather than the 21 cycles required for sample 47. Because the sample became ohmic in one iteration, only two I-V curves are shown in Figure 7. The as-deposited I-V data show that sample 43 was initially less resistive than sample 47.

The influence of the metal sequence on the time required for conversion to an ohmic contact has not previously been reported for the Al-Ge-Ni ohmic contact metallization and represents an important finding from this research. For the Au-Ge-Ni ohmic contact system, Murakami et al.<sup>15</sup> reported that placing Ni at the metal-semiconductor interface reduced the minimum in the specific contact resistance versus heat treatment temperature, as well as reduced the scatter in these data. However, they did not report an effect on the time at temperature required for conversion to ohmic behavior.

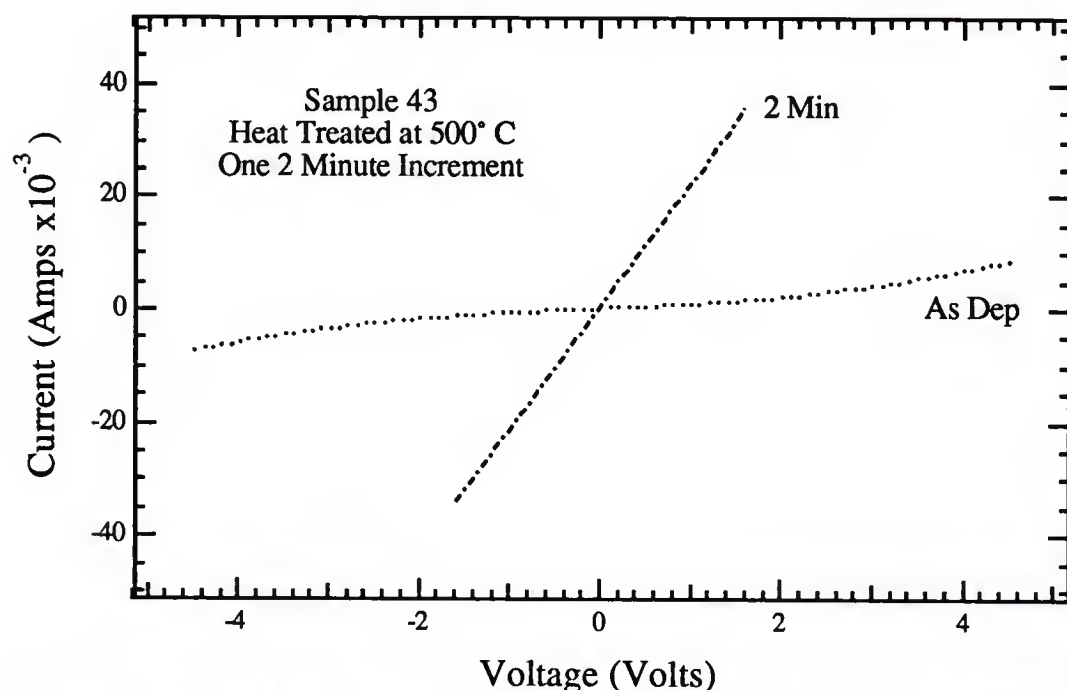


Figure 7. Series of I-V curves with increasing heat treatment time for Sample 43, electrical measurements between lines 1 and 2.

Table 1. Metallization of GaAs.

Sample Number	Dopant/Concentration	Interface Metal	Heat Treatment Temp Time		I-V Results
19	Si - 1.0X10E18-.16um 2.9X10E17-34um	300Å Ge	425	3+2+2+3+3	Ohmic after 13 Min
20	Si - 1.0X10E18-.16um 2.9X10E17-34um	50Å Ni	500	1+2	Ohmic after 3 Min
25	Si - 1.1X10E18-.16um 3.0X10E17-34um	251Å Ge	425	2+2+2+2 3+3+3+3	Ohmic after 20 Min
26	Si - 1.1X10E18-.16um 3.0X10E17-34um	51Å Ni	500	2	Ohmic after 2 Min
27	Si - 1.1X10E18-.16um 3.0X10E17-34um	251Å Ge	500	3+2+2+2	Ohmic after 9 Min
28	Si - 1.1X10E18-.16um 3.0X10E17-34um	52Å Ni	Ramped Real Time to 425		Turned Ohmic quickly at ~180 C
29	Si - 1.6X10E18-.25um 2.7X10E17-.63um	251Å Ge	Ramped Real Time ~20 Min to 425		Ohmic after ~15 Min
30	Si - 1.6X10E18-.25um 2.7X10E17-.63um	51Å Ni	500	3	Ohmic after 3 Min
39	Si - ~~5x10E16-2.0um	52Å Ni	425	2 Lines - 2 Min 3rd Line - 50 Min	2Min & 50 Min 2 ea to 40+10 to 50
43	Si - ~~5x10E16-2.0um	51Å Ni	500	2	Ohmic after 2 Min
45	Si - ~~5x10E16-2.0um	252Å Ge	425	2 + 2...= 40 then +10 to 100	Almost, Not Quite
47	Si - ~~5x10E16-2.0um	254Å Ge	500	2 ea to 44 Min	Ohmic after 42 Min

The elapsed time required to form ohmic contacts was also influenced by the heat treatment temperature. The metallizations which were Schottky as-deposited and became ohmic after heat treatment are listed in Table 1. The samples made early in this study did not have the same thickness ratios as samples numbered with 25 or higher (as reported above). Therefore caution must be used in the comparisons of the time it took for samples numbered less than 25 to convert from Schottky to ohmic behavior.

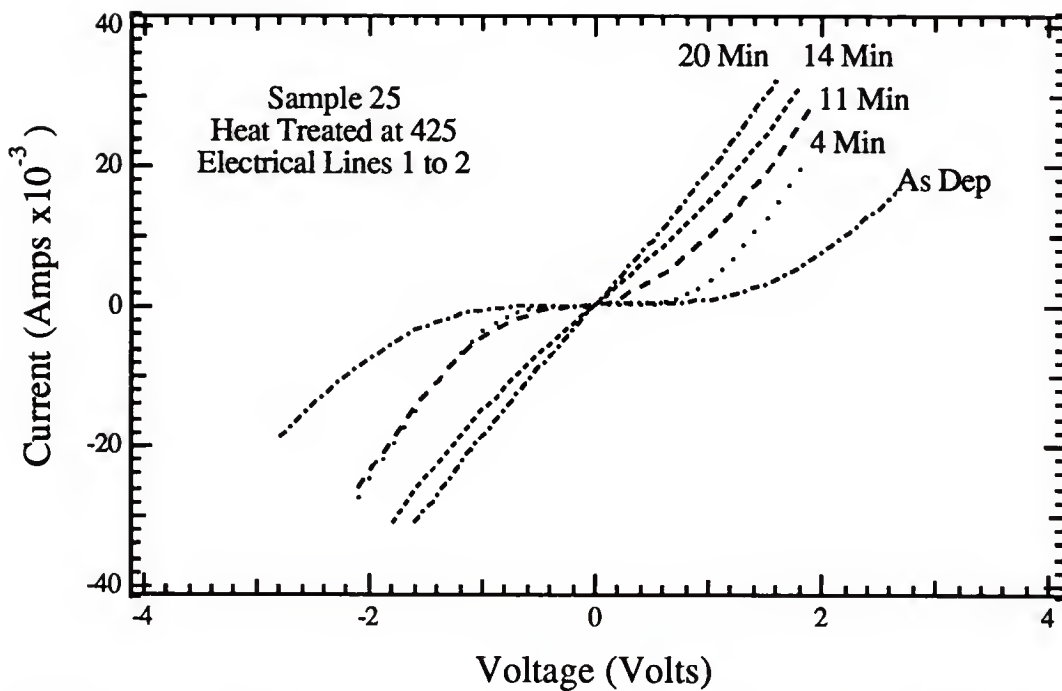


Figure 8. Series of I-V curves with increasing heat treatment time at 425° C for sample 25, electrical measurements between lines 1 and 2.

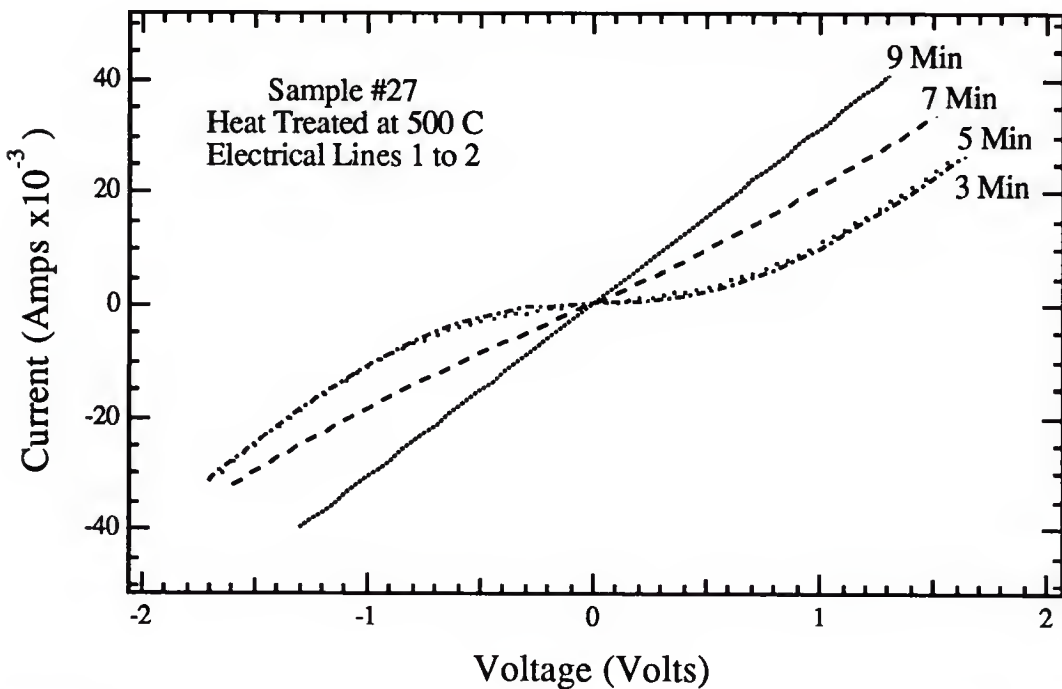


Figure 9. Series of I-V curves with increasing heat treatment time at 500° C for Sample 27, electrical measurements between lines 1 and 2.

Samples 25 and 27 were taken from the same 3 inch wafer, a LEC semi-insulating GaAs wafer with an ion implanted active layer ( $2.9 \times 10^{17} \text{ cm}^{-3}$  Si to a depth of 0.34  $\mu\text{m}$ ) and an ion implanted contact layer ( $1.0 \times 10^{18} \text{ cm}^{-3}$  Si to a depth of 0.16  $\mu\text{m}$ ). Both samples also have the same metal deposition sequence of Al/Ni/Ge/GaAs, but sample 25 was heat treated at 425° C for four 2 minute increments then for four 3 minute increments, totaling 20 minutes. The I-V profiles of sample 25 are shown in Figure 8. Sample 27 was heat treated at 500° C for one 3 minute increment and for three 2 minute increments, totaling 9 minutes. The I-V profiles of sample 27 are shown in Figure 9. The slope of the I-V plot of sample 25 was approximately 60% of that of sample 27 (i. e. sample 25 was more resistive). Thus to achieve a similar conversion to ohmic behavior requires slightly more than a factor of 2 longer time at 425° C than at 500° C. This clearly suggests that a thermally activated rate limiting mechanism was controlling the conversion from Schottky to ohmic behavior for the samples which have Ge adjacent to GaAs.

An effect due to changing from 425 to 500° C was not detected for samples with Ni adjacent to GaAs. The conversion from Schottky to ohmic behavior generally occurred in just a few minutes (refer to Table 1) when heat treated at either 425° C or 500° C. However, the real time I-V data reported below show that a temperature activated process is operative in conversion to ohmic behavior. There is clearly a difference in the mechanism or rate limiting step with Ni versus Ge adjacent to the GaAs.

The time required for the metallization to convert from Schottky to ohmic behavior was also dependent on the doping concentration of the contact layer. This effect was also observed only in samples with Ge adjacent to GaAs. For this comparison it was not possible to use the same GaAs wafer as the substrate for both samples, since the contact layer and its doping concentration were an integral part of the substrate. The series of I-V curves of samples 27 and 47, in Figures 9 and 6 respectively, show the

effect of substrate doping. Both samples were heat treated at 500° C and both samples had approximately 250Å of Ge as the first metal layer at the metal-semiconductor interface. The more heavily doped sample 27, with a Si ion implanted contact layer of  $1.0 \times 10^{18} \text{ cm}^{-3}$ , required 9 minutes to convert from Schottky to ohmic behavior. Sample 47, with a Si MBE grown contact layer of  $5.0 \times 10^{16} \text{ cm}^{-3}$  required 42 minutes to make the same conversion, a difference of nearly 5 times. Since the only major difference in these samples was the doping concentration of their contact layers, it was reasonable to attribute the difference in conversion time to the time required to create a Ge degenerative doped surface layer, probably due to Ge doping. Incorporation of Ge in the contact layer of the GaAs, as stated earlier, was a key part of the generally accepted mechanism for the formation of an ohmic contact from metal alloys such as Al-Ge-Ni or Au-Ge-Ni.

#### Real Time I-V Measurement and Heat Treatment

Because heat treatment temperatures apparently affected contacts differently depending upon whether Ge or Ni was adjacent to the GaAs, real time I-V measurements were used to investigate the effects of time. Both of the samples (28 and 29, see the appendices) used in this experiment became ohmic. The initial I-V curve of the as-deposited metallization of both samples was that of a Schottky barrier, as measured on the same system as samples measured iteratively. Both samples for the real time studies were also taken from the same 3 inch GaAs as samples 25 and 27, discussed above. The first sample, sample 28, had a layer sequence of Al/Ni/Ge/Ni/GaAs and the as-deposited I-V data are shown in Figure 10. After these data were collected, the sample was mounted on a quartz holder for insertion into the heat treatment furnace. The holder was equipped with thermocouple and electrical leads spring loaded to make contact with the TLM pads 1 and 3 on the sample.

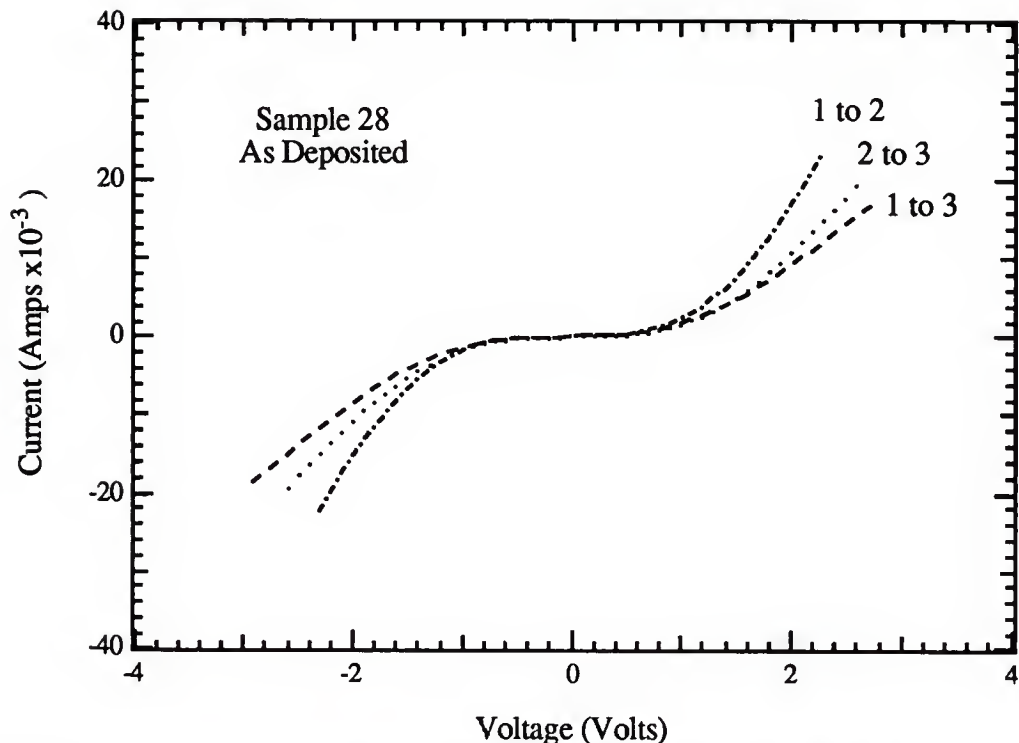


Figure 10. Room temperature I-V measurement of sample 28, as-deposited.

The I-V measurement made in the real time measurement system was also initially Schottky. As sample 28 was slowly inserted toward the furnace hot zone the I-V curve changed very quickly (less than 1 minute), the curve began to change at approximately 110° C. The changes were so rapid that they could not be photographed on the oscilloscope. As the sample was inserted further into the furnace, the temperature continued to rise and the I-V curve became linear at 150° C and less resistive as indicated by greater current at the same voltage (i. e. an increase in the slope of the I-V curve). By 180° C the changes in the I-V curve slowed dramatically, although the change in the slope of the I-V curve continued to slowly increase to approximately 300-325° C; by 380° C the slope had stopped increasing. The sample was inserted into the center of the furnace (425° C) and left there for approximately 2 min. Only a slight decrease was observed in the slope of the I-V curve during this time. As the sample was slowly removed from the furnace, the slope continued to decrease slowly. The entire experiment

occurred in 4 to 5 minutes. The I-V curve at room temperature after heating in the real time system was very similar to the curve shown in Figure 11, for sample 29.

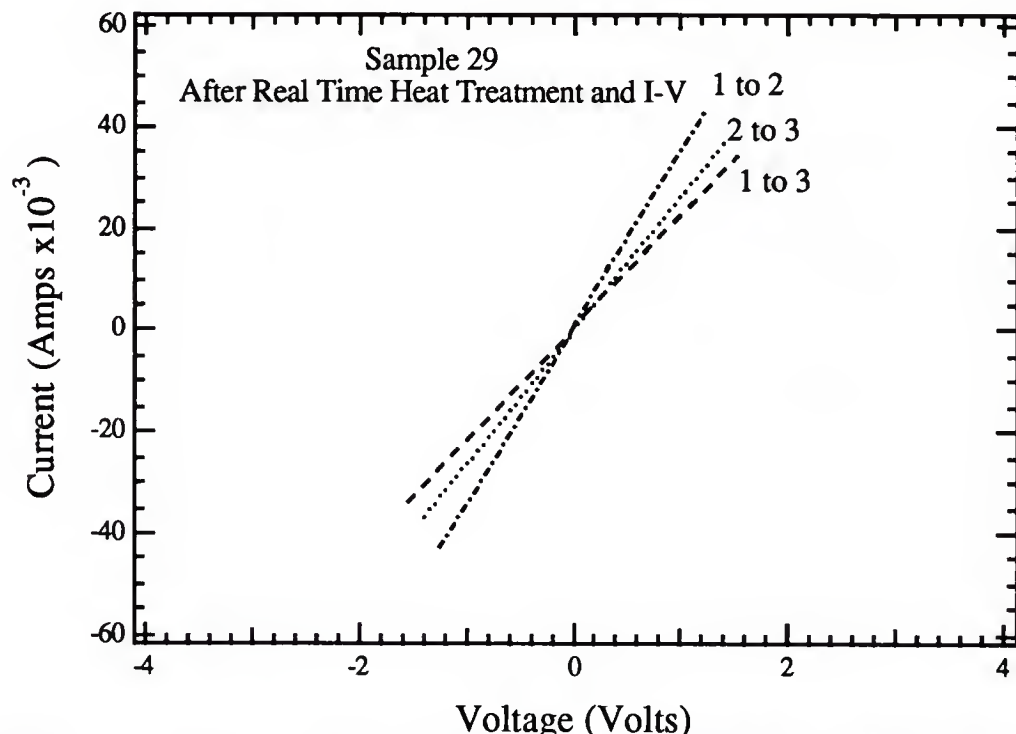


Figure 11. I-V measurement of sample 29 after the real time I-V measurement and heat treatment.

The second sample (sample 29) had a layer sequence of Al/Ni/Ge/GaAs. The initial I-V curve was Schottky as-deposited. This sample was moved toward the hot zone of the furnace more slowly and the I-V curve changed much more gradually than sample 28, consistent with the previous results for samples with Ge at the metal-semiconductor interface. Approximately 7 minutes elapsed before it reached a temperature of 275° C with little or no change in the I-V curve. At 275° C the breakdown voltage and the effective resistance decreased slowly. At a temperature of 340° C and an elapsed time of 10 minutes, the I-V curve became slightly asymmetric. By 350° C and an elapsed time of 12 minutes, the I-V curve was again symmetric with further reduction

in the breakdown voltage and effective resistance. The sample did not become ohmic until its temperature reached 430° C after approximately 15 minutes. Shortly after the sample became ohmic, electrical contact to this sample was lost. It was heat treated to a total of 20 minutes, then removed from the furnace. Of the 20 minutes, insertion of the sample to the center of the furnace consumed 15 minutes. The changes observed in the I-V curves are very similar to the series of I-V curves of sample 25, shown in Figure 8. The room temperature I-V curves for sample 29 after heating are shown in Figure 11.

The results from both samples 28 and 29 were completely consistent with the results from the samples iteratively heat treated and electrically characterized, even the observation of the I-V curves becoming asymmetric. In addition, the amount of heat treatment time required for the samples to become ohmic during the two different types of heat treatment was equal to within experimental error when the heat up and cool down for the iterative heat treatments were considered. The real time I-V measurement and heat treatment do show, however, that the sample with Ni adjacent to GaAs began to exhibit ohmic behavior as low as 180° C and had reached its lowest resistivity by approximately 325° C.

#### Summary of Current-Voltage Data

In summary, the electrical characterization has been used to demonstrate dramatic differences in the amount of heat treatment time and temperature required to convert Al-Ge-Ni from Schottky to ohmic behavior, depending on whether Ge or Ni was at the metal-semiconductor interface. The times and temperatures needed to become ohmic were also found to be dependent on the doping concentration of the contact layer. For samples with Ge at the metal-semiconductor interface, the time required to convert from Schottky to ohmic behavior took longer with lower doping concentration and with lower heat treatment temperature. For samples with Ni at the metal-semiconductor interface, the

time required to convert from Schottky to ohmic behavior was much less and about the same for both high and low doping at either 425 or 500° C. As indicated by the real time I-V measurement during heat treatment, the samples with Ni at the metal-semiconductor interface show ohmic behavior at lower temperature, similar to reports by Murakami et al.<sup>15</sup> A possible explanation for the longer times required to convert from Schottky to ohmic behavior for the low doped substrates with Ge at the metal-semiconductor interface, may be the time required for enough Ge incorporation into the GaAs to degenerately dope the contact layer n<sup>+</sup>. The contacts with Ni at the metal-semiconductor interface; however, convert from Schottky behavior to ohmic behavior much faster. It has been reported that Ni dissociates GaAs.<sup>27, 28</sup> Thus, a more likely explanation for degenerative doping for both types of samples is that Ni dissociates GaAs and causes faster incorporation of Ge. For the samples with Ge at the metal-semiconductor interface, the rate limiting step may simply be the time required for diffusion of Ni through the Ge layer to the metal-semiconductor interface. Further details on elemental profiles and phase formation are given in the next section.

The electrical lines defined by the Ta mask were intended to provide only a qualitative measurement of electrical performance, i.e. to determine when or if the Al-Ge-Ni metallizations converted to ohmic behavior. The emphasis of this study was to describe the metallurgical effects of changing the layering sequence. This study has not attempted to optimize the elemental ratios or the heat treatment processing to produce the lowest resistivity ohmic contact. However, it was possible to make an estimate of the contact resistivity by making several assumptions, all of which have deleterious effects on the accuracy of the measurement and would lead to overestimating the specific contact resistance. For example, the probe contact resistance was assumed to be negligible, the sheet resistance of the interface layer was assumed to be equivalent to the sheet resistance of the metal contact, and the contact spacings were assumed to be uniform from sample to sample and equal to the mask spacings; all of these assumptions are well known to cause

Table 2. Specific contact resistance estimate, assuming  $R_c = R_{sc}$ .

Sample Number	Specific Contact Resistance ohm·cm <sup>-2</sup>	Interface Metal	Heat Treatment	
			Time Min.	Temperature °C
19	$2.8 \times 10^{-2}$	Ge	13	425
20	$1.7 \times 10^{-1}$	Ni	3	500
25	$3.9 \times 10^{-1}$	Ge	20	425
26	$2.6 \times 10^{-2}$	Ni	2	500
27	$3.7 \times 10^{-2}$	Ge	9	500
28	$1.1 \times 10^{-1}$	Ni	~5	425
29	$7.4 \times 10^{-1}$	Ge	~20	425
30	$2.2 \times 10^{-1}$	Ni	3	500
39	$5.0 \times 10^{-2}$	Ni	2-50	425
43	$8.8 \times 10^{-2}$	Ni	2	500
47	$2.5 \times 10^{-6}$	Ge	44	500

inaccuracies in the specific contact resistivity. The calculated values are listed in Table 2. The calculation of specific resistivity is made from the equation  $r_c = R_c^2 W^2 / R_{sc}$  ( $r_c$  ≡ specific contact resistivity,  $R_c$  ≡ contact resistivity,  $R_{sc}$  ≡ sheet resistivity of the metal contact/semiconductor interface layer,  $W$  ≡ length of the contact). Values for  $R_c$  and  $R_{sc}/W$  are taken from plots of the resistance calculated from the I-V curves versus the contact spacing,  $R_c/2$  is the y-intercept and  $R_{sc}/W$  is the slope. R. E. Williams<sup>19</sup> has succinctly described of the TLM measurement technique and typical measurement errors. The large range specific contact resistance ( $10^{-6}$  to  $10^{-1}$ ) in Table 2 probably indicate random error in measurement in addition to the systematic errors associated with contact probe resistance and contact spacing. Minor errors in measurement of  $R$  or spacing can cause large errors (orders of magnitude) in contact resistance. The measurements would also be improved by using a wire bonded to the contact rather than contact probes and by more accurate placement of the line spacings.

### Elemental Depth Profiles

#### Three Element Contacts

Auger depth profiling was used to investigate the interdiffusion of the contact metals and the semiconductor as-deposited and after heat treating to form an ohmic contact. The Auger survey scans of the as-deposited metals indicated the surface layer of the metal has the usual contamination from O and C of surfaces exposed to the atmosphere. The Auger survey scan of sample 20, shown in Figure 12, is typical for all of the as-deposited metallized samples. These surface contaminants were quickly sputtered away (~2 minutes) during the Auger depth profiling. The metal films contained very little or no C or O below the sample surface. A few of the early metallized substrates were not cleaned and they had C and O at the metal-semiconductor interface.

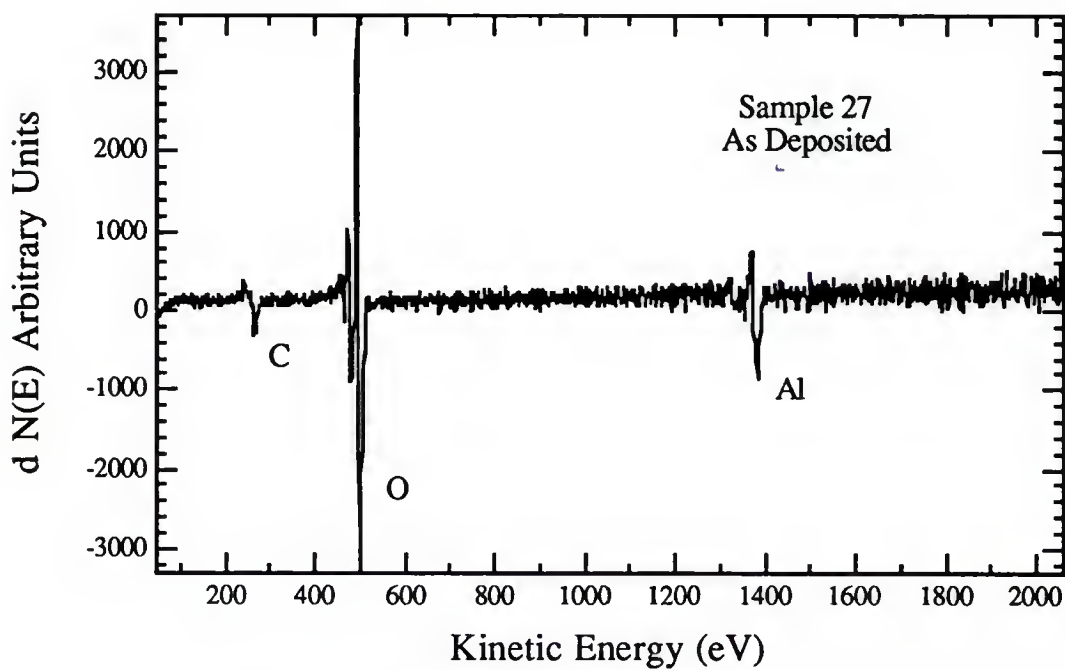


Figure 12. Auger survey scan of sample 27, as-deposited.

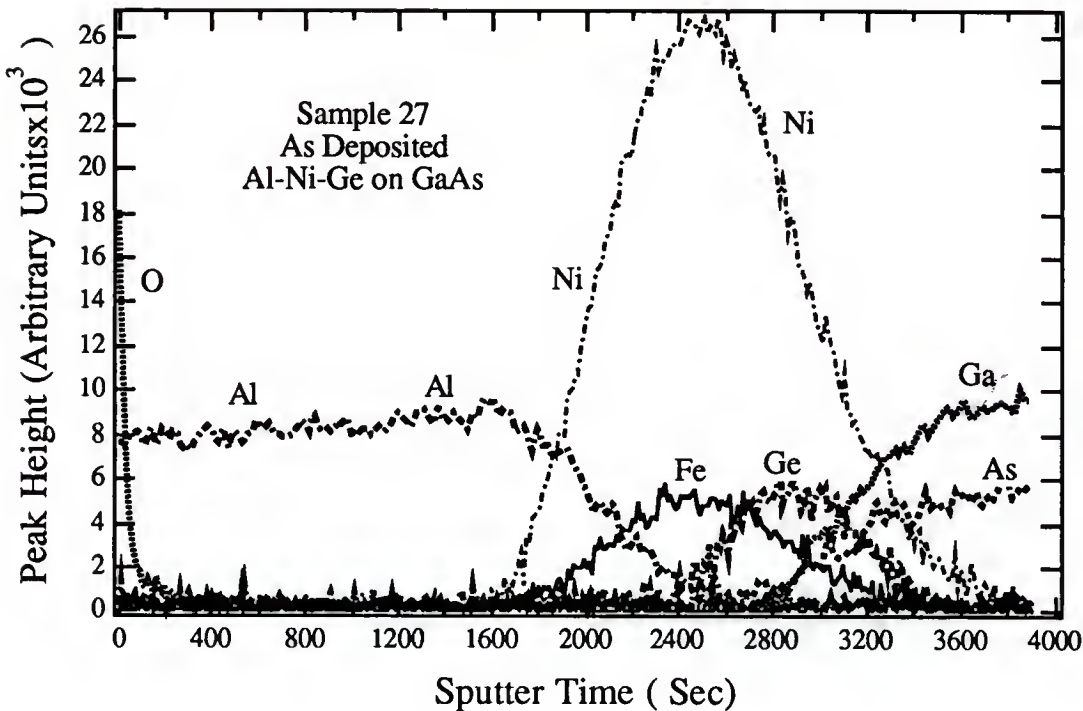


Figure 13. Auger depth profile of sample 27, as-deposited, Al/Ni/Ge on GaAs.

Auger depth profiles appear to indicate a slight interdiffusion between Al and Ni, and a very extensive interdiffusion between Ni and Ge in the as-deposited condition. This is shown in Figure 13 for sample 27, which consists of Al (2000 Å)/Ni (500 Å)/Ge (250 Å)/ion implanted GaAs. There appears to be some in-diffusion between Ni and Ge with GaAs, with little out-diffusion of the Ga or As into the metal layers. The suggestion from Auger depth profiles of interdiffusion of Ni and Ge agrees with the results of Liliental-Weber et al.<sup>20</sup> and Graham et al.<sup>21, 23</sup> who reported interdiffusion and Ge-Ni phase formation in their electron beam as-deposited samples. However, they also report out-diffusion of Ga and As into the metals, which was not observed in this study.

There was no observable difference in the Auger depth profiles of as-deposited contact metallizations with and without the 50 Å of Ni at the metal-semiconductor interface. Sample 26 had the Ni at the interfacial layer and only limited interdiffusion of the Al and Ni is seen in Figure 14. The depth profiles for samples 26 and 27 are very

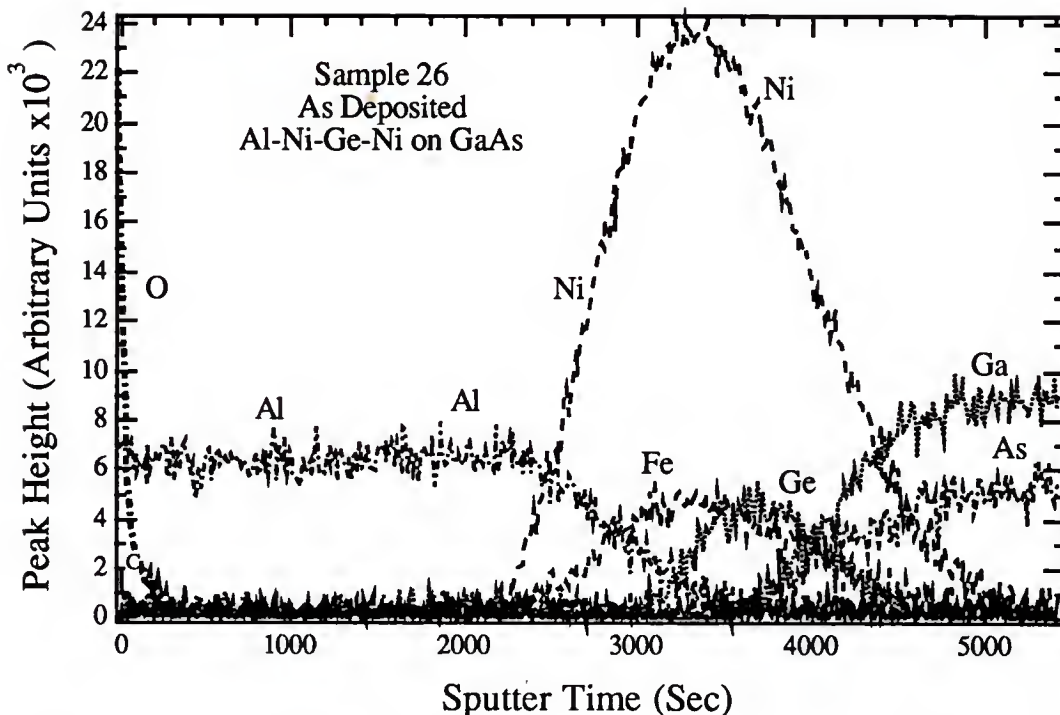


Figure 14. Auger depth profile of sample 26, as-deposited, Al/Ni/Ge/Ni on GaAs.

similar with respect to interdiffusion as found by comparing data in Figures 14 and 13, respectively. It was apparent however, that the Ni and Ge profiles overlap slightly more in sample 26 versus sample 27. This was attributed to Ni being at the metal-semiconductor interface and the interdiffusion of Ni into the Ge from both directions for sample 26. There may also be deeper Ni penetration into the GaAs substrate in sample 26. Note that the sputter time for sample 26, shown in Figure 14, is much greater than for sample 27, shown in Figure 13 because the ion beam raster size was increased for sample 26 to sputter at a slower rate and increase the depth resolution. The difference in the sequence of the metals at the substrate interface in the as-deposited contact samples as well as the claims of interdiffusion cannot be easily discerned from these Auger depth profiles due to intermixing during the deposition during the sputtering process. The ion sputtering process can also cause ion mixing and ion knock-on.<sup>76</sup> Therefore the interdiffusion must be corroborated with another analytical technique.

Contamination by Fe was detected on many of the samples. The Fe was always associated with the Ni layers, and is known to be a frequent contaminant of even highly refined Ni. The Fe concentration was 10 - 15% of the Ni layer based on quantitation using Auger peak-to-peak values and handbook sensitivities.<sup>77</sup> However, the depth profiles show that the Fe did not interdiffuse in the metal layers as much as the Al, Ni, and Ge and therefore probably did not modify diffusion between and phase reaction of the contact metals with the semiconductor. Fe in the GaAs is a deep level electron trap which would impede charge transfer required for ohmic conduction and make the contact more resistive. Because of the lack of diffusion and the fact that ohmic contacts were observed, the Fe is not believed to have an important effect on the behavior of this contact metallization system.

Heat treated samples showed varying degrees of further intermixing of metal layers, the degree of which correlates with temperature and time. Nearly complete interdiffusion of the metal layer components was observed for samples heat treated at higher temperature or for longer periods of time at the lower temperature, while less interdiffusion was observed at lower temperatures for shorter times. For example, sample 27 was iteratively heat treated at 500° C for 9 minutes total. From the I-V data in Figure 7, sample 27 converted from Schottky to ohmic behavior between 7 and 9 minutes. The Auger depth profile in Figure 15 shows that the contact metals have completely interdiffused after 9 minutes at 500° C. The Al appears to have completely intermixed with the Ni and Ge layers and was present at the metal-semiconductor interface. While reaction of Al to form an AlGaAs layer was suggested by Graham et al.<sup>22, 23</sup> as a possible explanation of the conversion to ohmic behavior, no evidence to support such a mechanism was found in previous studies or this study. The Ni appears to have diffused towards and away from the metal-semiconductor toward the surface and is distributed throughout the metal contact. The Ni and Ge penetration into the GaAs does not appear to be much different for sample 27 before or after heat treatment. While

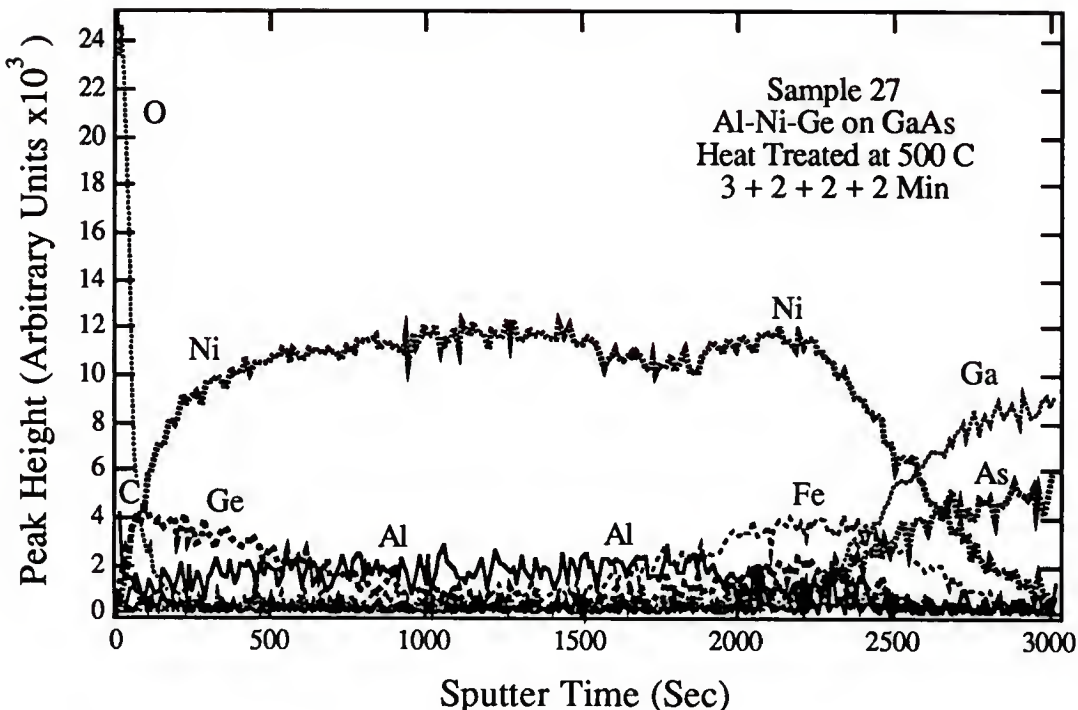


Figure 15. Auger depth profile of sample 27, after 500° C heat treatment for 9 minutes total time, Al/Ni/Ge on GaAs.

the Ga and As appear to have interdiffused with the metal layer slightly more than in the as-deposited samples, no Ga or As were detected at the ambient interface of in the metal layers. This indicates no out-diffusion occurred for either element. The Ge is concentrated both at the metal/semiconductor and at the metal/ambient interfaces. This depth profile was representative of the depth profiles for all of the samples heat treated at 500° C.

Samples heat treated at 425° C exhibited less interdiffusion for time shorter than 15 minutes. The Auger depth profile of sample 19 (Al (2000Å)/ Ni (400Å)/ Ge (300Å)/ GaAs) was heat treated at 425° C for a total time of 13 minutes in increments of 3, 2, 2, 3, and 3 minutes, as shown in Figure 16. Diffusion of Ni into both Al and Ge is evident, but no Ge was detected at the ambient interface. Interdiffusion of the metal layer components was observed for samples heat treated at higher temperature or for longer periods of time at the lower temperature, while less interdiffusion was observed at lower

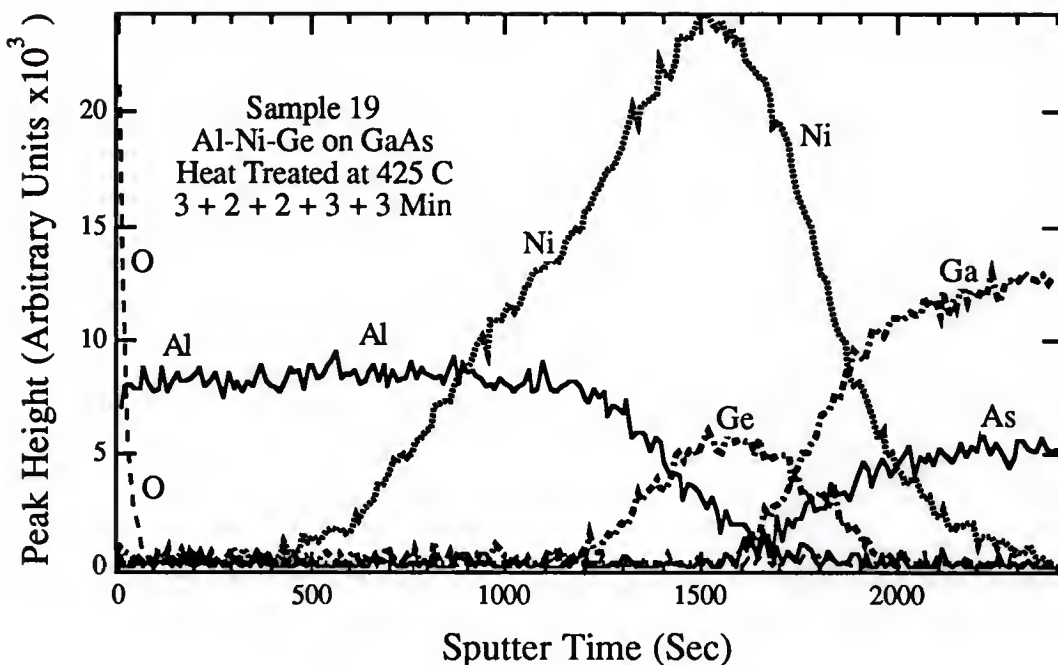


Figure 16. Auger depth profile of sample 19, after 425° C heat treatment for 13 minutes total time, Al/Ni/Ge on GaAs.

temperatures for shorter times. For example, sample 27 was iteratively heat treated at 500° C for 9 minutes total. From the I-V data in Figure 7, sample 27 converted from Schottky to ohmic behavior between 7 and 9 minutes. The Auger depth profile in Figure 15 shows that the contact metals have completely interdiffused after 9 minutes at 500° C. The Al appears to have completely intermixed with the Ni and Ge layers and was present at the metal-semiconductor interface. While reaction of Al to form an AlGaAs layer was suggested by Graham et al.<sup>22, 23</sup> as a possible explanation of the conversion to ohmic behavior, no evidence to support such a mechanism was found in previous studies or this study. The Ni appears to have diffused towards and away from the metal-semiconductor toward the surface and is distributed throughout the metal contact. The Ni and Ge penetration into the GaAs does not appear to be much different for sample 27 before or after heat treatment. While the Ga and As appear to have interdiffused with the metal layer slightly more than in the as-deposited samples, no Ga or As were detected at the

ambient interface or in the metal layers. This indicates no out-diffusion occurred for either element. The Ge is concentrated both at the metal/semiconductor and at the metal/ambient interfaces. This depth profile was representative of the depth profiles for all of the samples heat treated at 500° C.

In the early samples, Ge was seen quite distinctly to form dendritic-like florets on the surface of metal on either GaAs or sapphire substrates. Florets were observed on samples with a high Ge concentration (e. g. a Ge/Ni ratio of 3:4), but not on samples with a lower Ge/Ni ratio (e. g. 1:2) and did not depend on whether Ge or Ni was adjacent to the substrate. An SEM image of sample 20, heat treated at 500° C for 3 minutes (Figure 17) shows the Ge florets. Precipitates of Ge were observed by Graham et al.<sup>22, 23</sup> for Al-Ge-Ni ohmic contact samples with similar Ge to Ni (1:1) ratios, and have been reported for excess Ge in the Au-Ge-Ni contacts.<sup>28, 44-46</sup> After Ar<sup>+</sup> sputtering to remove surface contamination, Auger analysis showed that the florets were pure Ge.



Figure 17. SEM micrograph of sample 20 after heat treatment at 500° C for 3 min.

Samples with various Al-Ge-Ni sequences deposited on sapphire were also depth profiled before and after heat treatment. Their Auger depth profiles were very similar to those of the contacts grown on GaAs. For example, the depth profiles of those samples heat treated at 500° C indicated the same interdiffusion. As stated previously, even the Ge out-diffusion and floret growth on the surface was observed for a 3 to 4 ratio of Ge to Ni.

### Two Element Metallizations

To better understand intermixing, samples without the outer 2000Å layer of Al were Auger sputter profiled. The 1 to 2 ratio of Ge to Ni [Ge(250Å)/Ni(500Å) or Ni(50Å)/Ge(250Å)/Ni(450Å)] was grown on both GaAs and sapphire. Depth profiles of as-deposited samples indicated that the metals did not interdiffuse as much when Al was present. The Auger depth profile of sample 34 [Ni(450Å)/Ge(250Å)/Ni(50Å)/sapphire] shown in Figure 18, and the 50Å layer of Ni is easily observed. This was also true for similar metallizations on GaAs. Auger depth profiles of samples with Ge adjacent to the substrate indicated the Ni has penetrated the Ge layer, but not nearly as much as indicated in the depth profiles of contacts with all three elements. This result was consistent with the difference in electrical characterization results for heat treatment times required to convert the samples from Schottky to ohmic behavior, which indicated a major difference with and without Ni at the GaAs interface. The two component system on sapphire show the Ni/Ge/Ni layers did not completely intermix during deposition.

In another type of the 2-element sample, two of the three metals were deposited in four alternating layers of 250Å each (i. e. a 1:1 ratio) onto both GaAs and sapphire. Auger depth profiles of the as-deposited samples of Ni and Ge and similar samples of Al and Ni deposited on both GaAs and sapphire appeared to be layered with some interdiffusion between the layers. While the three layers of Ni/Ge/Ni for sample 34 were obvious, as shown Figure 18, the four layer samples of Al/Ge/Al/Ge/GaAs appeared to

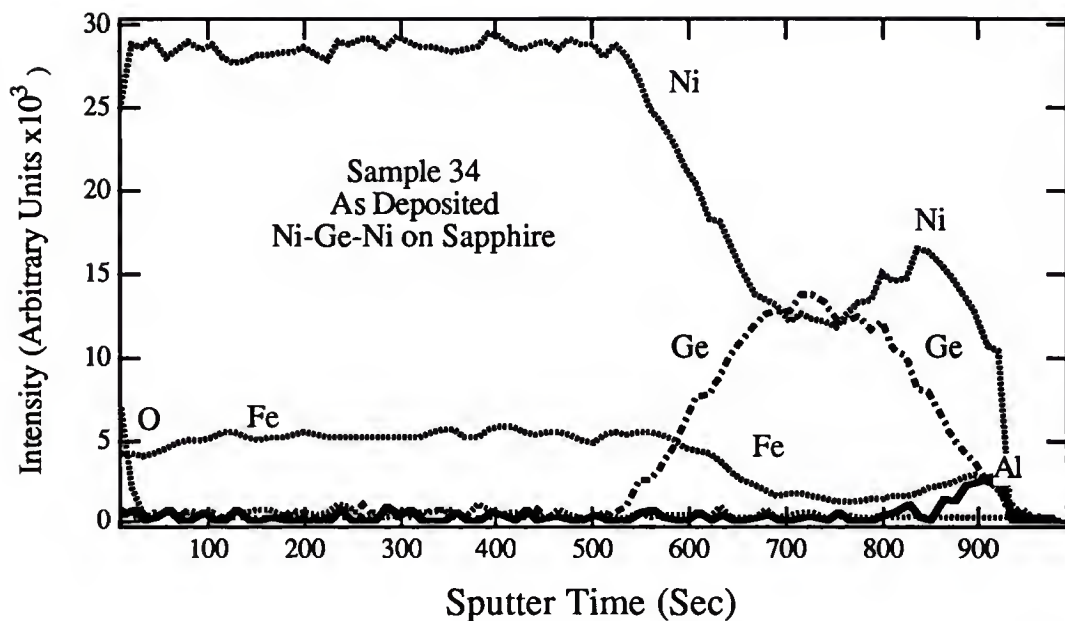


Figure 18. Auger depth profile of sample 34, as-deposited, Ni/Ge/Ni on sapphire.

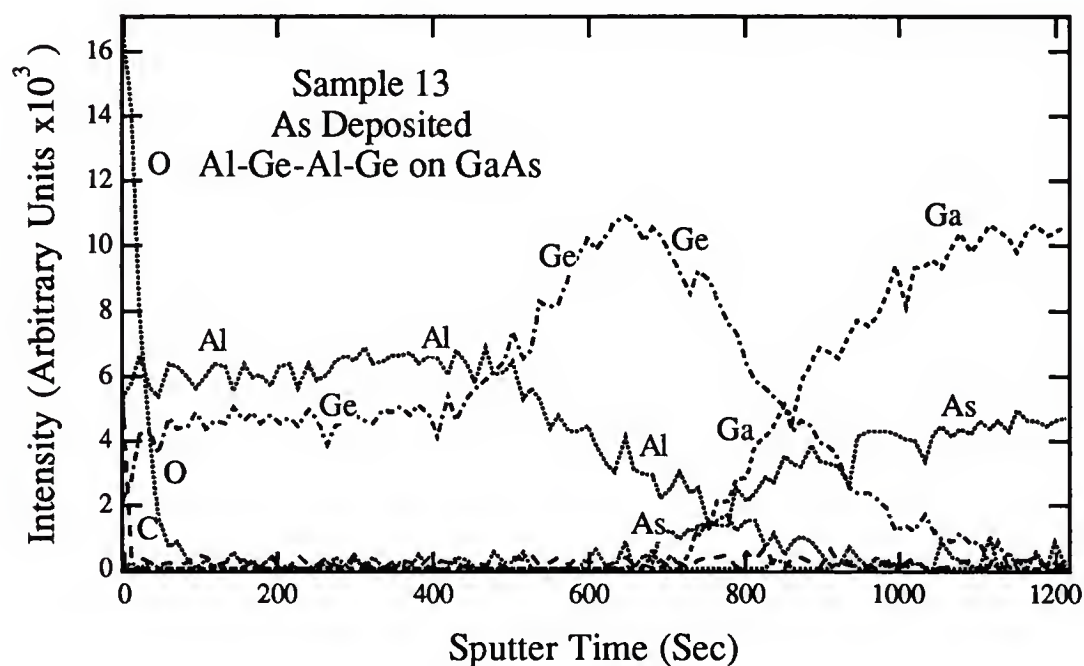


Figure 19. Auger depth profile of Sample 13, as-deposited, Al/Ge/Al/Ge, 250 Å each, on GaAs.

have rearranged themselves as indicated by the Auger depth profile of sample 13, shown in Figure 19. The Auger depth profile would suggest that the four layers have rearranged with Ge diffusing to the substrate and Al diffusing to the ambient during deposition in the Al/Ge samples. The Auger depth profile of the same metallization deposited onto sapphire during the same deposition, also exhibited this rearrangement.

The 2-element 4 layer samples on GaAs and sapphire were heat treated at 500° C for 4 minutes. The Auger depth profiles of the Ni and Ge samples deposited on both GaAs and sapphire indicate complete interdiffusion. The Auger depth profiles of the Al and Ni samples deposited on GaAs and sapphire were different, with limited interdiffusion on GaAs but complete on sapphire. The depth profiles of Al and Ge deposited on both GaAs and sapphire after heat treatment appear to be dominated by their original surface morphology.

#### Summary of Elemental Depth Profiles

Auger survey scans have been used to demonstrate that the surfaces of the samples exposed to the atmosphere were contaminated with O and C. The Auger survey scans were also used to identify surface florets on high Ge:Ni ratio samples as being pure Ge. At Ge:Ni ratios  $\leq 2$ , the layers remain uniform; however, if the ratio of Ge:Ni was  $\sim 3:4$ , the contact layer became laterally nonuniform, similar to the Au-Ge-Ni contacts.<sup>44</sup> Thus the ratio of Ge to the other materials is important with excess Ge causing out-diffusion and precipitation on the surface during heat treatment.<sup>28, 44-46</sup> Crouch et al.<sup>45</sup> have reported a dendritic growth precipitating to the surface which they identify as a 1 to 1 Ge to Au for Au-Ge contacts heated by RTA. Precipitation of Ge rich compounds on the surface of the sample was shown to be controlled in this study by reducing the ratio of Ge to Ni.

Although the depth profiles of the thicker, complete contact samples must be interpreted with caution, the Al and Ni layers and the Ni and Ge layers appear to exhibit some interdiffusion both as-deposited and heat treated. The difference in layering sequence of the Ni and Ge layers was only evident in the Auger depth profiles without the thick Al layer due to artifacts causing poor depth resolution in the sputter profiles. However, intermixing during deposition is in agreement with previous works on both the Al-Ge-Ni and the Au-Ge-Ni contact systems. For example, as-deposited samples of Al-Ge-Ni contacts from separately evaporated Ni-Ge layers were found to be intermixed on a GaAs substrate as determined with convergent beam electron diffraction (CBED) by Liliental-Weber et al.<sup>20</sup> Depth profiles after conversion from Schottky to ohmic electrical behavior indicate varying degrees of interdiffusion. Interdiffusion was extensive for samples heat treated at 500° C and limited for heat treatment at 425° C for times <15 minutes. For Au-Ge-Ni contacts, the sequence of evaporation was reported not to affect the final arrangement of constituents after heat treatment.<sup>28, 37, 40, 47, 49, 63</sup> While a difference in the mixing between the two different sequences was not obvious from Auger depth profiles, the electrical results were dramatically affected by the layering sequence. According to the elemental profiles, the arrangement of metal components after conversion from Schottky to ohmic behavior ranges from limited interdiffusion to extensive interdiffusion. These results demonstrate that the electrical measurements are sensitive to small metallurgical changes, and that complete interdiffusion was not critical to ohmic contact formation. Even limited metallurgical changes obviously were sufficient to form the phase or cause the diffusion necessary to achieve ohmic behavior. In fact the increased resistance at longer times during real time I-V measurement suggest complete interdiffusion may be detrimental. Further details of phase formation based upon X-ray diffraction analysis are discussed below.

## Diffraction Analysis of Phase Formation in Al-Ge-Ni Thin Films

### Three Element Metallization

As stated earlier, X-ray diffraction was chosen to identify the phases formed during the heat treatment necessary for conversion from Schottky to ohmic electrical behavior. Glancing angle X-ray diffraction was performed on various samples, such as those with complete three element or two element metallization on either GaAs or sapphire. The goal of the XRD analysis was to identify the phases present after processing and to correlate this information with the interdiffusion results of the Auger depth profiles and the electrical characterization results.

Both of the different layering sequences for the complete contact metallization were examined with X-ray diffraction. As-deposited, diffraction peaks were strong from elemental Al, with much weaker peaks due to GaAs, elemental Ge, and elemental Ni. Very weak peaks consistent with  $\text{Al}_3\text{Ni}$ ,  $\text{GeNi}$ , and  $\text{Ge}_3\text{Ni}_5$  were also detected. For example, an XRD spectra from sample 43 taken at  $8^\circ$  incidence angle is shown in Figure 20. The chances of diffraction from the single crystal substrate is greatly reduced in the glancing angle mode since the incidence angle is fixed. To increase the probability of diffraction from the sample, data was collected at two incidence angles ( $4^\circ$  and  $8^\circ$ ). Common to nearly all samples were broad peaks at the peak positions of GaAs and/or Ge. It is difficult to conclude on the basis of position alone, whether the diffraction is from Ge or GaAs, since their lattice parameters are so similar. However, the low intensity, broadened peaks were also seen in spectra of the two element samples without Ge. Therefore, the broad low intensity peaks were attributed to strain induced in the GaAs by the thin metal films in the absence of Ge. Ge may contribute to these peaks when it is present. Diffraction peaks can be broad if the sample has phases with very small crystallite sizes, or contain microstresses, disorder, stacking faults, dislocations, and/or inhomogeneous solid solutions. The width of the diffraction peak will also

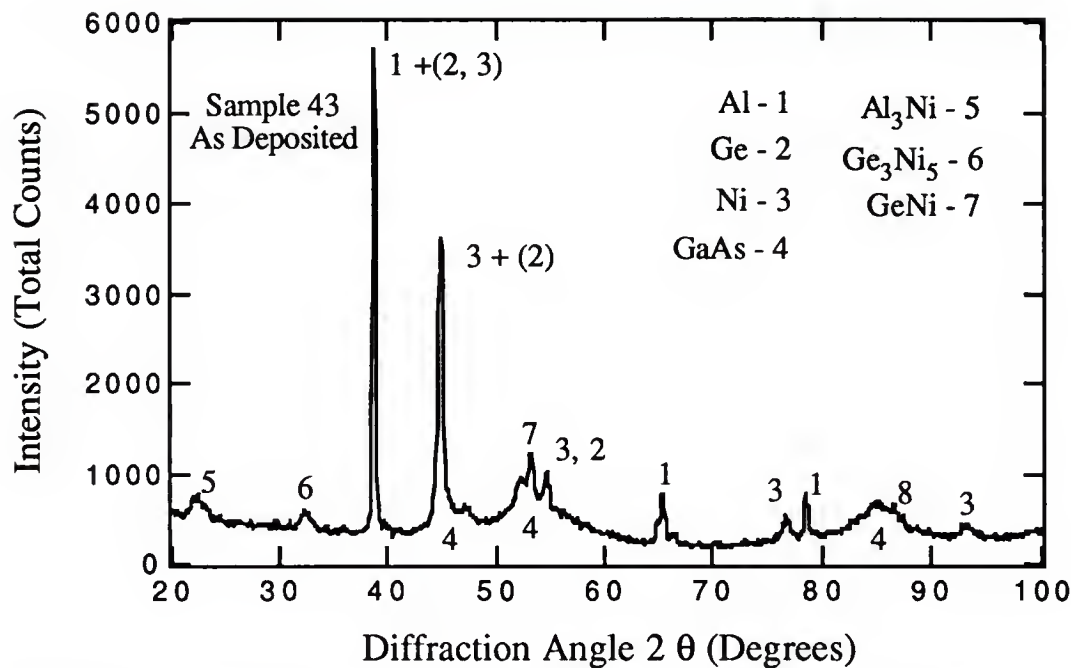


Figure 20. XRD Spectra of Sample 43, as-deposited, Al-Ni/Ge/Ni on GaAs

Table 3. X-ray Diffraction data for as-deposited Al-Ge-Ni metallization. The numbers indicate the probability that the phase is present. (4 - Many of the peaks, 3 - Some of the peaks, 2 - Several of the peaks, 1 - One or two of the peaks from the phase detected, No entry - No indication of the phase).

Sample Number	43	43	47	47
Layering	Al-Ni-Ge-Ni	Al-Ni-Ge-Ni	Al-Ni-Ge	Al-Ni-Ge
Incidence Angle	8	4	8	4
Al	4	4	4	4
Ge	2	2	2	2
Ni	3	3	3	3
GaAs	2	2	2	2
Al <sub>3</sub> Ni	1	2	2	3
GeNi	1		1	
Ge <sub>3</sub> Ni <sub>5</sub>	2		2	3

increase as the film thickness decreases. Thus, the peak broadening of GaAs and/or Ge peaks seen in Figure 20 can be attributed to microstresses in the GaAs substrate caused by the metal overlayer, an amorphous or small crystallite size for Ge, the thinness of the Ge layer, or a combination of these factors.

X-ray diffraction data from as-deposited samples 43 (Al/Ni/Ge/Ni) and 47 (Al/Ni/Ge), are summarized in Table 3. The table utilizes numbers to indicate the existence of the particular phases, with 4 indicating the highest probability and 1 indicating the lowest probability of the presence of that phase. No entry means that no evidence for that phase was detected in that particular sample. There were no differences in the phases identified in the three element as-deposited samples for Ni versus Ge adjacent to GaAs.

For contact metallizations heat treated at either 500° C or 425° C, XRD data were collected from a cross-section of samples with both types of layering sequences. Common to all heat treated samples was the increased formation of the Al<sub>3</sub>Ni phase, with nearly all of the peaks from this phase being present. Their peak intensities did not correspond to those of the ICDD card, as the data were collected in the glancing angle mode. Also common to nearly all of the heat treated samples were broad peaks at the peak positions of GaAs and/or Ge. The XRD spectra for sample 43 after heat treatment for 2 minutes at 500° C is shown in Figure 21. In addition to the Al<sub>3</sub>Ni and the broad GaAs and/or Ge peaks, peaks from elemental Al, AlNi<sub>3</sub>, GeNi, GeNi<sub>2</sub>, Ge<sub>3</sub>Ni<sub>5</sub>, Ga<sub>2</sub>Ni<sub>3</sub>, Ni<sub>4</sub>GaGe<sub>2</sub>, and Ni<sub>5</sub>As<sub>2</sub> phases have been identified. For samples with Ni at the metal semiconductor interface and heat treated at 500° C, the XRD data have strong peaks from Al<sub>3</sub>Ni as well as elemental Al and GaAs. The indications of GeNi, Ge<sub>3</sub>Ni<sub>5</sub>, Ga<sub>2</sub>Ni<sub>3</sub>, Ga<sub>3</sub>Ni<sub>2</sub>, Ni<sub>5</sub>As<sub>2</sub>, and Ni<sub>4</sub>GaGe<sub>2</sub> phases were based on peak position, but the intensities of the peaks from these phases were weak even after collecting data for 69 hours. Samples heat treated to 500° C with interfacial Ni always converted from Schottky to ohmic behavior in 2 to 4 minutes, allowing less time for interdiffusion or extensive phase

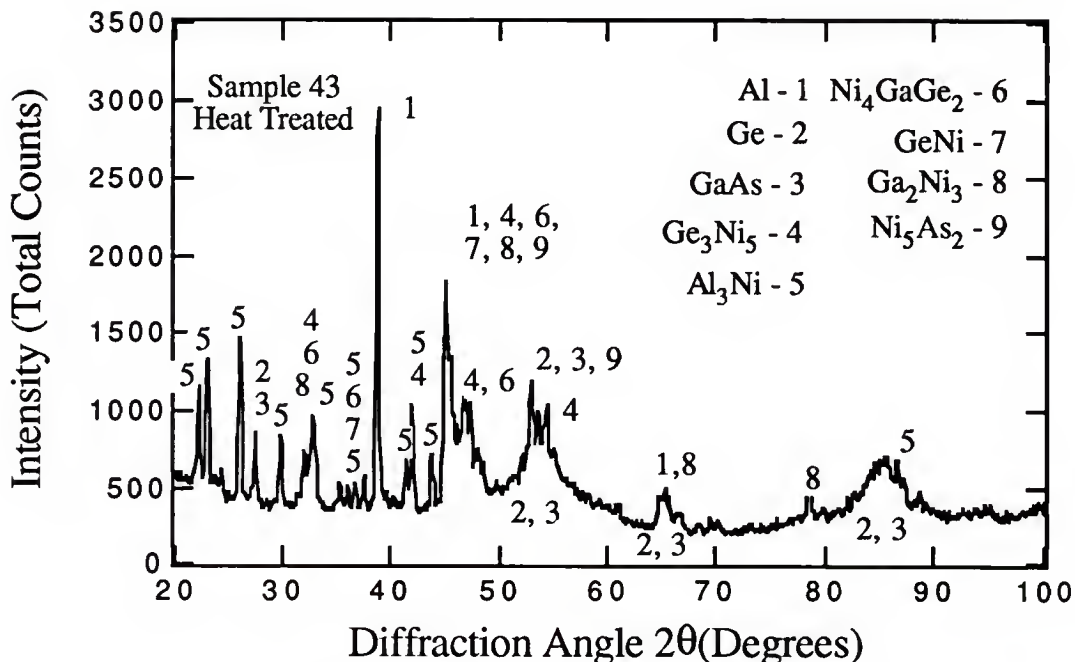


Figure 21. XRD Spectra of Sample 43, After 500° C Heat Treatment for 2 Minutes.

formation. In addition, peak overlaps from these phases are quite extensive, so they cannot be unambiguously identified. Few if any diffraction peaks could ever be identified with iron, presumably because Fe was in solid solution with Ni and XRD from a separate phase was unlikely. Representative examples of X-ray diffraction data from samples 31 (Al/Ni/Ge), 43 (Al/Ni/Ge/Ni), and 47 (Al/Ni/Ge) after being heat treated at 500° C are summarized in Table 4. All of the samples listed in this table were heat treated and electrically characterized by the iterative procedure described earlier. According to the XRD data, the samples with Ge at the metal semiconductor interface (samples 31 and 47) heat treated for 50 and 44 minutes, respectively, have many of the same phases as sample 43 (e. g. Al<sub>3</sub>Ni, GeNi, Ni<sub>4</sub>GaGe<sub>2</sub>). These type of samples exhibit more NiAs<sub>2</sub> and Ni<sub>5</sub>As<sub>2</sub> phases. Although no effort was made to quantify the XRD data due to the large number of peaks which overlap, the peaks assigned to the Ni<sub>4</sub>GaGe<sub>2</sub> phase were more intense for sample 47 than for sample 31. Despite these similarities, sample 47 converted from Schottky to ohmic behavior, while sample 31 did not convert

to ohmic behavior. With Ni at the interface (sample 43) more  $\text{Ge}_3\text{Ni}_5$ ,  $\text{GeNi}_2$  phases were observed (higher percent Ni concentration). The samples with Ni at the interface have slightly greater indication of Ge-Ni and Ga-Ni phases while those with Ge at the interface have more indication of Ni-As phases and the NiGe phase (lower percent Ni concentration).

Table 4. X-ray diffraction data after heat treatment at 500° C from the complete contact metallization with Ni at the metal/semiconductor interface. The numbers indicate the probability that the phase is present. (4 - Many of the peaks, 3 - Some of the peaks, 2 - Several of the peaks, 1 - One or two of the peaks from the phase detected, No entry - No indication of the phase).

Sample Number	43	43	31	31	47	47
Layering	Al-Ni-Ge-Ni	Al-Ni-Ge-Ni	Al-Ni-Ge	Al-Ni-Ge	Al-Ni-Ge	Al-Ni-Ge
Temperature	500	500	500	500	500	500
Time (Min)	2	2	50	50	44	44
Incidence Angle	8	4	8	4	8	4
Al	3	3	1		1	
Ge	3	3	2	2	1	1
Ni					1	
GaAs	3	3	2	2		1
$\text{Al}_3\text{Ni}$	4	4	4	4	4	4
$\text{AlNi}_3$	1	1		1	3	3
$\text{GeNi}$	3	3	2	3	3	3
$\text{Ge}_3\text{Ni}_5$	4	3	1	1		
$\text{GeNi}_2$	3	3				
$\text{Ga}_2\text{Ni}_3$	4	4		3		
$\text{NiAs}(\text{Ge})$			1	3	3	2
$\text{NiAs}_2$			3	3	3	2
$\text{Ni}_5\text{As}_2$	1	1	2	3	3	2
$\text{Ni}_4\text{GaGe}_2$	4	3	3	3	3	3

For samples heat treated at 425° C, the X-ray diffraction data are summarized in Tables 5 and 6 for samples with Ge or Ni at the metal/semiconductor interface, respectively. All of the samples heat treated at 425° C, similar to those heat treated at

Table 5. X-ray diffraction data after heat treatment at 425° C from the complete contact metallization with Ge at the metal/semiconductor interface. The numbers are as described in the caption for Table 4.

Sample Number	29	29	45	45
Layering	Al-Ni-Ge	Al-Ni-Ge	Al-Ni-Ge	Al-Ni-Ge
Temperature	425	425	425	425
Time (Min)	RT ~20	RT ~20	100	100
Incidence Angle	8	4	8	4
Al	1	1	1	1
Ge	3	3	3	3
GaAs	3	3	3	3
Al <sub>3</sub> Ni	4	4	4	4
AlGe	3	3	3	3
GeNi	3	3	3	3
GeNi <sub>2</sub>			1	1
Ga <sub>2</sub> Ni <sub>3</sub>			1	1
NiAs <sub>2</sub>		1	2	2
Ni <sub>5</sub> As <sub>2</sub>	1	1	2	2

500° C, had XRD spectra with indications of Al<sub>3</sub>Ni and the broad GaAs/Ge peaks. Samples 29 (Al/Ni/Ge) and 28 (Al/Ni/Ge/Ni) were heat treated and electrically characterized in real time. The primary difference in the XRD data from these two samples was, again, that with Ge first more GeNi phase was present, while with Ni first more Ge<sub>3</sub>Ni<sub>5</sub>, GeNi<sub>2</sub>, and Ga<sub>2</sub>Ni<sub>3</sub> phases were present, similar to samples 43 and 47. There generally seems to be more Ni-As phases present with Ge first; however, some was observed with Ni first also. Recall that sample 29 (heated to 425° C) took several times longer to convert from Schottky to ohmic behavior compared to sample 28 (heated to 500° C). Samples 45 (Al/Ni/Ge) and 39 (Al/Ni/Ge/Ni) were heat treated and electrically characterized by the iterative procedure. Sample 45, with Ge first, did not completely convert to ohmic behavior even after 100 minutes at 425° C, since its I-V curve was nearly, but not completely linear. Sample 39 converted from Schottky to

Table 6. X-ray diffraction data after heat treatment at 425° C from the complete contact metallization with Ni at the metal/semiconductor interface. The numbers are as described in the caption for Table 4.

Sample Number	28	28	39	39
Layering	Al-Ni-Ge-Ni	Al-Ni-Ge-Ni	Al-Ni-Ge-Ni	Al-Ni-Ge-Ni
Temperature	425	425	425	425
Time (Min)	RT ~5	RT ~5	50	50
Incidence Angle	8	4	8	4
Al	1	1		
Ge	2	2	2	2
Ni	1	1		
GaAs	3	3	2	2
Al <sub>3</sub> Ni	4	4	4	4
Ge <sub>3</sub> Ni <sub>5</sub>	2	2	2	2
GeNi <sub>2</sub>	2	2		
Ga <sub>2</sub> Ni <sub>3</sub>	2	2	3	3
NiAs(Ge)			3	3
NiAs <sub>2</sub>			1	1
Ni <sub>5</sub> As <sub>2</sub>	1	1	2	2

ohmic behavior, with two of the electrical lines being converted in 4 minutes, while the last line required 50 minutes. Each sample was electrically characterized and heat treated in 2 minute increments up to 40 minutes, then in 10 minute increments to 50 minutes total time for sample 39 and to 100 minutes total time for sample 45. The primary difference, as indicated by XRD data, was the presence of Al<sub>3</sub>Ni and Ni<sub>3</sub>Ge for sample 45 with Ge deposited first, and the presence of Ge<sub>3</sub>Ni<sub>5</sub>, Ga<sub>2</sub>Ni<sub>3</sub>, and NiAs(Ge) for sample 39 with Ni deposited first, similar to the samples discussed previously. The XRD data for samples 45 and 39, which were heat treated several times longer than either sample 29 or sample 28, also indicate the presence of NiAs and Ni<sub>5</sub>As<sub>2</sub> phases. Sample 39 with Ni adjacent to GaAs was heat treated much longer than other Ni adjacent to GaAs samples. While it does exhibit more NiAs<sub>x</sub>, it nevertheless exhibits Ni-Ga and the higher Ni concentration Ni-Ge phases.

### Three Element Metallization on Sapphire

Because of the complexity of the XRD spectra for the three element contact metallizations, two-element samples on GaAs or sapphire and the complete three element metal depositions on sapphire were made to aid in the interpretation of the X-ray data. As stated previously, the metal on the sapphire substrates were deposited simultaneously with those on GaAs. XRD data of the complete contact metallizations grown on sapphire, similar to the contacts grown on GaAs, strongly indicate the Al<sub>3</sub>Ni phase. In addition, common to samples with both type of layering sequence, sapphire was detected along with elemental Al and Ge, while there is weak indication for the formation of several Ge-Ni and Al-Ge compounds. Again the most prominent phase in the spectra of both types of samples was Al<sub>3</sub>Ni. The presence of the elemental Ge phase after the 500° heat treatment lends credence to its identification on GaAs. Other than the absence of Ga and As containing phases, the phases from the complete metallization on GaAs and sapphire were similar. XRD data for representative examples of the complete contact metallizations on sapphire is summarized in Table 7.

### Two Element Metallization

Because of the dominance of the Al<sub>3</sub>Ni phase in the XRD spectra of the complete contact metallization, samples with the same Ni:Ge or Ni:Ge:Ni ratio and sequence were examined with XRD. Samples of Ni (500Å)/Ge (250Å) and Ni (450Å)/Ge (250Å)/Ni (50Å) on both GaAs and sapphire substrates were heat treated at either 425° C or 500° C. XRD data for the Ni-Ge and Ni-Ge-Ni samples is summarized in Tables 8 and 9 respectively. Qualitatively, the phases identified on both types of samples grown on GaAs and heat treated at 425° C and 500° C were similar. Samples with both types of layering sequence and heat treated at 425° C have less indication of NiAs(Ge), while samples with both types of layering sequence and heat treated at 500° C have less indication of elemental Ni. Sample 35, with Ni at the metal/semiconductor interface and

Table 7. X-ray diffraction data from the three element contact metallization on sapphire. The numbers are as described in the caption for Table 4.

Sample Number	27	27	31	31
Layering	Al-Ni-Ge	Al-Ni-Ge	Al-Ni-Ge-Ni	Al-Ni-Ge-Ni
Temperature	500	500	500	500
Time (Min)	9	9	3	3
Incidence Angle	8	4	8	4
Al	3	3	4	4
Ge	3		3	3
Sapphire	4	4	4	4
Al <sub>3</sub> Ni	4	4	4	4
AlNi	3	3		
Al <sub>2</sub> Ge			2	2
GeNi	2	2	2	2
Ge <sub>3</sub> Ni <sub>5</sub>	2	2		
GeNi <sub>2</sub>	1		2	2
Gamma-Al <sub>2</sub> O <sub>3</sub>	1	1		3

Table 8. X-ray diffraction from the two element Ni-Ge metallization on GaAs. The numbers are as described in the caption for Table 4.

Sample Number	33	33	44	44
Layering	Ni-Ge	Ni-Ge	Ni-Ge	Ni-Ge
Temperature	500	500	425	425
Incidence Angle	8	4	8	4
Ge	4	4	3	3
Ni		1	3	1
GaAs	4	4	2	3
Ni <sub>4</sub> GaGe <sub>2</sub>	2	1	2	3
NiAs(Ge)	2	2	1	2
Ga <sub>3</sub> Ni <sub>2</sub>	1	1	1	1
Ga <sub>2</sub> Ni <sub>3</sub>	1	1	1	1
GeNi	3	3	3	2
GeNi <sub>2</sub>	1	1	1	1
Ge <sub>3</sub> Ni <sub>2</sub>	1	1	3	
Ge <sub>3</sub> Ni <sub>5</sub>	1	1	3	1
Ge <sub>12</sub> Ni <sub>19</sub>	1	1		

heat treated at 500° C, has more indication of the Ni<sub>4</sub>GaGe<sub>2</sub> and NiAs(Ge) phases. In addition, XRD data from all of the samples indicate the same Ge-Ni and Ga-Ni phases as the complete contact samples. Again intensities of most of these peaks were weak, in spite of long collection times, due to the thinness of the metal layers. XRD data for these samples on sapphire substrates also exhibit Ge-Ni phases, again similar to the complete contact metallization on sapphire.

Table 9. X-ray diffraction data from Ni-Ge-Ni two element metallization on GaAs. The numbers are as described in the caption for Table 4.

Sample Number	34	34	35	35
Layering	Ni-Ge-Ni	Ni-Ge-Ni	Ni-Ge-Ni	Ni-Ge-Ni
Temperature	425	425	500	500
Incidence Angle	8	4	8	4
Ge	3	4	3	3
Ni	2	2	1	1
GaAs	3	4	3	3
Ni <sub>4</sub> GaGe <sub>2</sub>	1	3	4	4
NiAs(Ge)	1	1	3	3
Ga <sub>3</sub> Ni <sub>2</sub>	1	1		1
Ga <sub>2</sub> Ni <sub>3</sub>	1	1	1	1
GeNi	3	3	3	3
GeNi <sub>2</sub>		1	2	1
Ge <sub>3</sub> Ni <sub>2</sub>		2	1	3
Ge <sub>3</sub> Ni <sub>5</sub>	3	3	2	4
Ge <sub>12</sub> Ni <sub>19</sub>	1	1	1	1

#### Summary of Phase Formation in Al-Ge-Ni Thin Films

In summary, X-ray diffraction data demonstrated that the films interdiffused during the deposition process as shown by Al<sub>3</sub>Ni, GeNi and Ge<sub>3</sub>Ni<sub>5</sub> phase formation, consistent with TEM and EDS results.<sup>20-23</sup> In previous studies the phases could have formed during TEM sample preparation. However, the XRD results in this study indicated that the phases were formed during deposition, since the samples did not

indicated that the phases were formed during deposition, since the samples did not receive further processing. These phases, in addition to GaAs, elemental Al, Ge, and Ni, were all detected from as deposited samples, independent of whether Ge or Ni was at the metal semiconductor interface. For the samples deposited onto sapphire, in addition to sapphire, elemental Al, Ge, Ni, and Al<sub>3</sub>Ni were observed. For all heat treated contacts, the dominant phase observed from deposited layers was Al<sub>3</sub>Ni. All of the samples generally had indications of many of the same phases, with only slight differences due to the layering sequence and heat treatment time. These differences are summarized in Table 10. It should be pointed out again, that in general, the heat treatment times for the Ge first samples were much longer than for the Ni first times. For the complete contact samples with Ge at the metal semiconductor interface and heat treated at 425° C, there was a stronger indication of the NiGe phase than of the Ge<sub>3</sub>Ni<sub>5</sub> phase, that is, the Ni-Ge phase with higher Ge concentration. For the complete contact samples with Ni at the metal semiconductor interface and heat treated at 425° C, peaks from Ge<sub>3</sub>Ni<sub>5</sub>, Ga<sub>2</sub>Ni<sub>3</sub>, and NiAs(Ge) phases were more numerous, that is, Ni-Ge phases with higher Ni concentration and Ni-Ga phases. In addition, samples heat treated for longer time to convert contacts to ohmic behavior also show more evidence for Ni-As phases. For the complete contact samples heat treated at 500° C, the difference due to layering sequence was more dramatic, consistent with the fact that with Ni at the metal/semiconductor interface, less time was required to convert from Schottky to ohmic behavior. The limited time at temperature may inhibit the amount of phases formed. Electrical measurements were obviously more sensitive to metallurgical changes than were XRD measurements. XRD data for the complete contact samples with Ni at the metal semiconductor interface and heat treated at 500° C did indicate elemental Al and Al<sub>3</sub>Ni was present. In addition there were slight indications for GeNi<sub>2</sub>, Ge<sub>3</sub>Ni<sub>5</sub>, Ga<sub>2</sub>Ni<sub>3</sub>, Ga<sub>3</sub>Ni<sub>2</sub> and Ni<sub>4</sub>GaGe<sub>2</sub> phases when data were collected for 69 hours. The

samples with Ge at the metal/semiconductor interface and heat treated at 500° C required longer periods at temperature to convert to ohmic behavior, and generally their XRD data

Table 10. Summary of thin film X-ray diffraction results for complete contact metallizations on GaAs.

<b>As-Deposited</b> Elemental Al, Ni, and Ge $\text{Al}_3\text{Ni}$ and $\text{Ni}_5\text{Ge}_3$ form during deposition
<b>Heat Treated</b> All samples dominated by $\text{Al}_3\text{Ni}$ Other common phases: -- $\text{NiGe}$ , $\text{Ni}_5\text{Ge}_3$ , $\text{Ni}_3\text{Ga}_2$ , $\text{NiAs}(\text{Ge})$ , $\text{NiAs}_2$ , $\text{Ni}_5\text{As}_2$ , $\text{Ni}_4\text{GaGe}_2$
425° C -- Ge First Greater indication of $\text{NiGe}$ than $\text{Ni}_5\text{Ge}_3$ (e. g. higher Ge concentration Ni-Ge phase) Longer heat treatment -- more Ni-As phases
425° C -- Ni First Greater indication of $\text{Ni}_5\text{Ge}_3$ , $\text{Ni}_3\text{Ga}_2$ , and $\text{NiAs}(\text{Ge})$ (e. g. higher Ni concentration Ni-Ge phases) Longer heat treatment -- more Ni-As phases Greater indication of decomposition GaAs substrate
500° C -- Ge First Less indication of Ni-Ge phases Greater indication of Ni-As, $\text{Ni}_4\text{GaGe}_2$
500° C -- Ni First More elemental Al and Ge Less indication of $\text{NiGe}$ , $\text{Ni}_5\text{Ge}_3$ , $\text{Ni}_2\text{Ga}_3$ , and $\text{Ni}_4\text{GaGe}_2$ Greater indication of decomposition GaAs substrate

had stronger indication of Ni-As,  $\text{NiGe}$ , and  $\text{Ni}_4\text{GaGe}_2$  phases with weaker indications of Ge-Ni phases with higher concentrations of Ni. While there are similar phases indicated for both types of samples, there are some different trends for samples with Ni adjacent to the GaAs versus samples with Ge adjacent to the GaAs. Ni first samples always have more Ni-Ge phases with higher concentration of Ni and more Ni-Ga phases

present. Ge first samples always have the NiGe phase present, that is, the phase with less Ni. The Ge first samples have Ni-As phases present, but so did the Ni first sample which was heat treated for a longer period. While the XRD data was taken for only before and after the formation of ohmic contacts, these phase formations are consistent with diffusion couple reaction paths for each of the layers. The Ni first samples appear to be reactive with the GaAs substrate, as indicated by recent work by Chambers and Loebs.<sup>78</sup> XRD results for three element metallizations on sapphire and the two element samples on both GaAs and sapphire exhibited similar phases when the missing components were considered.

## CHAPTER 5 DISCUSSION

In this discussion section, important new results will be discussed and summarized. This is followed by discussion of reaction paths to help explain the phases observed. Next, a mechanism of surface doping during the reaction to form the ohmic contact is discussed. Finally a comprehensive model for ohmic contacts from Al-Ge-Ni on n-type GaAs is presented and discussed. Electrical measurements have been used to demonstrate dramatic differences in the times and temperatures required to convert the Al/Ni/Ni/GaAs versus Al/Ni/Ge/Ni/GaAs metallizations from Schottky to ohmic electrical behavior. For samples with Ge at the metal-semiconductor interface, the times required to become ohmic behavior were shown to be dependent on both the doping concentration of the contact layer of the GaAs, and on the heat treatment temperature. The times were longer for contact layers with low doping concentration and for lower heat treatment temperature. For samples with Ni at the metal-semiconductor interface, the times required to convert from Schottky to ohmic behavior at either 425 or 500° C were much less and did not depend on doping concentration or temperature. Real time I-V measurements indicated that samples with Ni at the metal-semiconductor interface had an onset of ohmic behavior as low as 180° C. Conversion to ohmic behavior at such a low of temperature confirms the speculation of Edwards et al.<sup>23</sup> that molten eutectics are not required for contact formation. The kinetic effect has not been previously reported for any ohmic contact system.

One objective of this research was to demonstrate that the Al-Ge-Ni metallization was a viable candidate for ohmic contacts to all ranges of doping in GaAs. Since Al-Ge-Ni ohmic contacts have only been reported for doping concentration levels in the

high- $10^{17}$  cm $^{-3}$  and above range,<sup>1,2, 20-23</sup> lightly doped (Si @ 10 $^{16}$  cm $^{-3}$ ) as well as heavily doped (Si @ $10^{18}$  cm $^{-3}$  and above) n-type GaAs were tested. In all cases, ohmic contacts were observed to form. The electrical data shows that Al-Ge-Ni converts to ohmic behavior on contact layers grown by MBE and VPE in addition to ion implanted layers. These different substrates were used because of the reported difficulty of converting Al-Ge-Ni contacts to ohmic behavior on layers other than ion implanted contact layers.<sup>22</sup> This difficulty was not observed in this study. Thus it appears that this metallization is a good candidate for ohmic contacts for GaAs devices.

Auger survey scans have been used to demonstrate that surfaces which have been exposed to the atmosphere were contaminated with O and C. The scans were also used to show that the dendritic precipitates on some of the samples were pure Ge. The cause of Ge precipitation in the early samples was shown to be a high ratio of Ge to Ni (~1:1). Precipitation was controlled by reducing the ratio of Ge to Ni (~1:2). Auger depth profiles were also used to demonstrate that interdiffusion took place during deposition of the metals and during the heat treatment procedure. This interdiffusion was consistent with phase changes as analyzed by XRD.

### Reaction Path Analysis

Auger depth profiles after heat treatment times and temperatures necessary to convert from Schottky to ohmic electrical behavior indicated varying degrees of interdiffusion. This interdiffusion behaved as expected with extensive interdiffusion for samples heat treated at 500° C or 425° C for longer than 15 min. and limited interdiffusion for heat treatment at 425° C for shorter times. Unlike the electrical data, the Auger depth profiles were not dramatically affected by the layering sequence. The effects of deposition sequence have been studied using Auger depth profiles and RBS for Au-Ge-Ni, Pd-Ge, and Pd-Si metallizations.<sup>28, 33, 37, 40, 45, 47, 49, 64</sup> The conclusions

were similar, that is interdiffusion and phase formation were detected, but not all of these events correlated well with electrical behavior of the contacts. In addition, layer sequence effects have only been reported for magnitude and variation in resistance and not the time to form ohmic contacts. The Auger depth profiles illustrate that Ni diffused to the metal-semiconductor interface during heat treatment, as reported for the Au-Ge-Ni system by Robinson.<sup>40</sup> It was reported that Ni increased the solubility of Ge in GaAs.<sup>28, 40, 48</sup>

X-ray diffraction data demonstrate that the films interdiffused during the deposition process consistent with the Auger depth profile data. These data indicate the formation of Al<sub>3</sub>Ni, Ge<sub>3</sub>Ni<sub>5</sub>, and GeNi phases during deposition, which were reported in the literature based upon EDS and TEM data.<sup>20-23</sup> Al<sub>3</sub>Ni was the primary phase observed by XRD spectra for all of the contacts after heat treatment, but all samples exhibited many of the same phases (see Table 10 for a summary of differences due to the layering sequence and heat treatment time). Samples with Ni adjacent to GaAs converted quickly to ohmic behavior and exhibited Ni-Ge, Ni-Ga, Ni-As and Ni-Ga-Ge phases. These samples exhibited more Ni-Ga and Ni-Ge (with higher concentration of Ni) phases than samples with Ge adjacent to GaAs. Samples heat treated at 500° C had more indication of Ni<sub>4</sub>GaGe<sub>2</sub> and NiGe phases than samples heat treated at 425° C. All samples with Ge adjacent to GaAs converted to ohmic behavior after longer times and had more NiGe, Ni-As, and NiAs(Ge) phases. These samples exhibited more NiGe (with higher concentration of Ge) and fewer Ni-Ga phases. The Al-Ni and Ni-Ge phases identified in this study were also reported in the previous Al-Ge-Ni literature.<sup>20-23</sup> However, the Ni-Ga and Ni-As phases identified here were not reported previously. As pointed out in the literature review, calculated and experimental phase diagrams show that the only phases in thermodynamic equilibrium with GaAs at temperatures below ~ 800° C would be NiGa, Ni<sub>2</sub>Ga<sub>3</sub>, and NiAs binaries.<sup>73</sup> This is consistent with the observation of Ni-Ga and Ni-As phases.

One of the controls of this study was to maintain the same total amount of each element for both the Ni first and the Ge first samples. Although the reaction paths are obviously different dependent upon whether Ni or Ge is adjacent to GaAs, the reactions will proceed toward the same end point and should reach the same end point given enough time. Since both types of samples, Ni first and Ge first, were heat treated until they did become ohmic, the phases present could be expected to be similar if ohmic contacts require a particular phase or phases to be present independent of reaction pathways. Obviously the reaction pathways will be different between these two conditions. For the two different layer sequences, i. e. Al/Ni/Ge/Ni/GaAs versus Al/Ni/Ge/GaAs, reactions with the semiconductor will begin as Ni-GaAs or Ge-GaAs. Ge-GaAs is a stable system as shown below by diffusion calculations and in the MBE literature<sup>79-81</sup> for Ge epitaxially grown on GaAs. Ballingall et al.<sup>80</sup> estimated that interdiffusion of MBE Ge-GaAs heterojunctions to be ~10Å after 1 hour at 400° C. On the other hand, Ni has been reported to decompose GaAs quickly and at low temperatures.<sup>78</sup> Therefore, dissociation of GaAs and formation of Ni-Ga and Ni-As phases is expected to occur with Ni adjacent to GaAs while Ge adjacent to GaAs is expected to be nonreactive. At the Ni-Ge interfaces the two components will behave as a diffusion couples, with Ni rich compounds at the Ni side and Ge rich compounds at the Ge side. If the Ge-GaAs interface is stable, then presumably Ni had to reach the GaAs to cause ohmic contacts, even when the Ge was first. If this is true, slow conversion to ohmic contacts may have resulted from both kinetic (time for Ni diffusion through Ge) as well as thermodynamic factors (formation of  $\text{NiGe}_x$  reduces the driving force to form Ni-Ga and Ni-As phases).

Mechanism of Doping

As discussed above, in-diffusion of Ge to form a heavily doped n<sup>+</sup> layer under the metal contact is the most common explanation for forming ohmic contacts on GaAs. The depletion width is reduced by the n<sup>+</sup> layer and carrier are transported by a tunneling mechanism. However, this model does not appear to be appropriate for the Al-Ge-Ni contact system. It is well known that Ge-GaAs is a very stable system. Recently Ge diffusion in GaAs has been quantified using a concentration dependent diffusion equation.<sup>82</sup> In-diffusion was modeled using a vacancy mechanism and compared to SIMS profiles of annealed Ge implanted into GaAs. The effective diffusion coefficient was determined to be  $D_{eff} = 2 \times 10^{-3} \text{ cm}^2/\text{sec} \exp [ -2.9eV/kT ] (n/n_i)^2$ , where n and n<sub>i</sub> are the doping concentration of the contact layer and the intrinsic doping concentration of the GaAs respectively. Using the times and temperatures required to convert to ohmic behavior for Ge first samples (20 min/425° C and 9 min/500° C for depositions on heavily doped substrates), the calculated values are  $D_{eff}/500 = 3.9 \times 10^{-16} \text{ cm}^2/\text{sec}$  and  $D_{eff}/425 = 1.5 \times 10^{-17} \text{ cm}^2/\text{sec}$ . Using these diffusivities in an error function diffusion distance calculation gives values of  $X_{500} = 45.8\text{\AA}$  and  $X_{425} = 13\text{\AA}$ . Similar calculations of diffusion distances for low doped ( $5 \times 10^{16} \text{ cm}^{-3}$ ) substrates yield diffusion distances of less than 1 $\text{\AA}$ . The calculated diffusion distances are less than the depletion width of ~100-150 $\text{\AA}$  for heavily doped substrates. Therefore, the commonly used diffusion argument does not seem appropriate for the Al-Ge-Ni contacts in this study since it does not appear to provide enough Ge for the n<sup>+</sup> layer.

General Model of Ohmic Contact Formation

It is now possible to postulate a model that will explain the conversion of Al-Ge-Ni contacts to ohmic behavior based on results and previous literature described

above. As stated earlier, the contacts with Ni at the metal-semiconductor interface converted from Schottky to ohmic behavior much faster, therefore, the Ni at the metal-semiconductor interface must have enhanced the conversion to ohmic contact. It has been reported that Ni dissociates GaAs.<sup>28, 78</sup> It has also been reported that intermediate phases of GaAs with Pd and Ni form at low temperature,<sup>31-35, 83, 84</sup> and conversion to ohmic behavior has been reported at the onset of their decomposition and concomitant regrowth of the substrate. For example, Pd<sub>4</sub>GaAs has been reported to form at temperatures as low as ~100° C. At higher temperature Ge reacted with this ternary compound resulting in formation of PdGe and regrowth of a GaAs layer.<sup>84</sup> This regrown layer/PdGe contact was ohmic, presumably due to heavy doping of the GaAs during regrowth. This is an extension of the model for Au-Ge-Ni/GaAs ohmic contacts when some investigators suggested that GaAs regrew upon cooling the from the Au-GaAs solid solutions which had formed during heating. Recall that Yeh and Holloway<sup>28</sup> showed that decomposition and regrowth of GaAs took place during heat treatment of Au contacts to Si doped GaAs. In this case, regrowth occurred during isothermal heat treatments rather than during cool-down. In a continuation of this work Li and Holloway<sup>68</sup> showed that GaAs will regrow during isothermal heating of GaAs covered by discrete layers of As and Ga under an outer film of either Au or Au-Ge. In addition, Li and Holloway<sup>30</sup> have measured the specific contact resistance of ohmic contacts using this regrown GaAs technique and found values of  $10^{-5} \Omega \cdot \text{cm}^2$ . Thus it is certain that regrowth of GaAs can lead to formation of ohmic contacts. Finally the presence of a dopant in the Au may not be necessary since Holloway et al.<sup>29</sup> demonstrated that dopant segregation occurred upon reaction of Au with GaAs. They showed that Si dopant from the contact layer was concentrated in the near-surface regions where GaAs decomposed in order to react with the Au contacts. They suggested that the concentrations of Si were sufficient to reduce the depletion distance and allow tunneling transport of charge carriers across the interface for ohmic behavior.

For the Al-Ge-Ni system it is suggested that a similar decomposition and regrowth mechanism is operable for Al/Ni/Ge/Ni contacts. For these samples, elemental Ni would dissociate the GaAs to form an intermediate  $Ni_xGaAs$  ternary phase at low temperature. During further heat treatment the layers would continue to interdiffuse. At longer times, formation of Al-Ni and Ni-Ge phases would remove the Ni from and destroy the Ni-Ga-As phase causing regrowth of a heavily doped GaAs(Ge) layer under the  $Ni_5Ge_3$ , NiGe,  $Ni_xAs$ , and NiAs(Ge) phases observed by XRD. Admittedly, no Ni-Ga-As ternary phase was detected in this study; however, the model is equally valid if the NiAs, NiGa, and  $Ni_4GaGe_2$  identified in this study serve the same purpose as the postulated Ni-Ga-As phase. These phases may well be the unidentified binary or ternary phases shown in the deconvoluted XPS spectra by Chambers and Loebs.<sup>78</sup> Their data also show that Ni adjacent to GaAs is much more reactive than either AlNi or Al. The Al-Ga reaction was very limited and the Al-As reaction did not appear to occur at all. In other words, with Ni adjacent to GaAs, reaction products are Ni-Ga and Ni-As or Ni-Ga-As phases which are subsequently reduced by Al-Ni and Ni-Ge phase formation. It is also possible that segregation of Si from the n-type contact layer might be involved in the heavy doping of the regrown layer as discussed above for Au contacts.<sup>29, 30, 68</sup> In all instances, an  $n^+$  doped GaAs region, sufficient to reduce the depletion distance and permit tunneling transport of the charge across the metal/semiconductor interface, is postulated to result in ohmic behavior. This Ni dissociation and GaAs regrowth mechanism is completely consistent with the observations for samples with Ni adjacent to the GaAs. The elemental profiles show that diffusion takes place during heat treatment. The resultant phase formation observed by XRD can be interpreted to be reaction products which form due to decomposition and regrowth.

It seems likely that a similar mechanism should explain the samples with Ge next to GaAs. The extra time required to convert to ohmic behavior could be due to the time required for Ni to diffuse to the metal/semiconductor interface. In addition, the reaction

pathway would cause rapid formation of Ni-Al and Ni-Ge phases in this case, which would reduce Ni-Ga and Ni-As phase formation. However, one observation which needs explanation is that longer times were required to convert samples with low doped versus high doped substrates. Thus the rate limiting step must either proceed at a different rate or proceed along a different path for changes in doping. Both possibilities exist based on the model and the literature cited above. For example, the data for Ge diffusion in GaAs shows that the rate depends upon the square of the doping density. If a similar dependence existed for Ni in Ge the short time for high doping, longer time for low doping is easily accounted for. This is especially true since with the Al/Ni/Ge/GaAs sequence, the Ni must first react with Ge before it can reach the GaAs. If Ni-Al and/or Ni-Ge phases lead to decomposition of NiGa and Ni-As or Ni-Ga-As phases, then the amount of Ni reaching the Ge/GaAs interface would be very limited. Presumably a regrowth layer approximately the thickness of the depletion width must be regrown to form a good ohmic contact. Since the depletion width is larger at low doping, more regrowth and therefore more reaction and therefore longer diffusion times would be required. A second effect leading to longer time at low doping could result from segregation of the Si dopant.<sup>29, 30, 68</sup> If segregated dopant led to the n<sup>+</sup> region and ohmic behavior, again a larger volume of GaAs would need to react at low versus high doping densities. For either regrowth and/or dopant segregation, limited transport of Ni in Ge would require longer times at low versus high doping levels.

Segregation of dopant to the metal/semiconductor interface may be indicated by the results of Graham et al.<sup>21-23</sup> Recall that they reported Al-Ge-Ni contacts converted to ohmic behavior on both n and p-type GaAs. If Ge is incorporated to form an n<sup>+</sup> layer, the metallization on p-GaAs should have resulted in a pn junction. Alternatively, their p-type Al/Ni/Ge/GaAs contacts may have converted to ohmic behavior due to Zn segregation to the metal/semiconductor interface during decomposition of the GaAs substrate. If GaAs regrowth occurred, Ge could be incorporated into the regrowth layer.

Presumably this is consistent with their results since their p-GaAs substrates were heavily doped and Ge incorporation may have been only partially compensated the Zn dopant.

As reported above, there was no dependence upon temperature or doping concentration for ohmic formation when Ni was adjacent to GaAs. This probably results because the times of heat treatment were long compared to fast reactions between Ni and GaAs at the interface. If these samples were heat treated for much shorter periods or at much lower temperatures, an effect of doping concentration upon heat treatment time required for conversion to ohmic behavior would be observed.

The different times required for conversion to ohmic behavior based on contact layer sequence, temperature, and doping of the contact layer are the basis for the building blocks for a process model of the conversion of Al-Ge-Ni contacts from Schottky to ohmic behavior. One of the more widely used process model simulators is SUPREM (Stanford University Process Emulator). This model predicts distribution of elements that result from a given process treatment for a certain time. The process model simulations for silicon devices are now well developed in SUPREM, and include the one and two dimensional distributions of oxide layers ( $\text{SiO}_2$ ) onto Si resulting from a given treatment in an oxidation furnace for a specified time and temperature. Process modeling for Si based devices is much more advanced than for GaAs based devices. Nonetheless, the work reported in this dissertation is a first crude step in building a process model for ohmic contact formation in GaAs for the Al-Ge-Ni system. In this work, the distribution of elements resulting from specified time-temperature treatments have been determined. More precise knowledge of the distributions of dopant are clearly needed and could probably be obtained by SIMS profiles of the ohmic contact. This work should be conducted in future experiments.

## CHAPTER 6 CONCLUSIONS

Electrical and metallurgical properties of Al/Ge/Ni ohmic contacts have been studied with I-V, Auger electron spectroscopy, and X-ray Diffraction. The objective of this study was to identify the interfacial chemistry between the Al-Ge-Ni metallization and the surface of very clean GaAs in order to rationalize alloy formation and elemental profiles to currently accepted ohmic contact models. The approach adopted was to vary the sequencing, layer thickness and thermal processing of the Al-Ge-Ni layers to determine elemental distributions and phase formations present after the conversion from Schottky to ohmic behavior.

Electrical characterization has been used to demonstrate dramatic differences in the amount of heat treatment time required to convert Al-Ge-Ni metallizations on GaAs from Schottky to ohmic behavior, depending on whether Ge or Ni was at the metal/semiconductor interface. Differences in heat treatment times were also found to depend on the doping concentration of the contact layer and on the heat treatment temperature for Ge first samples, but not for Ni first samples.. For samples with Ge at the metal-semiconductor interface the time required to convert from Schottky to ohmic behavior varied inversely with doping concentration and directly with temperature. For samples with Ni at the metal-semiconductor interface, the time required to convert from Schottky to ohmic behavior was much less and there was little dependence on the doping concentration or the heat treatment temperature.

The effects of the electrical behavior has been correlated with the interdiffusion of the Al, Ge, Ni, Ga, and As components with Auger Electron Spectroscopy. Phase identification was accomplished with X-ray Diffraction. Key phases were identified as

$\text{Al}_3\text{Ni}$ ,  $\text{GeNi}$ ,  $\text{Ge}_3\text{Ni}_5$ ,  $\text{Ni}_4\text{GaGe}_2$ ,  $\text{NiAs}$ ,  $\text{Ni}_5\text{As}_2$ ,  $\text{NiAs}(\text{Ge})$ ,  $\text{Ni}_2\text{Ga}_3$ . It has been proposed that the difference in the time to convert from Schottky to ohmic behavior was the result of the reaction kinetics involved in the formation of these phases. It was further proposed that different reactions occurred due to the different layering sequence of the metal layers. This speculation was based on the phase formation differences for the two different types of sample layering sequences. The samples with Ni adjacent to GaAs converted to ohmic behavior quickly, and XRD data exhibit Ni-Ga, Ni-As, and Ni-Ga-Ge phases after short heat treatment. These results were consistent with phase diagram predictions<sup>70-73</sup> and recent XPS studies.<sup>78</sup> It was suggested that these were reaction products which resulted from the rapid reaction of Ni and GaAs. Samples with Ge adjacent to GaAs converted to ohmic behavior more slowly (and much more slowly for contacts on low doped substrates) and XRD data exhibited NiGe (with lower concentration of Ge) and Ni-As phases, but much less Ga containing phase formation. It was suggested that for samples with Ge adjacent to GaAs the Ge/GaAs or NiGe reactions inhibit conversion to ohmic behavior. A decomposition and regrowth model was proposed to correlate the electrical behavior with the observed interfacial phase formations. Substrate dopant segregation was suggested to explain the observation of longer times required to convert samples on low doped substrates.

## **APPENDIX A**

### **GaAs SUBSTRATE AND SAMPLE CLEANING**

Appendix: A					
Sample Number	Substrate	Substrate Type	Date Grown	Dopant/Concentration	Substrate Cleaning
91-064-11	Sumitomo 802055-012-D045-54	MBE-147-As Capped	5-Mar-91	Si-10exp18 (1/cm)3	Thermal Desorption In Deposition System
91-073-12	Sumitomo 802055-012-D045-54	MBE-147-As capped	14-Mar-91	Si-10exp18 (1/cm)3	Thermal Desorption In Deposition System
91-078-13	Sumitomo 802055-012-D045-54	MBE-147-As capped	19-Mar-91	Si-10exp18 (1/cm)3	Thermal Desorption In Deposition System
91-085-14	Sumitomo 802055-012-D045-54	MBE-147-As capped	26-Mar-91	Si-10exp18 (1/cm)3	Thermal Desorption In Deposition System
91-099-15	Sumitomo 802055-012-D045-54	MBE-147-As capped	9-Apr-91	Si-10exp18 (1/cm)3	Thermal Desorption In Deposition System
91-105-16	Sumitomo 802055-012-D045-54	MBE-147-As capped	15-Apr-91	Si-10exp18 (1/cm)3	Thermal Desorption In Deposition System
91-110-17	Sumitomo 802055-012-D045-54	MBE-147-As capped	20-Apr-91	Si-10exp18 (1/cm)3	Thermal Desorption In Deposition System
91-115-18	Raytheon/2467-47	Ion Implanted	25-Apr-91	Si - 1.0X10E18-.16um * 2.9X10E17-.34um	None
91-119-19	Raytheon/2467-47	Ion Implanted	29-Apr-91	Si - 1.0X10E18-.16um * 2.9X10E17-.34um	None
91-121-20	Raytheon/2467-47	Ion Implanted	1-May-91	Si - 1.0X10E18-.16um * 2.9X10E17-.34um	None
					* Contact/Active Layers

APPENDIX: A	Sample Number	Substrate Mfg /Wafer Number	Substrate Type	Date Grown	Dopant/Concentration	Substrate Cleaning
91-124-21	Raytheon/2467-47	Ion Implanted	4-May-91	Si - 1.0X10E18-.16um * 2.9X10E17-.34um	None	
91-126-22	Raytheon/2467-47	Ion Implanted	6-May-91	Si - 1.0X10E18-.16um 2.9X10E17-.34um	None	
91-151-23	Professor Peng/R 3889	UF / EE Sample	31-May-91	Prof. Peng Sample	Chem Cleaned	
91-155-24	Professor Peng /R 3895	UF / EE Sample	4-Jun-91	Prof. Peng Sample	Chem Cleaned	
91-180-25	Raytheon/2467-28	Ion Implanted	29-Jun-91	Si - 1.1X10E18-.16um * 3.0X10E17-.34um	None	
91-186-26	Raytheon/2467-28	Ion Implanted	5-Jul-91	Si - 1.1X10E18-.16um * 3.0X10E17-.34um	None	
91-189-27	Raytheon/2467-28	Ion Implanted	8-Jul-91	Si - 1.1X10E18-.16um * 3.0X10E17-.34um	None	
91-192-28	Raytheon/2467-28	Ion Implanted	11-Jul-91	Si - 1.1X10E18-.16um * 3.0X10E17-.34um	Chem Cleaned	
91-194-29	Raytheon/18P139	Vapor Phase Epitaxy	13-Jul-91	Si - 1.6X10E18-.25um * 2.7X10E17-.63um		
91-196-30	Raytheon/18P139	Vapor Phase Epitaxy	15-Jul-91	Si - 1.6X10E18-.25um 2.7X10E17-.63um	None	
					* Contact/Active Layers	

APPENDIX: A	Sample Number	Substrate Mfg /Wafer Number	Substrate Type	Date Grown	Dopant/Concentration	Substrate Cleaning
91-198-31	Raytheon/18P139	Vapor Phase Epitaxy	17-Jul-91	Si - 1.6X10E18-.25um * 2.7X10E17-.63um	Chem Cleaned	
91-200-32	Raytheon/18P139	Vapor Phase Epitaxy	19-Jul-91	Si - 1.6X10E18-.25um * 2.7X10E17-.63um	Chem Cleaned	
91-202-33	Raytheon/18P139	Vapor Phase Epitaxy	21-Jul-91	Si - 1.6X10E18-.25um * 2.7X10E17-.63um	Chem Cleaned	
91-204-34	Raytheon/18P138	Vapor Phase Epitaxy	23-Jul-91	Si - 1.6X10E18-.25um * 2.7X10E17-.63um	Chem Cleaned	
91-206-35	Raytheon/2467-28	Ion Implanted	25-Jul-91	Si - 1.1X10E18-.16um * 3.0X10E17-.34um	Chem Cleaned	
91-208-36	Sumitomo 802055-012-D045-54	MBE-147-As capped	27-Jul-91	Si-Md 10E18	Thermal Desorption In Deposition System	
91-252-37	Sumitomo 004570-016-D015	HB-GaAs Bulk Doped - Si	9-Sep-91	Si-1x10E18	Chem Cleaned	
91-260-38	Sumitomo 802055-012-D085-95	MBE-182-As Capped	17-Sep-91	Si - ~~5x10E16-2.0um	Thermal Desorption In Deposition System	
91-263-39	Sumitomo 802055-012-D085-95	MBE-182-As Capped	20-Sep-91	Si - ~~5x10E16-2.0um	Thermal Desorption In Deposition System	
91-266-40	Sumitomo 802055-012-D085-95	MBE-182-As Capped	23-Sep-91	Si - ~~5x10E16-2.0um	Thermal Desorption In Deposition System	
						* Contact/Active Layers

APPENDIX: A					
Sample Number	Substrate Mfg /Wafer Number	Substrate Type	Date Grown	Dopant/Concentration	Substrate Cleaning
91-267-41	Sumitomo 802055-012-D085-95	MBE-182- As Capped	24-Sep-91	Si - ~~5x10E16-2.0um	Thermal Desorption In Deposition System
91-269-42	Sumitomo 802055-012-D085-95	MBE-182- As Capped	26-Sep-91	Si - ~~5x10E16-2.0um	Thermal Desorption In Deposition System
91-273-43	Sumitomo 802055-012-D085-95	MBE-182- As Capped	30-Sep-91	Si - ~~5x10E16-2.0um	Thermal Desorption In Deposition System
91-277-44	Sumitomo 802055-012-D085-95	MBE-182- As Capped	4-Oct-91	Si - ~~5x10E16-2.0um	Thermal Desorption In Deposition System
91-280-45	Sumitomo 802055-012-D085-95	MBE-182- As Capped	7-Oct-91	Si - ~~5x10E16-2.0um	Thermal Desorption In Deposition System
91-283-46	Sumitomo 802055-012-D085-95	MBE-182- As Capped	10-Oct-91	Si - ~~5x10E16-2.0um	Thermal Desorption In Deposition System
91-290-47	Sumitomo 802055-012-D085-95	MBE-182-As Capped	17-Oct-91	Si - ~~5x10E16-2.0um	Thermal Desorption In Deposition System
91-292-48	Bertram Laboratories 1373UN-39	HB-GaAs	19-Oct-91	Si - 2.6 to 3.5 x 10 E16	Chem Cleaned
91-294-49	Bertram Laboratories 1373UN-39	Bulk Doped-Si			
91-296-50	Bertram Laboratories 1373UN-39	HB-GaAs	23-Oct-91	Si - 2.6 to 3.5 x 10E16	Chem Cleaned
		Bulk Doped-Si			



## **APPENDIX B**

### **SAMPLE METALLIZATION, HEAT TREATMENT, AND ELECTRICAL RESULTS**

Appendix: B		Metallization Sequence	Heat Treatment		I-V Results
Sample Number			Temp	Time	
91-064-11		GaAs/249Å Ni/250Å Ge/250Å Ni/250Å to 290Å Ge sapphire/249Å Ni/250Å Ge/250Å Ni/250Å to 290Å Ge	500	2+2	Ohmic as dep
91-073-12		GaAs/250Å Ni/250Å Al/252Å Ni/250Å Al sapphire/250Å Ni/250Å Al/252Å Ni/250Å Al	500	2+2	Ohmic as dep
91-078-13		GaAs/250Å Ge/251Å Al/251Å Ge/251Å Al sapphire/250Å Ge/251Å Al/251Å Ge/251Å Al	500	2+2	Ohmic as dep
91-085-14		100Å Ge/220Å Al	No	No	No
91-099-15		101Å Ge/300Å Al/100Å Ge/Approx. 100Å Al	No	No	No
91-105-16		100Å Ge/301Å Al	No	No	No
91-110-17		GaAs/100Å Ge/300Å Al/100Å Ge/120Å Al sapphire/100Å Ge/300Å Al/100Å Ge/120Å Al	No	No	No
91-115-18		GaAs/300Å Ge/401Å Ni/2004Å Al sapphire/300Å Ge/401Å Ni/2004Å Al	425	3+2+2	Ohmic as dep Turned Schottky
91-119-19		GaAs/300Å Ge/400Å Ni/2001Å Al sapphire/300Å Ge/400Å Ni/2001Å Al	425	3+2+2+3+3	Ohmic after 13 Min
91-121-20		GaAs/50Å Ni/300Å Ge/351Å Ni/2001Å Al sapphire/50Å Ni/300Å Ge/351Å Ni/2001Å Al	500	1+2	Ohmic after 3 min

APPENDIX: B Sample Number	Metallization Sequence	Heat Treatment	I-V Results
		Temperature	Time
91-124-21	50Å Ni/401Å Ge/250Å Ni/2018Å Al	425	100
91-126-22	51Å Ni/400Å Ge/300Å Ni/2059Å Al	425	7
			Ohmic as deposited
			Became Schottky
91-151-23	400Å Ge/300Å Ni/2001Å Al	UF Sample	UF Sample
91-155-24	51Å Ni/400Å Ge/304Å Ni/2141Å Al	UF Sample	Sent to Prof. Peng at UF
91-180-25	251Å Ge/502Å Ni/2004Å Al	425	2+2+2+2
			Ohmic at 20 Min
			3+3+3+3
91-186-26	51Å Ni/256Å Ge/448Å Ni/2000Å Al	500	2
			Ohmic at 2 minutes
91-189-27	GaAs/251Å Ge/501Å Ni/2001Å Al sapphire/251Å Ge/501Å Ni/2001Å Al	500	3+2+2+2
			Ohmic at 9 minutes
91-192-28	GaAs/52Å Ni/25Å Ge/452Å Ni/2007Å Al sapphire/52Å Ni/25Å Ge/452Å Ni/2007Å Al	Ramped to 425	Real Time
			Turned Ohmic quickly at ~180 C
91-194-29	GaAs/251Å Ge/501Å Ni/2000Å Al sapphire/251Å Ge/501Å Ni/2000Å Al	Ramped to 425	Real Time
			Ohmic at ~15 Min
91-196-30	GaAs/51Å Ni/250Å Ge/451Å Ni/2001Å Al sapphire/51Å Ni/250Å Ge/451Å Ni/2001Å Al	500	3
			Ohmic at 3 minutes

APPENDIX: B Sample Number	Metallization Sequence	Heat Treatment	I-V Results
		Temperature	Time
91-198-31	GaAs/251Å Ge/501Å Ni/2003Å Al sapphire/251Å Ge/501Å Ni/2003Å Al	500	1st-2+2 2nd-+10 to 30
91-200-32	GaAs/51Å Ni/250Å Ge/450Å Ni/2002Å Al sapphire /51Å Ni/250Å Ge/450Å Ni/2002Å Al	425	20 Never turned Ohmic
91-202-33	GaAs/250Å Ge/500Å Ni sapphire /250Å Ge/500Å Ni	500	3 N/A
91-204-34	GaAs/51Å Ni/251Å Ge/451Å Ni sapphire/51Å Ni/251Å Ge/451Å Ni	425	2 + 2 N/A
91-206-35	GaAs/51Å Ni/253Å Ge/451Å Ni sapphire/51Å Ni/253Å Ge/451Å Ni	500	3 N/A
91-208-36	GaAs/51Å Ni/250Å Ge/450Å Ni/2000Å Al sapphire/51Å Ni/250Å Ge/450Å Ni/2000Å Al	None	None Ohmic As Deposited
91-252-37	50Å Ni/250Å Ge/451Å Ni/2006Å Al	Lost	N/A N/A
91-260-38	51Å Ni/252Å Ge/452Å Ni/2001Å Al	Destroyed	N/A N/A
91-263-39	52Å Ni/251Å Ge/451Å Ni/2002Å Al	425	2 Lines - 2 Min 2 Min & 50 Min
91-266-40	51Å Ni/252Å Ge/450Å Ni/2002Å Al	Available	N/A

APPENDIX: B Sample Number	Metallization Sequence	Heat Treatment	I-V Results
		Temperature	Time
91-267-41	Samples used for Hall & PL Substrate Check	N/A	N/A
91-269-42	51Å Ni/252Å Ge/452Å Ni/2003Å Al	Available	N/A
91-273-43	51Å Ni/250Å Ge/451Å Ni/2000Å Al	500	2 Turned Ohmic at 2 Min
91-277-44	251Å Ge/450Å Ni	425	2+2 N/A
91-280-45	252Å Ge/502Å Ni/2007Å Al	425 2 Pieces	2 ea to 40 & 2+2+2 Almost, Not Quite
91-283-46	250Å Ge/502Å Ni/2007Å Al	Available	N/A
91-290-47	254Å Ge / 508Å Ni / 2018Å Al	500 10 to 44 Min	2+2...+2 Turned Ohmic at 42 Min
91-292-48	250Å Ge / 502Å Ni / 2003Å Al	500	2ea to 40 then Never turned Ohmic
91-294-49	50Å Ni / 251Å Ge / 454Å Ni / 2011Å Al	500 to 48	5+4+4+3 to 56 2+2...+2 Never turned Ohmic
91-296-50	51Å Ni / 254Å Ge / 453Å Ni / 2003Å Al	No	0 N/A



## REFERENCES

1. R. Zuleeg, P. E. Frieberthshauser, J. M. Stephens, and S. H. Watenabe, "Al-Ge Ohmic Contacts to n-type GaAs," IEEE Electron Device Letters, Vol. EDL-7, No. 11, pg. 603-604, 1986.
2. R. Zuleeg, P. E. Frieberthshauser, J. M. Stephens, and S. H. Watenabe, "Al-Ge Contacts to n-type GaAs," Presentation at the Electrochemical Society Meeting, San Diego, CA, 19 to 24 October, 1986.
3. F. Braun, "Über die stromleitung durch schefelmetalle," Ann. Physica Chem., Vol. 153, pg. 556, 1884.
4. W. Schottky, "Halbleitertheorie der Sperrsicht," Naturwissenschaften, Vol. 26, pg. 843, 1938.
5. W. F. Mott "Note on the Contact between a Metal and an Insulator or Semiconductor" Proc. Camb. Phil. Soc., Vol. 34, pg. 568-572, 1938.
6. J. Bardeen, "Surface States and Rectification at a Metal Semi-Conductor Contact," Physical Review, Vol. 71, No. 10, pg. 717-727, 1947.
7. W. E. Spicer, I. Lindau, P. Skeath, C. Y. Su, and P. Chye, "Unified mechanism for Schottky-barrier formation and III-V oxide interface states," Physical Review Letters, Vol. 44, pg. 420, 1980.
8. L. J. Brillson, M. L. Slade, R. E. Viturro, M. K. Kelly, N. Tache, G. Margaritondo, J. M. Woodall, P. D. Kirchner, G. D. Pettit, and S. L. Wright, "Fermi level pinning and chemical interaction at metal-InGaAs (100) interfaces," Journal of Vacuum Science and Technology, Vol. B 4, pg. 919, 1986.
9. J. L. Freeouf and J. M. Woodall, "Schottky barriers: an effective work function model," Applied Physics Letters, Vol. 39, pg. 727-729, 1981.
10. V. Heine, "Theory of surface states," Physical Review A, Vol. 138, pg. 1689, 1965.
11. S. M. Sze, Physics of Semiconductor Devices (John Wiley and Sons, New York, 1981).
12. V. L. Rideout, "A Review of the Theory and Technology for Ohmic Contacts to Group III-V Compound Semiconductors," Solid-State Electronics, Vol. 18, pg. 541-550, 1975.

13. A. Piotrowska, A. Guvarc'h, and G. Pelous, "Ohmic Contacts to III-V Compound Semiconductors: A Review of Fabrication Techniques," Solid-State Electronics, Vol. 26, No. 3, pg. 179-197, 1983.
14. T. Sands, "Compound Semiconductor Contact Metallurgy," Materials Science and Engineering, Vol. B1, pg. 289-312, 1989.
15. M. Murakami, "Development of Ohmic Contact Materials for GaAs Integrated Circuits," Materials Science Reports, Vol. 5, No. 6, pg. 273-317, 1990.
16. A. Piotrowska and E. Kaminska, "Ohmic Contacts to III-V Compound Semiconductors," Thin Solid Films, Vol. 193, pg. 511-527, 1990.
17. R. E. Williams, in Gallium Arsenide Processing Techniques, Chapter 11, "Ohmic Contacts," pg. 225-257 (Artec House, Inc. Dedham MA, 1984).
18. B. L. Sharma in Semiconductors and Semimetals, Vol. 15, Chapter 1, "Ohmic Contacts to III-V Compound Semiconductors," pg. 1-38 (Academic Press, New York, 1981).
19. G. Y. Robinson in Physics and Chemistry of III-V Compound Semiconductor Interfaces, Chapter 2, "Schottky Diodes and Ohmic Contacts for III-V Semiconductors," pg. 73-154, Ed. C. W. Wilmsen (Plenum Press, New York, 1985).
20. Z. Liliental-Weber, J. Washburn, C. Musgrave, E. R. Weber, R. Zuleeg, W. V. Lampert, and T. W. Haas, "New Al-Ge-Ni Contacts on GaAs; Their Structure and Electrical Properties," Materials Research Society Symposium Proceedings, Vol. 126, pg. 295-301, 1988.
21. R. J. Graham, H. H. Erkasya, and R. J. Roedel, "Preliminary Studies of the Al-Ge-Ni Ohmic Contacts to p- and n-type GaAs," Journal of Electrochemical Society, Vol. 35, pg. 266-267, 1988.
22. R. J. Graham, H. H. Erkasya, J. L. Edwards, and R. J. Roedel, "High-resolution Transmission Electron Microscope Studies of an Al-Ge-Ni Ohmic Contact to GaAs," Journal of Vacuum Science and Technology, Vol. B 6, No. 5, pg. 1502-1505 1988.
23. R. J. Graham, R. W. Nelson, P. Williams, T. B. Haddock, E. P. Baaklini, and R. J. Roedel, "Investigation of the Structural and Electrical Properties of Al-Ge-Ni Contacts to GaAs," Journal of Electronic Materials, Vol. 19, No. 11, pg. 1257-1263, 1990.
24. N. Braslau, J. B. Gunn, and J. L. Staples, "Metal-Semiconductor Contacts for GaAs Bulk Effect Devices," Solid-State Electronics, Vol. 10, pg. 381-383, 1967.
25. R. H. Cox and H. Strack, "Ohmic Contacts for GaAs Devices," Solid-State Electronics, Vol. 10, pg. 1213-1218, 1967.
26. N. Braslau, "Alloyed Ohmic Contacts to GaAs," Journal of Vacuum Science and Technology, Vol. 19, No. 3, pg. 803-807, 1981.

27. W. T. Anderson Jr., A. Christou, and J. E. Davey, "Development of Ohmic Contacts for GaAs Devices Using Epitaxial Ge Films," IEEE Journal of Solid-State Circuits, Vol. B 4, pg. 430-435, 1978.
28. M. Ogawa, "Alloying Behavior of Ni/Au/Ge Films on GaAs," Journal of Applied Physics, Vol. 51, No. 1, pg. 406-412, Jan. 1980.
29. P. H. Holloway, L. L.-M. Yeh, D. H. Powell, and A. Brown, "Mechanism of forming ohmic contacts to GaAs," Applied Physics Letters, Vol. 59 No.8, pg. 947-949, 1991.
30. L. L.-M. Yeh and P. H. Holloway, "Mechanism of Au-GaAs reaction and Effects on Ohmic Formation," Materials Research Society Proceedings, Vol. 144, pg. 607-612, 1989.
31. L. C. Wang, B. Zhang, F. Fang, E. D. Marshall, S. S. Lau, T. Sands, and T. F. Kuech, "An investigation of a nonspiking Ohmic contact to n-GaAs using Si/Pd system," Journal of Materials Research, Vol. 3, No. 5, pg. 922-930, 1988.
32. L. S. Yu, L. C. Wang, E. D. Marshall, S. S. Lau, and T. F. Kuech, "The temperature dependence of contact resistivity of the Ge/Pd and the Si/Pd nonalloyed contact scheme on n-GaAs," Journal of Applied Physics, Vol. 65, No. 4, pg. 1621-1625, 1989.
33. E. D. Marshall, L. S. Yu, S. S. Lau, T. F. Kuech, and K. L. Kavanaugh, "Planar Ge/Pd and alloyed Au-Ge-Ni ohmic contacts to n-Al<sub>x</sub>Ga<sub>1-x</sub>As (0 ≤ x ≤ 0.3)," Applied Physics Letters, Vol. 54. No.8, pg. 721-723, 1989.
34. C. J. Palmstrøm, S. A. Schwarz, E. Yablonovitch, J. P. Harbison, C. L. Schwartz, L. T. Florez, T. J. Gmitter, E. D. Marshall, and S. S. Lau, "Ge redistribution in solid-phase Ge/Pd/GaAs ohmic contact formation," Journal of Applied Physics, Vol. 67, No. 1, pg. 334-339, 1990.
35. T. Sands, E. D. Marshall, and L. C. Wang, "Solid-phase regrowth of compound semiconductors by reaction-driven decomposition of intermediate phases," Journal of Materials Research, Vol. 3, No. 5, pg. 914-921, 1988.
36. A. M. Andrews and N. Holonyak Jr., "Properties of N Type Ge-Doped Epitaxial GaAs Layers Grown From Au-Rich Melts," Solid-State Electronics, Vol. 15 pg. 601-604, 1972.
37. M. Heiblum, M. I. Nathan, and C. A. Chang, "Characteristics of AuGeNi Ohmic Contacts to GaAs," Solid-State Electronics, Vol. 25, No. 3, pg. 185-195, 1982.
38. O. Aina, W. Katz, B. J. Baliga, and K. Rose, "Low Temperature Sintered Au Ge/GaAs Ohmic Contacts," Journal of Applied Physics, Vol. 53, No. 1, pg. 777-780, Jan. 1982.
39. O. Aina, S. W. Chiang, Y. S. Liu, F. Bacon, and K. Rose, "Microstructure and Resistivity of Laser-Annealed AuGe Ohmic Contacts on GaAs," Journal of Electrochemical Society: Solid-State Science and Technology, Vol. 128, No. 10, pg. 2183-2184, Oct. 1981.

40. G. Y. Robinson, "Metallurgical and Electrical Properties of Alloyed Ni/Au-Ge Films on N-type GaAs," Solid-State Electronics, Vol. 18, pg. 331-342, 1975.
41. R. P. Gupta and W. S Kohkle, "Gallium-Vacancy-Dependent Diffusion Model of Ohmic Contacts to GaAs," Solid-State Electronics, Vol. 28, No. 8, pg. 823-830, 1985.
42. J. Dell, H. L. Hartnagel, and A. G. Nassibian, "Ultrathin-film Ohmic Contacts for GaAs FET," Journal of Physics D: Applied Physics, Vol. 16, pg. L243-L245, 1983.
43. A. Iliadis and K. E. Singer, "The Role of Germanium in Evaporated Au-Ge Ohmic Contacts to GaAs," Solid-State Electronics, Vol. 26, pg. 7-14, 1983.
44. M. Wittmer, T. Finstad, and M.A. Nicolet, "Investigation of the Au-Ge-Ni and Au-Ge-Pt System used for Alloy Contacts to GaAs," Journal of Vacuum Science and Technology, Vol. 14, No. 4, pg. 935-936, 1977.
45. M. A. Crouch, S. S. Gill, J. Woodward, S. J. Courtney, G. M. Williams, and A. G. Cullis, "Structure and Electrical Properties of Ge/Au Ohmic Contacts to n-Type GaAs Formed by Rapid Thermal Annealing," Solid-State Electronics, Vol. 33, No. 11, pg. 1437-1446, 1990.
46. W. Wittmer, R. Pretorius, J. W. Mayer, and M. A. Nicolet, "Investigation of Au-Ge-Ni System Used for Alloyed Contacts to GaAs," Solid-State Electronics, Vol. 20, pg. 433-439, 1977.
47. F. Vidimari, "Improved Ohmic Properties of Au-Ge Contacts to Thin n-GaAs Layers Alloyed with an SiO<sub>2</sub> Overlayer," Electron Letters, Vol. 15, pg. 675-677, 1979.
48. M. Ogawa, "Alloying Reaction in Thin Nickel Films Deposited on GaAs," Thin Solid Films, Vol. 70, pg. 181-189, 1980.
49. I. R. Hill, W. M. Lau G. R. Yang, and R. A. North, "Combined EBIC-Auger Analysis of AuGeNi/n-GaAs Ohmic Contact Formation," Surface and Interface Analysis, Vol. 11, No. 12, pg. 596-598, 1988.
50. A. Lahav and M. Eizenberg, "Interfacial Reactions of Ni-Ta Thin Films on GaAs," Applied Physics Letters, Vol. 45, No. 3, pg. 256-432, 1984.
51. A. Lahav and M. Eizenberg, "Effect of Phase Separation on the Electrical Properties of the Interface Between Ni-Ta Thin Films and GaAs Substrate," Applied Physics Letters, Vol. 46, No. 4, pg. 430-432, 1985.
52. T. Sands, V. G. Kermidas, A. J. Yu, K-M. Yu, R. Gronsky, and J. Washburn, "Ni, Pd, and Pt on GaAs: A Comparative Study of Interfacial Structures, Compositions, and Reacted Film Morphologies," Journal of Materials Research, Vol. 2, No. 2, pg. 262-275, 1987.
53. S. H. Chen, C. B. Carter, C. J. Palmstrøm, and T. Ohashi, "Transmission Electron Microscopy Studies on Lateral Reaction of GaAs with Ni," Applied Physics Letters, Vol. 48, No. 12, pg. 803-805, 1986.

54. S. A. Schwarz, C. J. Palmstrøm, C. L. Schwartz, T. Sands, L. G. Shantharama, J. P. Harbinson, L. T. Florez, E. D. Marshall, C. C. Han, S. S. Lau, L. H. Allen, and J. W. Mayer, "Backside Secondary Ion Mass Spectrometry Investigation of Ohmic and Schottky Contacts on GaAs," Journal of Vacuum Science and Technology, Vol. A 8, No. 3, pg. 2079-2083, 1990.

55. J. R. Shappirio, R. T. Lareau, R. A. Lux, J. J. Finnegan, D. D. Smith, L. S. Heath, and M. Taysing-Lara, "Metal Penetration and Dopant Redistribution Beneath Alloyed Ohmic Contacts to n-GaAs," Journal of Vacuum Science and Technology, Vol. A 5, No. 4, pg. 1503-1507, 1987.

56. W. Patrick, W. S. Mackie, S. P. Beaumont, and D. W. Wilkinson, "Low Temperature Annealed Contacts to Very Thin GaAs Epilayers," Applied Physics Letters, Vol. 48, No. 15, pg. 986-988, 1986.

57. Z. Liliental, R. W. Carpenter, J. Escher, "Electron Microscopy Study of the AuGe/Ni/GaAs Contacts on GaAs and GaAlAs," Ultramicroscopy, Vol. 14, pg. 135-144, 1984.

58. G. S. Marlow, M. B. Das, L. Tongson, "The Characteristics of Au-Ge Based Ohmic Contacts to n GaAs including the Effects of Aging," Solid-State Electronics, Vol. 26, No. 4, pg. 259-266, 1983.

59. A. K. Kulkarni and C. Lai, "New Models for Ohmic Contacts to GaAs," Thin Solid Films, Vol. 164, pg. 435-439, 1988.

60. N. Braslau, "Ohmic Contacts to GaAs," Thin Solid Films, Vol. 104, pg. 391-394, 1983.

61. M. Murakami, K. D. Childs, J. M. Baker, and A. Callegari, Microstructure Studies of AuNiGe Ohmic Contacts to n-type GaAs," Journal of Vacuum Science and Technology, Vol. B 4, No. 4, pg. 903-911, 1986.

62. Y.-C. Shih, M. Murakami, E. L. Wilkie, and A. C. Callegari, "Effects of Interfacial Microstructure on Uniformity and Thermal Stability of AuNiGe Ohmic Contact to n-type GaAs," Journal of Applied Physics, Vol. 62, No. 2, pg. 582-590, 1987.

63. M. Hansen, Constitution of Binary Alloys, 2nd Edition (McGraw-Hill, New York, 1958).

64. T. S. Kuan, P. E. Batson, T. N. Jackson, H. Rupprecht, E. L. Wilkie, "Electron Microscope Studies of an alloyed Au/Ni/Au-Ge Ohmic Contact to GaAs," Journal of Applied Physics, Vol. 54, No. 12, pg. 6952-6957, 1985.

65. T. S. Kuan, "Structural Analysis of Metal / GaAs Contacts and Ge/Ga As and Al As/GaAs Heterojunctions," Journal Applied Physics, Vol. 54, pg. 6975, 1985.

66. R. A. Bruce and G. R. Piercy, "An Improved Au-Ge-Ni Ohmic Contact to n-Type GaAs," Solid-State Electronics, Vol. 30, No. 7, pg. 729-737, 1987.

67. A. P. Botha and E. Relling, "Interface Reactions and Electrical Behaviour of Ni-AuGe Contacts on GaAs," Materials Research Proceedings, Vol. 54, pg. 421-426, 1986.

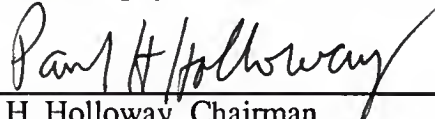
68. B. Li and P. H. Holloway, "Regrowth of GaAs at the Au-Ge-Ga/GaAs interface under an As flux," Journal of Vacuum Science and Technology, Vol. A 9, No. 3, pg. 944-948, 1991.
69. C. Thomas Tsai and R. Stanley Williams, "Solid Phase Equilibria in the Au-Ga-As, Au-Ga-Sb, Au-In-As, and Au-In-Sb Ternaries," Journal of Materials Research, Vol. 1, No. 2, pg. 352-360, 1986.
70. R. Beyers, K. B. Kim, and R. Sinclair, "Phase Equilibria in Metal-Gallium-Arsenic Systems: Thermodynamic Considerations for Metallization Materials," Journal of Applied Physics, Vol. 61, No. 6, pg. 2195-2202, 1987.
71. R. Schmid-Fetzer "Stability of Metal/GaAs-Interfaces: A Phase Diagram Survey," Journal of Electronic Materials, Vol. 17, No. 2, pg. 193-200, 1988.
72. A. Guivarc'h, R. Guerin, J. Caulet, A. Poudoulec, and J. Fontenille, "Metallurgical Study of Ni/GaAs Contacts. II. Interfacial Reactions of Ni Thin Films on (111) and (100) GaAs," Journal of Applied Physics, Vol. 66, No. 5, pg. 2129-2136, 1989.
73. A. Guivarc'h and R. Guerin, "Metallurgical Study of Ni/GaAs Contacts. I. Experimental Determination of the Solid Portion of the Ni-Ga-As ternary-phase Diagram," Journal of Applied Physics, Vol. 66, No. 5, pg. 2122-2128, 1989.
74. W. Shockley, AI-TDR-64-207, Air Force Avionics Laboratory, Wright-Patterson AFB, OH, 1964.
75. Powder Diffraction File, International Centre for Diffraction Data, Swarthmore, PA, 1991
76. G. K. Wehner, in Methods of Surface Analysis, Chapter 1, "The Aspects of Sputtering in Surface Analysis Methods," pg 5-35, Ed. A. W. Czanderna (Elsevier, New York, 1975).
77. L. E. Davis, N.C. MacDonald, P. W. Palmberg, G. E. Riach, R. E. Weber, Handbook of Auger Electron Spectroscopy (Perkin-Elmer Corp., Eden Prairie, MN, 1978).
78. S. A. Chambers and V. A. Loeb, "Chemistry of Formation, Structure, and Band Bending at Epitaxial Ni, Al, and NiAl/GaSe<sub>x</sub>As<sub>1-x</sub>GaAs(001)-(2x1) Interfaces," Materials Research Society Proceedings, Vol. 221, pg. 283-288, 1991
79. J. H. Neave, P. K. Larsen, B. A. Joyce, J. P. Gowers, and J. F. van der Veen, "Some observations on Ge:GaAs (001) and GaAs:Ge (001) interfaces and films," Journal of Vacuum Science and Technology, Vol. B 1, No. 3, pg. 688-674, 1983.
80. J. M Ballingall, C. E. C. Wood, and L. F. Eastman, "Electrical measurements of the conduction band discontinuity of the abrupt Ge-GaAs <001> heterojunction," Journal of Vacuum Science and Technology, Vol. B 1, No. 3, pg. 675-681, 1983.

81. A. D. Katnani, P. Chiaradia, H. W. Sang, Jr., and R. S. Bauer, "Fermi level position and valence band discontinuity at GaAs/Ge interfaces," Journal of Vacuum Science and Technology, Vol. B 2, No. 3, pg. 471-475, 1984.
82. E. L. Allen, Defense Advanced Research Projects Agency Contract Report No.DAAL-01-88-K-0828, 1991.
83. T. Sands, V. G. Keramidas, A. J. Yu, K.-M. Yu, R. Gronsky, and J. Washburn, "Ni, Pd, and Pt on GaAs: A comparative study of interfacial structures, compositions, and reacted film morphologies," Journal of Materials Research, Vol. 2, No. 2, pg. 262-275, 1987.
84. T. Sands, E. D. Marshall, and L. C. Wang, "Solid-phase regrowth of compound semiconductors by reaction-driven decomposition of intermediate phases," Journal of Materials Research, Vol. 3, No. 5, pg. 914-921, 1988.

## BIOGRAPHICAL SKETCH

William V. Lampert was born in Piqua, Ohio, USA, on January 3, 1948. He graduated from New Bremen Local High School, New Bremen, Ohio, in 1966. While attending Wright State University in Fairborn, Ohio he joined the Air Force Materials Laboratory at Wright-Patterson Air Force Base, Ohio, in 1975 as a co-op student in the Mechanics and Surface Interactions Branch of the Nonmetallic Materials Division. He received he received his Bachelor of Science in Materials Science and Engineering from Wright State University in 1977 and continued to work in the Surface Interactions group. His work at that time focused on the application of surface analytical techniques to develop models to provide new and improved cathode materials and materials processing for traveling wave tubes. In 1981 he was selected for the Air Force long-term full-time training program and entered the University of Florida Department of Materials Science and Engineering receiving a Master of Engineering in 1982. Subsequently he returned to the Materials Laboratory to continue to apply surface analytical techniques and the cathode modeling to resolve production problems with cathodes to be used in traveling wave tubes for MILSTAR satellites. In 1985 he returned to the Materials Science and Engineering Department through an agreement with the University of Florida to allow him to pursue the degree of Doctor of Philosophy by conducting his research off campus at the Materials Laboratory. His research has been on metallization of GaAs with emphasis on elevated temperature applications. After the long-term full-time training program is completed he will continue research, at the Materials Directorate, on ohmic contacts on III-V and IV-IV semiconductors for high temperature applications.

I certify that I have read this study and that in my opinion it conforms to acceptable standards of scholarly presentation and is fully adequate, in scope and quality, as a dissertation for the degree of Doctor of Philosophy.



Paul H. Holloway, Chairman  
Professor of Materials Science and  
Engineering

I certify that I have read this study and that in my opinion it conforms to acceptable standards of scholarly presentation and is fully adequate, in scope and quality, as a dissertation for the degree of Doctor of Philosophy.



Reza Abbaschian  
Professor of Materials Science and  
Engineering

I certify that I have read this study and that in my opinion it conforms to acceptable standards of scholarly presentation and is fully adequate, in scope and quality, as a dissertation for the degree of Doctor of Philosophy.



Robert T. DeHoff  
Professor of Materials Science and  
Engineering

I certify that I have read this study and that in my opinion it conforms to acceptable standards of scholarly presentation and is fully adequate, in scope and quality, as a dissertation for the degree of Doctor of Philosophy.



Kevin S. Jones  
Associate Professor of Materials Science  
and Engineering

I certify that I have read this study and that in my opinion it conforms to acceptable standards of scholarly presentation and is fully adequate, in scope and quality, as a dissertation for the degree of Doctor of Philosophy.



Sheng S. Li  
Professor of Electrical Engineering

I certify that I have read this study and that in my opinion it conforms to acceptable standards of scholarly presentation and is fully adequate, in scope and quality, as a dissertation for the degree of Doctor of Philosophy.

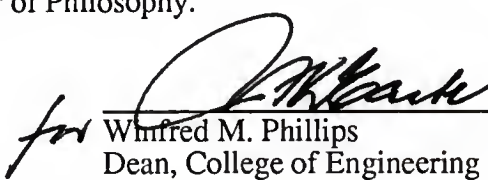
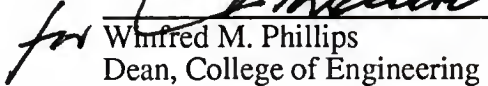


---

T. Walter Haas  
Group Leader, Wright Laboratory  
Materials Directorate

This dissertation was submitted to the Graduate Faculty of the college of Engineering and to the Graduate School and was accepted as partial fulfillment of the requirements for the degree of Doctor of Philosophy.

August 1992

  
*for*   
Winfred M. Phillips  
Dean, College of Engineering

---

Madelyn M. Lockhart  
Dean, Graduate School

UNIVERSITY OF FLORIDA



3 1262 08554 0507